Stable Limits of the Khovanov Homology and L-S-K Spectra for Infinite Braids

Michael Sean Willis
Charlottesville, Virginia

Bachelor of Science in Mathematics, Pennsylvania State University, 2004

A Dissertation presented to the Graduate Faculty
of the University of Virginia in Candidacy for the Degree of
Doctor of Philosophy

Department of Mathematics

University of Virginia
August, 2017

_____

_____

_____

_____

Contents

Acknowledgements

I would like to thank Robert Lipshitz for many helpful conversations full of mathematical encouragement and guidance. I would also like to thank Nicholas Kuhn, Peter Bonventre, and John Berman for their willingness to share their stable homotopy theory and category theory expertise. Gabriel Islambouli has been invaluable as both a collaborator and a good friend, and for that I am grateful. Finally, I would like to thank my advisor Slava Krushkal for all of his patience, guidance, honesty, and support as I have prepared this thesis.

Chapter 1

INTRODUCTION

Classical knot theory, that is the study of knots and links in 3-space, is a large and important area of study in low-dimensional topology. For a given link L, we have three particular invariants—the Jones polynomial $V(L)$, the Khovanov homology $Kh(L)$, and the Lipshitz-Sarkar-Khovanov (L-S-K) spectrum $\mathcal{X}(L)$—that stand at the intersection of knot theory with quantum topology, mathematical physics, and representation theory. The hierarchy of these invariants is illustrated in Figure 1.1.

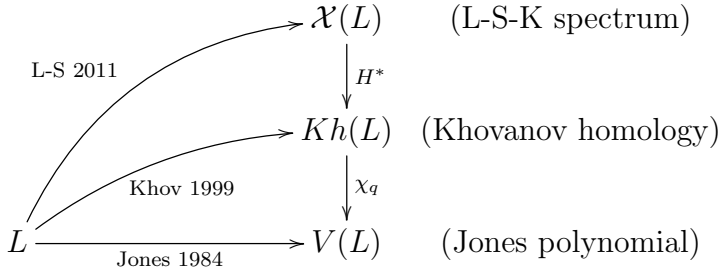

Figure 1.1: A diagram of invariants for a link L; $V(L)$ can be obtained from $Kh(L)$ which contains more information about L, and similarly $Kh(L)$ can be obtained from $\mathcal{X}(L)$ which contains still more information about L.

The celebrated Jones polynomial $V(L)$ was discovered by Vaughn Jones in 1984

[Jon97]. Besides being able to distinguish many different links in S^3, it also provides a combinatorial obstruction to a link being alternating [Thi87]. In addition, the Jones polynomial has further relationships with Chern-Simons theory [Wit94] and the Vassiliev invariants of knots [KR00].

The Khovanov homology $Kh(L)$ was discovered by Mikhail Khovanov in 1999 [Kho00]. It is a bigraded (co-)homology theory that categorifies the Jones polynomial of L, with graded Euler characteristic recovering $V(L)$. In this way, the Khovanov homology $Kh(L)$ contains at least as much information about a link L as does $V(L)$, but its added algebraic structure has been used to see more than can be clearly seen from $V(L)$ alone; in particular $Kh(L)$ can detect the unknot U [KM11] (it is unknown whether or not the Jones polynomial can also detect U). Functorial properties of $Kh(L)$ also lead to bounds on the slice genus of links, which have been used to give a purely combinatorial proof of the Milnor conjecture on the slice genus of torus knots [Ras10].

The L-S-K spectrum $\mathcal{X}(L)$ of a link L was constructed by Robert Lipshitz and Sucharit Sarkar in 2011 [LS14a]. It is the suspension spectrum of a CW-complex that *spectrifies* the Khovanov homology, in the sense that the reduced singular cohomology $\tilde{H}^*(\mathcal{X}(L))$ recovers $Kh(L)$. As with the comparison between $Kh(L)$ and $V(L)$, the L-S-K spectrum $\mathcal{X}(L)$ contains at least as much information about L as does $Kh(L)$, but its added topological structure can allow one to see more. In particular, $\mathcal{X}(L)$ can be used to compute cohomological operations on $Kh(L)$ [LS14c] that can be used

to improve on the slice genus bounds found using Khovanov homology alone [LS14b].

On the other hand, given a framed link L and an irreducible representation of the Lie algebra $\mathfrak{sl}_2(\mathbb{C})$, as indexed by its dimension $n \in \mathbb{N}$, we can also define the *colored* Jones polynomial ($V_n(L)$) as follows. We cable L with n parallel strands (as defined by the framing of L) and insert a copy of the n^{th} Jones-Wenzl projector P_n [Wen87] into each component of L before taking the Jones polynomial as usual. P_n is a special idempotent element in the Temperley-Lieb algebra $TL_n(\mathbb{C}(q))$ on n strands. The resulting $V_n(L)$, besides being related to the representation theory of $\mathfrak{sl}_2(\mathbb{C})$, is also conjecturally related to the hyperbolic volume of knot complements [Kas97]. The Jones-Wenzl projector P_n itself has many important applications in quantum field theory and is used to build quantum invariants of 3-manifolds [KL94].

A categorification of P_n is then necessary to define a colored Khovanov homology $Kh_n(L)$ which categorifies $V_n(L)$ in the same sense that $Kh(L)$ categorifies $V(L)$. Lev Rozansky's approach to this problem was based upon replacing P_n by an infinite twist [Roz14a]. That is, after cabling the link L with n strands, we add k full twists into each component. The resulting link is denoted L_n^k. Then both colored invariants $J_n(L)$ and $Kh_n(L)$ are formed by taking a limit as the twisting $k \to \infty$ as in Figure 1.2. In this way, Rozansky showed that the Khovanov chain complex associated to an infinite twist provides a suitable categorification of the Jones-Wenzl projector P_n.

Chapter 2 will focus on clarifying and expanding upon the summary of previous work presented above. After that there are three main goals of this manuscript, all

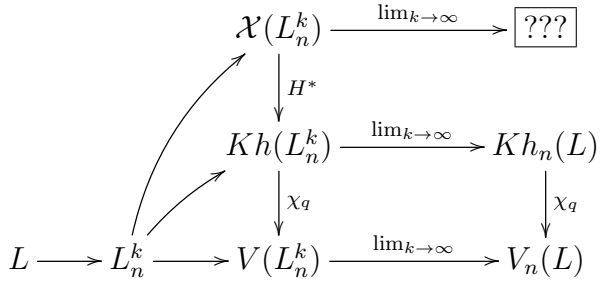

Figure 1.2: A diagram of colored invariants $V_n(L)$ and $Kh_n(L)$ that suggests the way towards a colored $\mathcal{X}_n(L)$.

related to Figure 1.2 and Rozansky's categorified projectors. The first goal is to fill in the upper-right hand box of Figure 1.2 with a colored version of the L-S-K spectrum $\mathcal{X}_n(L)$.

Theorem 1.0.1. *There exists a colored L-S-K spectrum for any $\mathfrak{sl}_2(\mathbb{C})$ colored link. Its reduced cohomology is isomorphic to the colored Khovanov homology defined in [CK12], [Roz14b].*

Theorem 1.0.1 provides an invariant which spectrifies the colored Khovanov homology $Kh_n(L)$ in the same sense that $\mathcal{X}(L)$ spectrifies $Kh(L)$; Corollary 1.0.5 further below will guarantee that there is indeed new information within $\mathcal{X}_n(L)$ for even the simplest case where $L = U$ the unknot. Loosely speaking, the process of proving Theorem 1.0.1 will involve a spectrification of the Jones-Wenzl projector P_n in a manner similar to the categorification of P_n using infinite twists.

Theorem 1.0.2. *For any link diagram D involving a finite number of Jones-Wenzl projectors, there exists an L-S-K spectrum $\mathcal{X}(D)$ with reduced cohomology isomorphic*

to the homology defined using the categorified Jones-Wenzl projectors as in [Roz14a] and [CK12].

An example of the type of diagram in the statement of Theorem 1.0.2 is provided in Figure 1.3. Notice that the Jones-Wenzl projectors themselves, and their categorifications, are defined using tangles. The L-S-K spectrum has not yet been defined for tangles, and so Theorem 1.0.2 requires that the projectors involved are closed in some way to form a link diagram. Nevertheless we will also prove several properties of such spectra, such as being 'killed by turnbacks', that the projectors and their categorifications satisfy. In this sense, Theorem 1.0.2 spectrifies the notion of Rozansky's categorified projector, lifting the important element P_n of TL_n into the stable homotopy category. Theorems 1.0.1 and 1.0.2 will be the focus of Chapter 3.

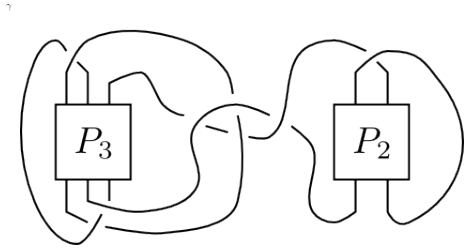

Figure 1.3: An example diagram for which Theorem 1.0.2 defines an L-S-K spectrum.

The second goal of this manuscript is to analyze the behavior of colored L-S-K spectra as the coloring parameter n goes towards infinity. For a certain special class of links (called B-adequate links), the work of Armond and Garoufalidis-Le shows that the coefficients of the colored Jones polynomial stabilize as $n \to \infty$ [GL15, Arm13].

For these same links, Rozansky also showed that the colored Khovanov homology groups stabilize as the coloring grows [Roz14b]. In Chapter 4 we will adapt these techniques to give a similar stabilization result for colored L-S-K spectra as $n \to \infty$.

Theorem 1.0.3. *The L-S-K spectra of n-colored B-adequate links stabilize as $n \to \infty$.*

We will also present a separate, simpler argument giving sharper bounds on stabilization of the colored L-S-K spectra (and thus the colored Khovanov homology and colored Jones polynomial) for the unknot U. In this case, cabling and twisting U results in constructing torus links $T(n,k)$, whose stable Khovanov homology has been extensively studied [GORS14, GOR13, Hogb], and so we state the theorem below accordingly.

Theorem 1.0.4. *In the case of the unknot U, the n-colored L-S-K spectra $\mathcal{X}_n(U) = \mathcal{X}(T(n,\infty))$ stabilize as $n \to \infty$ and the stable limit $\mathcal{X}(T(\infty,\infty)) := \bigvee_{j\in(2\mathbb{N}\cup 0)} \mathcal{X}^j(T(\infty,\infty))$ satisfies*

$$\mathcal{X}^j(T(\infty,\infty)) \simeq \mathcal{X}^{j/2}(T(j/2,\infty)) \simeq \mathcal{X}^{(j/2)^2}(T(j/2,j/2)) \qquad \text{for } j > 0$$

$$\mathcal{X}^0(T(\infty,\infty)) \simeq \mathcal{X}^{-1}(T(1,\infty)) \simeq S^0$$

where S^0 denotes the standard sphere spectrum.

Here the superscripts on the spectra refer to the internal quantum grading, which we will describe in Chapter 2. The approach for this simplified case will also provide us with the following corollary.

Corollary 1.0.5. *For all $k \geq 3$, the L-S-K spectrum $\mathcal{X}(T(3,k))$ admits a non-trivial Sq^2 action.*

Theorem 1.0.3 shows that the limiting behavior of the colored invariants of Armond, Garoufalidis-Le, and Rozansky lifts to the corresponding colored spectra in the stable homotopy category, while Theorem 1.0.4 and Corollary 1.0.5 provide insight into the behavior of the L-S-K spectra for torus links, which are in some sense the simplest links with 'thick' Khovanov homology which allows for the possibility of much new information to be gained from their spectra.

Finally, the third goal of this manuscript is to generalize all of these results in a slightly different direction. In the building of the colored invariants for links, we cable the links and insert an infinite twist into each component. One might ask what would happen if some other infinite braid were inserted in place of the infinite twist. In Chapter 5 we will show that, with the addition of one extra assumption which we call *completeness* (which will be a very natural assumption to make), *any* positive, infinite braid can be used in place of the infinite twist to give the same result.

Theorem 1.0.6 (joint with G. Islambouli)**.** *Let $\mathcal{B}$ be any complete semi-infinite positive braid, viewed as the limit of positive braid words*

$$\mathcal{B} = \lim_{\ell \to \infty} \sigma_{j_1} \sigma_{j_2} \cdots \sigma_{j_\ell}.$$

Then the limiting Khovanov chain complex $KC(\mathcal{B})$ is chain homotopy equivalent to the categorified Jones-Wenzl projector, and $\mathcal{B}$ may be used in place of the infinite twist

in the construction of any of the $\mathfrak{sl}_2(\mathbb{C})$ *colored invariants* $V_n(L)$*,* $Kh_n(L)$*, or* $\mathcal{X}_n(L)$*.*

Chapter 5 will also include some simple considerations for more general classes of infinite braids. Theorem 1.0.6 shows that, up to the notion of completeness, any positive infinite braid can be used to categorify and spectrify the Jones-Wenzl projector P_n. This result also provides some indication that the stable behavior of both the Khovanov homology and L-S-K spectra for positive infinite braids is insensitive to the specifics of the braid, indicating that although the conjectures about such stable homology are often stated in terms of torus braids [GORS14, GOR13, Hogb], in fact these conjectures may be true in much greater generality.

Remark 1.0.1. *The majority of these results have appeared in the author's papers [Wil16, Wil, IW17]. The paper [Wil] was first published in* Algebraic & Geometric Topology *by Mathematical Sciences Publishers.*

Chapter 2

BACKGROUND AND CONVENTIONS

2.1 The Decategorified Story

The purpose of this section is to define the Jones and colored Jones polynomials for knots and links. Although the original definition of the Jones polynomial [Jon97] had roots in functional analysis and quantum mechanics, a purely combinatorial approach comes from the application of the Kauffman bracket [Kau88]. We follow Kauffman's approach here. An important aspect of the Jones polynomial is its local nature - computations are based on single crossings at a time. We thus begin by presenting the local picture via tangles and the Temperley-Lieb algebra. This approach allows for a relatively simple definition for the Jones-Wenzl projector and the colored Jones polynomial, which we present at the end of this section.

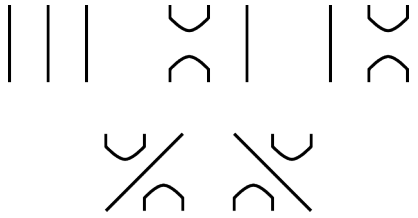

Figure 2.1: The five additive basis elements for $TL_3(R)$.

2.1.1 The Temperley-Lieb Algebra

Fix $n \in \mathbb{N}$ and a (commutative) ring R. The n^{th} *Temperley-Lieb algebra* over R is the algebra $TL_n(R)$ additively generated as a module over R by the set of crossingless planar matchings between two fixed sets of n points on opposite sides of a rectangle. The additive basis elements of $TL_3(R)$ are depicted in Figure 2.1.

Multiplication of basis elements is carried out by concatenating matchings. If a closed loop is created during concatenation, it is replaced by a scalar factor $d \in R$. To begin with, we set

$$R := \mathbb{Z}[q, q^{-1}]$$

$$d := q + q^{-1}.$$

The multiplicative identity is the diagram of n vertical lines, and will be denoted by I_n. It is well-known that $TL_n(R)$ is multiplicatively generated by the diagrams $\{e_i | i = 1, \ldots, n-1\}$ described in Figure 2.2. See Figure 2.3 for an example of multiplication in $TL_3(R)$. By convention, we can set $TL_0(R)$ to be a copy of the ground ring R, viewed as being generated by the empty diagram.

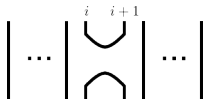

Figure 2.2: The diagrams $e_i \in TL_n(R)$ that form the standard multiplicative basis.

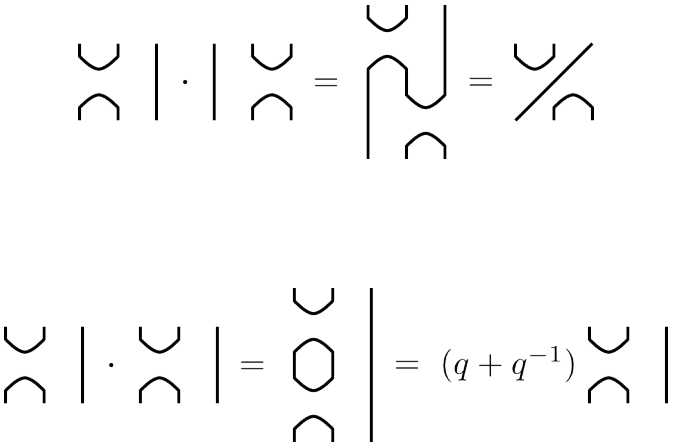

Figure 2.3: Two examples of multiplication in $TL_3(R)$. The first illustrates $e_1 \cdot e_2$. The second illustrates the computation $e_1 \cdot e_1 = (q + q^{-1})e_1$.

Figure 2.4: An example of a $(3, 3)$-tangle diagram.

Remark 2.1.1. *There is nothing particularly important about our choice of* $\mathbb{Z}$ *as the 'base' from which we choose our ground ring to be* $\mathbb{Z}[q, q^{-1}]$*. Other rings and fields are equally valid to work with, but we will usually work over* $\mathbb{Z}$*. If another ring is used (typically* $\mathbb{Z}/2\mathbb{Z}$*), we will make this clear within the notation.*

2.1.2 The Kauffman Bracket and the Jones Polynomial

Having fixed $n \in \mathbb{N}$, an (n, n)-tangle is an isotopy class of an embedding of n disjoint intervals, along with any number of disjoint circles, into the cube $[0, n+1] \times [-1, 1]^2$ with the $2n$ endpoints mapped to the fixed boundary points $(i, -1, 0)$ and $(i, 1, 0)$ for $i = 1, \ldots, n$. Intuitively, this gives a set of n strands connecting n endpoints on the top and bottom of a rectangular box (perhaps entwined with disjoint circles), and is drawn via a tangle diagram as shown in Figure 2.4. The Temperley-Lieb algebra $TL_n(\mathbb{Z}[q, q^{-1}])$ is related to (n, n)-tangles via the Kauffman bracket $\langle \cdot \rangle$, a function converting (n, n)-tangle diagrams into elements of TL_n (see [KL94]). There exist several different normalization conventions for defining the Kauffman bracket in the literature. We choose to adopt the following convention.

$$\left\langle \times \right\rangle = \left\langle \right\rangle \left\langle \right\rangle - q \left\langle \asymp \right\rangle \tag{2.1.1}$$

Figure 2.5: The crossing on the left is a positive crossing; the crossing on the right is negative.

The first local picture on the right hand side of Equation 2.1.1 will be referred to as the 0-resolution of the crossing, while the second picture will be the 1-resolution. This local relation, together with the Temperley-Lieb relation that replaces circles by the scalar factor $(q + q^{-1})$, allows any (n, n)-tangle diagram to be evaluated to an element of $TL_n(\mathbb{Z}[q, q^{-1}])$.

Under this convention, the Kauffman bracket is invariant under the Reidemeister moves only up to a degree shift. To build a true invariant of tangles, we orient the strands and let n^+ and n^- denote the number of positive and negative crossings respectively (positive and negative crossings are illustrated in Figure 2.5). Then the *Jones invariant* $V(\mathbf{T}) \in TL_n(\mathbb{Z}[q, q^{-1}])$ of an oriented (n, n)-tangle $\mathbf{T}$ can be defined as

$$V(\mathbf{T}) := (-1)^{n^-}(q)^{n^+-2n^-} \langle D_{\mathbf{T}} \rangle \tag{2.1.2}$$

where $D_{\mathbf{T}}$ is any diagram for the tangle $\mathbf{T}$. In particular, the *Jones polynomial* of a knot or link L is calculated as the Jones invariant of L viewed as a $(0, 0)$-tangle. Thus $V(L) \in TL_0(\mathbb{Z}[q, q^{-1}]) = \mathbb{Z}[q, q^{-1}]$ is a Laurent polynomial invariant of knots and links in S^3.

2.1.3 The Jones-Wenzl Projector and the Colored Jones Polynomial

If we enlarge R to the field $R := \mathbb{C}(q)$ of rational functions of q, we can find a special idempotent element in $TL_n(R)$, denoted P_n, characterized by the following axioms:

I. $P_n \cdot e_i = e_i \cdot P_n = 0$ for any of the standard multiplicative generators $e_i \in TL_n(R)$. This is often described by stating that P_n is "killed by turnbacks".

II. The coefficient of the n-strand identity tangle I_n in the expression for P_n is 1.

These are the Jones-Wenzl projectors (one for each $n \in \mathbb{N}$), originally defined in [Wen87]. The simplest non-trivial example is P_2, shown below.

$$P_2 = I_2 - \frac{1}{q^{-1}+q} \left\langle \asymp \right\rangle \tag{2.1.3}$$

Although the Jones-Wenzl projectors have been extensively studied in a variety of contexts [KL94], here we will focus on their use for defining the colored Jones polynomial of a link.

Let L be a framed, oriented ℓ-component link in S^3 with link diagram D_L. A coloring of a link L refers to assigning an irreducible $\mathfrak{sl}_2(\mathbb{C})$ representation to each component of L. Such representations are characterized by their dimension, allowing us to simply consider colorings as assignments of non-negative integers to each link component. Following the convention of Rozansky [Roz14a], we allow the color n to correspond to the $(n+1)$-dimensional $\mathfrak{sl}_2(\mathbb{C})$ representation. In this way, we define

a *coloring* γ of L to be an ordered ℓ-tuple of colors $\gamma := (n_1, \ldots, n_\ell) \in \mathbb{N}^\ell$ that assigns the color n_h to the h^{th} component of L. We denote the resulting *colored link* by L_γ. Then the *colored Jones polynomial* of the link L_γ is obtained by cabling each component with its designated n_h number of strands, inserting a copy of the n_h^{th} Jones-Wenzl projector P_{n_h} into each such cabled component, and then taking the usual Jones polynomial. See Figure 2.6.

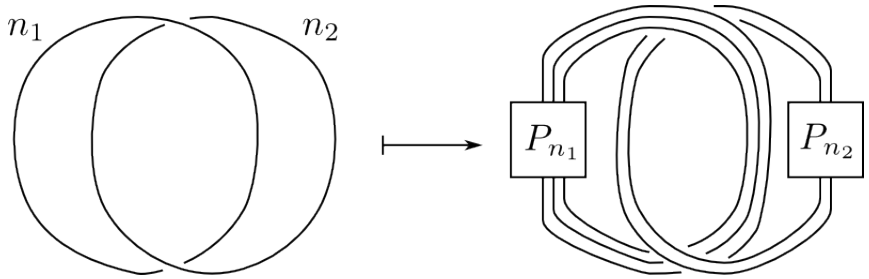

Figure 2.6: On the left is an example L_γ, with components colored n_1 and n_2; on the right is the resulting diagram D_{L_γ} for taking the colored Jones polynomial.

Remark 2.1.2. *The cabling of each component depends on the framing of that component. Note that it is always possible to represent a framed link L by a link diagram where each component is given the blackboard framing. This is accomplished by representing the unframed link L via any suitable projection to the plane as usual, and then adding positive or negative kinks (Reidemeister I moves) to the diagram which adjust the framing of the link as necessary. Unless otherwise stated, we will assume that this has been done for diagrams in this manuscript.*

2.2 The Categorified Story

The goal of this section is to categorify the concepts of the previous one. Roughly speaking, we would like to construct chain complexes whose Euler characteristics recover elements of the Temperley-Lieb algebra such as the Jones polynomial of a link, or the Jones-Wenzl projector (and thus the colored Jones polynomial). This was originally carried out by Mikhail Khovanov for the Jones polynomial of links [Kho00], and later with more algebraic sophistication for tangles as well [Kho02]. However, a simpler diagrammatic approach was discovered by Dror Bar-Natan [BN05] and that is the approach we follow here. The Jones-Wenzl projector was categorified later by Ben Cooper and Slava Krushkal [CK12], and independently by Lev Rozansky [Roz14a]. Both approaches use infinite chain complexes, but Rozansky's version presents such a complex with a clear interpretation as the Khovanov complex of an infinite twist. This viewpoint will be crucial throughout this manuscript, and so we will expand on it somewhat further below.

2.2.1 Bar-Natan's Graphical Temperley-Lieb Category

We present here a quick summary of Bar-Natan's diagrammatic categorification of the Temperley-Lieb algebra. The interested reader is strongly encouraged to turn to the source itself [BN05] for a much fuller account. The central idea, inspired by Equation 2.1.1, is essentially local in nature and somewhat formal. We seek to replace

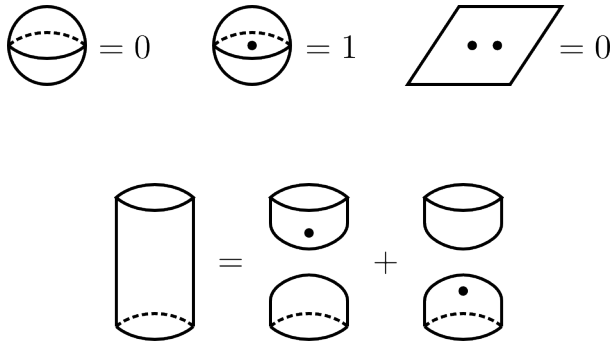

Figure 2.7: The local relations for the morphisms in the category $Cob_\bullet(n)$.

Equation 2.1.1 by a two term chain complex

$$[\![\diagup\!\diagdown]\!] \stackrel{?}{:=} [\![)\,(]\!] \stackrel{?}{\longrightarrow} \mathrm{q}\,[\![\asymp]\!] \tag{2.2.1}$$

where the first term has homological degree zero, and the q indicates a second formal grading which will be used to recover the polynomial coefficients in $R = \mathbb{Z}[q, q^{-1}]$.

In order to carry out this task, we first define a category $Cob_\bullet(n)$ whose objects are embedded 1-manifolds in a rectangle with boundary mapped to n fixed points on either side of the rectangle. Thus, the objects are precisely the basis diagrams of TL_n, but also allowing for disjoint circles to be present. The morphisms in $Cob_\bullet(n)$ are formal sums of 'dotted' cobordisms (with fixed boundary) between such diagrams, relative some local moves. Here 'dotted' simply means that dots may be drawn on any surface in our cobordism, and that such dots are free to slide along the surface. The local moves are described in Figure 2.7. The spherical relations ensure that no disjoint closed cobordisms are ever needed in a morphism, and the two-dot relation ensures that no more than one dot need ever be accounted for on any surface. The neck-

cutting relation eliminates the need for any genus. Both the objects and morphisms of $Cob_\bullet(n)$ allow for concatenation similar to $TL(n)$, although there is not yet a natural method for removing a disjoint circle. There is also not yet a notion of having coefficients to a diagram in the ground ring $\mathbb{Z}[q, q^{-1}]$.

We attempt to fix both of these problems using formal categorical notions. Starting with our category $Cob_\bullet(n)$, we begin by introducing a purely formal $\mathbb{Z}$-grading to objects, the quantum grading. We then take the *additive closure* of our q-graded $Cob_\bullet(n)$ by allowing for formal direct sums of objects, and matrices of morphisms between them. Finally, we consider the category of chain complexes (up to chain homotopy equivalence) over this additive closure of $Cob_\bullet(n)$, and call this category $\mathbb{TL}_n$. Although the objects are not groups and we do not have a meaningful notion of homology at this stage, we still gain a homological grading which, together with the formal q-grading, allows us to take the graded Euler characteristic of any such complex to recover elements of $TL_n(\mathbb{Z}[q, q^{-1}])$. This process respects the concatenation operation, where "concatenating" two complexes means taking their tensor product with diagrams and morphisms formed by concatenation. Furthermore, the local relations of Figure 2.7 can now be used to prove a chain homotopy equivalence that categorifies the relation of removing a disjoint circle:

$$[\![D \sqcup \bigcirc]\!] \cong \mathrm{q}\,[\![D]\!] \oplus \mathrm{q}^{-1}\,[\![D]\!] \tag{2.2.2}$$

Here the double brackets $[\![\cdot]\!]$ indicate that these are chain complexes, and the q symbol indicates a shift in the formal q-grading.

Remark 2.2.1. *We refer to the complexes built here (and throughout this manuscript) as chain complexes, but in fact the maps within any of these complexes are taken to increase homological grading by one, rather than decrease. Thus these complexes would be classically considered cochain complexes, but following the literature on the subject we still refer to them as chain complexes.*

Remark 2.2.2. *With the help of Equation 2.2.2 we can effectively remove all closed circles from a diagram within any term of a complex in $\mathbb{TL}_n$. In the case $n = 0$, which is of prime interest for invariants of knots and links, this means we can reduce the chain complex to one where every diagram is the empty diagram. That is to say, in each homological and q-degree we see only a direct sum of empty diagrams which can be interpreted as copies of $\mathbb{Z}$ (the q-gradings will recover the powers of q allowing the Euler characteristic to land correctly in $\mathbb{Z}[q, q^{-1}]$). Once we have done this, the local relations of Figure 2.7 also allow us to eliminate all closed surfaces, so that the maps involved will all be matrices of multiples of the empty cobordism. In this way we can already interpret an element of $\mathbb{TL}_0$ as a bigraded complex of free modules over $\mathbb{Z}$. We shall not pursue this viewpoint in this manuscript, but see Remark 2.2.3.*

2.2.2 The Chain Complex Associated to a Tangle and Khovanov Homology

With our category $\mathbb{TL}_n$ in place, we now provide an actual definition to the idea of Equation 2.2.1 by setting

$$[\![\times]\!] := [\!]\,)\,(\,[\!] \xrightarrow{s} \mathrm{q}\,[\![\asymp]\!] \tag{2.2.3}$$

where the map s indicates a saddle cobordism between the two resolutions of the crossing (the cobordism s is the identity cobordism everywhere away from the crossing). Here the 0-resolution $)\,($ is taken to be in homological degree zero, and the 1-resolution $\asymp$ is taken to be in homological degree one (see Remark 2.2.1). The full complex of a tangle is then a tensor product over all of these two term complexes (q-grading is taken to be additive under tensor product, just as the power of q in the Jones invariant is additive under multiplication), and so takes the form of a cubical complex, usually referred to as the *cube of resolutions*.

Similarly to the case of the Kauffman bracket, the chain complex built in this way is only invariant under Reidemeister moves up to degree shifts. In order to build a true invariant of tangles, we again introduce orientations on the strands, and let n^+ and n^- count the number of positive and negative crossings in the diagram $D_{\mathbf{T}}$ for a given tangle $\mathbf{T}$. We then make the following key definition.

Definition 2.2.1. *The* Khovanov chain complex *of an* (n,n)*-tangle* $\mathbf{T}$ *with diagram*

$D_{\mathbf{T}}$ will be denoted $KC(\mathbf{T})$, and is defined by

$$KC(\mathbf{T}) := \mathrm{h}^{-n^-}\mathrm{q}^{n^+-2n^-}\,[\![D_{\mathbf{T}}]\!] \tag{2.2.4}$$

where h *and* q *denote global homological and q-degree shifts that are applied to the entire complex. To isolate specific bigradings, we use superscripts $KC^{i,j}(\mathbf{T})$ where i indicates the homological grading, and j indicates the q-grading.*

It is proven in [BN05] that the formula of Equation 2.2.4 gives a well-defined $\mathbb{TL}_n$-valued invariant of tangles (that is to say, different diagrams for the same tangle produce chain homotopy equivalent complexes in $\mathbb{TL}_n$). Furthermore, by construction it is clear that the q-graded Euler characteristic of such a complex recovers the Jones invariant of the tangle. That is,

$$\chi_q(KC(\mathbf{T})) = V(\mathbf{T}). \tag{2.2.5}$$

In the particular case of a knot or link L viewed as a $(0,0)$-tangle, we can do even better. As currently constructed, $KC(L)$ would be a chain complex where the terms are given by resolutions of the link diagram D_L into diagrams of disjoint circles in the plane, and the differentials are comprised of saddle maps between them. In order to create a complex of actual modules of which we can take homology, we replace any resolution D with the free module over $\mathbb{Z}$ (or whatever base ring/field we like, see Remark 2.1.1) generated by $Cob_\bullet(\emptyset, D)$, the set of dotted cobordisms from the empty set to D. The relations of Figure 2.7 (particularly the neck-cutting relation) guarantee that we only need to consider discs giving birth cobordisms at each circle. This is

equivalent to *decorating* each circle in the diagram D with either a v_+ (standing for an undotted birth cobordism at that circle) or v_- (standing for a dotted birth cobordism at that circle). We call the result a *decorated diagram* or a *decorated resolution* of the link diagram D_L. In an abuse of nomenclature that we shall justify in Remark 2.2.3 below, we keep the same name and notation $KC(L)$ for the resulting complex. The saddle maps that make up the differential can be computed on the generators with the help of the local neck-cutting relation, and we arrive at the new definition below.

Definition 2.2.2. *Given a knot or link $L \subset S^3$ with diagram D_L, the* Khovanov chain complex *of L is denoted $KC(L)$ and is constructed as follows. As a module over the base ring (usually assumed to be $\mathbb{Z}$), $KC(L)$ is generated by all possible decorated resolutions of D_L. The differential on $KC(L)$ acts on any decorated resolution D by a sum of maps based on single saddle cobordisms going from 0-resolutions in D to 1-resolutions (together with a choice of sign convention mimicking the alternating signs used when taking the tensor product over the various* $[\![\times]\!]$ *for each crossing, see [BN05]). The effect on the decorations depends on whether the saddle merged two*

circles (multiplication m) or split one circle into two (co-multiplication Δ) as follows:

$$m(v_+, v_+) = v_+ \tag{2.2.6}$$

$$m(v_+, v_-) = m(v_-, v_+) = v_- \tag{2.2.7}$$

$$m(v_-, v_-) = 0 \tag{2.2.8}$$

$$\Delta(v_+) = (v_+, v_-) + (v_-, v_+) \tag{2.2.9}$$

$$\Delta(v_-) = (v_-, v_-) \tag{2.2.10}$$

All circles that are not affected by a saddle maintain their decorations. The homological degree and q-degree of any generator are determined by the following formulae:

$$\deg_h(\cdot) := \#(\textit{1-resolutions}) - n^- \tag{2.2.11}$$

$$\deg_q(\cdot) := \#(\textit{1-resolutions}) + (\#(v_+) - \#(v_-)) + (n^+ - 2n^-) \tag{2.2.12}$$

where n^+ and n^- count the number of positive and negative crossings in the original diagram D_L for the link L.

With this definition, it is not hard to show that the differentials respect the q-degree, and thus we can split $KC(L)$ as a direct sum over q-degrees:

$$KC(L) = \oplus_{j\in\mathbb{Z}} KC^{*,j}(L). \tag{2.2.13}$$

Thus when we take homology, our groups are bigraded.

Definition 2.2.3. *The* Khovanov homology *of a knot or link L is denoted $Kh(L)$ and is defined to be the homology of the Khovanov complex $KC(L)$. We again use*

superscripts $Kh^{i,j}(L)$ to isolate specific gradings (i for homological grading, j for q-grading).

Since the complex $KC(L)$ is well-defined for a link up to chain homotopy equivalence, the homology groups $Kh(L)$ are also well-defined up to isomorphism. For an excellent example showing the construction of $KC(L)$ for the trefoil, see Figure 1 in [BN05].

Remark 2.2.3. *The seemingly new version for $KC(L)$ given as Definition 2.2.2 is, in fact, chain homotopy equivalent to the chain complex one would get by constructing $KC(L)$ by viewing L as a $(0,0)$-tangle as before, and then using the chain homotopy equivalences of Equation 2.2.2 to arrive at a complex where every diagram is the empty set (see [BN07]), which can then be interpreted as a complex of modules over $\mathbb{Z}$ as in Remark 2.2.2. This equivalence justifies the use of the same name and notation for $KC(L)$ that is used for (n,n)-tangles where $n \neq 0$. It also guarantees that the graded Euler characteristic of $Kh(L)$ correctly recovers the Jones polynomial $V(L)$ in the same way as it did for any (n,n)-tangles.*

Remark 2.2.4. *As indicated earlier, this definition for Khovanov homology is not the one originally given by Khovanov himself [Kho00], but is easily shown to be equivalent [BN05]. For tangles, Khovanov's approach produces an actual complex of modules over a more complicated ring [Kho02], but we will not need this construction here.*

Remark 2.2.5. *The notations above assume a ground ring of $R = \mathbb{Z}[q, q^{-1}]$ for*

$TL_n(R)$. We will occasionally make use of allowing $\mathbb{Z}/2\mathbb{Z}$ coefficients instead, that is, allowing $R = \mathbb{Z}/2\mathbb{Z}[q, q^{-1}]$ (see Remark 2.1.1). In such cases, we will notate the Khovanov complex and homology as $KC(L; \mathbb{Z}/2\mathbb{Z})$ and $Kh(L; \mathbb{Z}/2\mathbb{Z})$ respectively.

2.2.3 Categorifying the Jones-Wenzl Projector and Colored Khovanov Homology

Our category of chain complexes $\mathbb{TL}_n$ was built with decategorification to $TL_n(\mathbb{Z}[q, q^{-1}])$ in mind. This allowed us to define the Khovanov homology $Kh(L)$ which categorifies the Jones polynomial $V(L)$. However, the colored Jones polynomial makes use of the Jones-Wenzl projectors $P_n \in TL_n(\mathbb{C}(q))$ - in particular, P_n contains terms with coefficients that are rational in q. The question of how to categorify these fractions was handled by Ben Cooper and Slava Krushkal [CK12], and independently by Lev Rozansky [Roz14a], at about the same time. Both approaches focused on one central idea: we expand the rational coefficients of P_n as power series in q (or q^{-1}, see Remark 2.2.6) and observe that all of the coefficients of this series are integral. Then we seek to categorify these terms via infinite chain complexes within $\mathbb{TL}_n$.

We begin with an axiomatic definition for precisely what we are looking for. Specifically, we seek a semi-infinite chain complex $\mathbf{P}_n \in \mathbb{TL}_n$ satisfying:

I. $\mathbf{P}_n \otimes \mathbf{e}_i \simeq \{*\}$ for any TL_n generator e_i viewed as a one-term complex in $\mathbb{TL}_n$. That is, $\mathbf{P}_n$ is "contractible under turnbacks".

II. The identity diagram I_n appears only once, in homological degree zero.

III. All negative homological degrees and q-degrees of $\mathbf{P}_n$ are empty, and the differentials are made up of degree zero maps.

Such a complex $\mathbf{P}_n$ is called a *categorified Jones-Wenzl projector*. For more details on this axiomatic definition, see [CK12] where such complexes are constructed inductively and are shown to be unique up to chain homotopy equivalence. The simplest non-trivial example is $\mathbf{P}_2$, shown below (compare to Equation 2.1.3).

$$\mathbf{P}_2 = \rangle\langle \longrightarrow q \asymp \longrightarrow q^3 \asymp \longrightarrow q^5 \asymp \longrightarrow \cdots \tag{2.2.14}$$

The maps in the complex (2.2.14) are given explicitly in [CK12]. Note that the graded Euler characteristic for $\mathbf{P}_2$ gives a power series representation of P_2 from Equation 2.1.3, as discussed above.

Remark 2.2.6. *The version of* $\mathbf{P}_n$ *described above is based upon expanding the ratios in* P_n *as power series in the variable* q*. However, it is equally valid to expand them as power series in the variable* q^{-1}*. Thus the third axiom of* $\mathbf{P}_n$ *could be replaced by a similar axiom declaring the* positive *homological and* q*-gradings to be empty.*

An attempt at spectrifying the Cooper-Krushkal construction of $\mathbf{P}_n$ was discussed, and accomplished for $n = 2$, by Andrew Lobb, Patrick Orson, and Dirk Schuetz [LOS], but problems occurred for $n \geq 3$. Instead, we will follow the construction in [Roz14a], where Lev Rozansky provided a categorification for any P_n via an infinite

torus braid. If we let $\sigma_1, \ldots, \sigma_{n-1}$ denote the standard generators of the braid group B_n, we introduce the following notation for full twists on n strands:

$$\mathbf{T}_n^k := (\sigma_1 \sigma_2 \cdots \sigma_{n-1})^{nk}. \tag{2.2.15}$$

After giving a well-defined notion for a stable limit of chain complexes, Rozansky proved the following theorem.

Theorem 2.2.4 (Rozansky)**.** *The (renormalized) Khovanov chain complexes of torus braids* $\mathrm{h}^{n^-}\mathrm{q}^{-(n^+-2n^-)}KC(\mathbf{T}_n^k)$ *stabilize up to chain homotopy as* $k \to \pm\infty$*. The limiting complex, denoted* $KC(\mathbf{T}_n^{\pm\infty})$*, satisfies the axioms of a categorified Jones-Wenzl projector, and so by the uniqueness result of [CK12] we may write*

$$\mathbf{P}_n \cong KC(\mathbf{T}_n^{\pm\infty}) \tag{2.2.16}$$

Proof. See [Roz14a], and also section 1.6 in [Roz14b]. □

We shall consider some details of this approach more carefully in Chapter 5 where they will be more immediately relevant. In essence, the stable limiting aspect of Theorem 2.2.4 means that if we are seeking a chain complex categorifying the Jones-Wenzl projectors up through a given homological degree, it is enough to replace any P_n in a diagram with a copy of $\mathbf{T}_n^{\pm k}$ for large k (we shall often refer to this as a 'finite-twist approximation'). The exact size of k needed depends on the homological degree we are interested in. The graded Euler characteristic of this complex stabilizes as $k \to \infty$ to give a power series representation of the rational terms appearing in the

usual formulas for the P_n. Positive (right-handed) twisting gives a power series in q, while negative (left-handed) twisting gives a power series in q^{-1}.

In particular, Theorem 2.2.4 gives a concrete approach to defining a colored Khovanov homology for knots and links in S^3. As illustrated in Figure 1.2 in the introduction, we take our framed link L and cable it according to the desired coloring γ, just as we would for the colored Jones polynomial. However, instead of inserting a copy of P_{n_h} into each cable, we insert a copy of the torus braid $\mathbf{T}^k_{n_h}$ for large k. The resulting link is denoted L^k_γ. We then take a stable limit of chain complexes $\mathrm{h}^{n^-}\mathrm{q}^{-N}KC(L^k_\gamma)$ as the twisting $k \to \infty$ to arrive at the *colored Khovanov complex* $KC_c(L_\gamma)$, and take homology to arrive at the *colored Khovanov homology* $Kh_c(L_\gamma)$.

2.3 The Spectrified Story

Having now a bi-graded chain complex $KC(L)$ whose graded Euler characteristic recovers the Jones polynomial $J(L)$, one might ask whether or not $KC(L)$ is isomorphic to the cochain complex of some space associated with L, perhaps even a cell complex whose cellular cochain complex recovers $KC(L)$. (Note that we ask for the cochain complex of the space, since the Khovanov complex has differentials that increase homological degree.) If such a space exists, one would hope that it splits as a wedge sum over the different q-degrees, just as $KC(L)$ splits in Equation 2.2.13. One might also hope that the space can be constructed combinatorially from a diagram for L, just as $KC(L)$ can be, and of course that the space so constructed does not depend

on the choice of diagram. Finally, one would hope that the space contains some new information about the link that was not available in $KC(L)$ and $Kh(L)$ alone.

In [LS14a], Robert Lipshitz and Sucharit Sarkar show that these hopes are very nearly fulfilled. The only caveat is that, rather than a space for L, we construct a spectrum $\mathcal{X}(L)$ in the stable homotopy category. Thus we refer to $\mathcal{X}(L)$ as a "spectrification" of $KC(L)$, which itself was a categorification of $V(L)$. The goal of this section is to first describe the invariant $\mathcal{X}(L)$ and its important properties before turning to an overview of its construction.

Remark 2.3.1. *Note that we only mention a spectrification $\mathcal{X}(L)$ for knots and links, rather than for tangles. As of this writing, there is no published work producing a well-defined space-like invariant for tangles that can recover the Khovanov homology of a tangle, which itself requires Khovanov's own more sophisticated algebraic machinery (see Remark 2.2.4). This will be an important point in deciding precisely what we should mean by "spectrifying" the Jones-Wenzl projector needed for colored Khovanov homology.*

2.3.1 The Lipshitz-Sarkar-Khovanov Spectrum of a Knot or Link

In this section we will expand upon several of the points about L-S-K spectra brought up during the Introduction. We begin with a more precise statement.

Theorem 2.3.1 ([LS14a])**.** *Given a link $L \subset S^3$ with diagram D_L, there exists a spectrum $\mathcal{X}(D_L)$ that satisfies the following properties:*

- *$\mathcal{X}(D_L)$ is the suspension spectrum of a CW complex.*
- *$\mathcal{X}(D_L)$ splits as a wedge sum $\mathcal{X}(D_L) := \bigvee_{j\in\mathbb{Z}} \mathcal{X}^j(D_L)$ such that $\tilde{H}^i(\mathcal{X}^j(D_L)) \cong Kh^{i,j}(L)$; that is, the reduced cohomology of $\mathcal{X}(D_L)$ recovers the Khovanov homology of the link L.*
- *The stable homotopy type of each $\mathcal{X}^j(D_L)$ is an invariant of the link L; that is, it does not depend on the choice of diagram D_L.*

The third item above in particular allows us to eliminate the diagram from the notation and define:

Definition 2.3.2. *Given a link L, the* L-S-K spectrum *of L is the spectrum $\mathcal{X}(L) := \bigvee_{j\in\mathbb{Z}} \mathcal{X}^j(L)$ of Theorem 2.3.1.*

We postpone discussion on the construction of $\mathcal{X}(L)$ and the proof of Theorem 2.3.1 for the moment and instead focus on some of its interesting properties, mostly presented here without proof. To begin with, there are some cases where $\mathcal{X}(L)$ is actually not interesting.

Proposition 2.3.3 ([LS14a])**.** *If L is an alternating link, $\mathcal{X}(L)$ is a wedge sum of Moore spaces, and thus is completely determined by $Kh(L)$.*

Fortunately, this is not the case in general.

Proposition 2.3.4 ([LS14c])**.** *There exist links L for which $\mathcal{X}(L)$ is not a wedge sum of Moore spaces.*

One important consequence of having a stable homotopy invariant for links is that the cohomology (that is, the Khovanov homology $Kh(L)$) admits an action by the Steenrod algebra.

Proposition 2.3.5. *Non-trivial Steenrod square operations on $\tilde{H}^i(\mathcal{X}^j(L);\mathbb{Z}/2\mathbb{Z}) = Kh^{i,j}(L;\mathbb{Z}/2\mathbb{Z})$ can serve to differentiate links with isomorphic Khovanov homology [LS14c] and also give rise to slice genus bounds [LS14b] for the link L.*

In fact, in [LS14c], Lipshitz and Sarkar derive a combinatorial formula for both Sq^1 and Sq^2 acting on the cochain level (that is, on generators of $KC(L)$), and they use this formula explicitly to calculate the invariant $\mathcal{X}(L)$ for some links with small crossing number via classification results of Whitehead [Whi50] and Chang [Cha56].

Proposition 2.3.6 ([LS14b])**.** *A cobordism between two links L and L' induces a map $\mathcal{X}(L) \to \mathcal{X}(L')$.*

This last proposition is used to produce the slice genus bounds of Proposition 2.3.5, but it is not yet clear in the literature whether or not there is such a map that is an invariant of the isotopy type of the cobordism. Indeed, Lipshitz and Sarkar construct these maps by decomposing a cobordism into elementary pieces, and the maps have not been shown to be independent of this decomposition.

The most important property of $\mathcal{X}(L)$ for our purposes comes from the following 'Collapsing Lemma'. Fixing $j \in \mathbb{Z}$, we use Equation 2.2.3 to consider the Khovanov chain complex $KC(L)$ represented as the mapping cone of a chain map:

$$KC^{j+N_L}(L) = \mathrm{Cone}\big(KC^{j+N_{L_0}}(L_0) \longrightarrow KC^{j-1+N_{L_1}}(L_1)\big) \tag{2.3.1}$$

where L_1 and L_0 are the links resulting from taking the 1-resolution and 0-resolution, respectively, of a single crossing in the diagram for L. The single superscripts stand for q-gradings, with N_L denoting the q-degree normalization shift $n^+ - 2n^-$ in the link diagram L, and similarly for N_{L_1} and N_{L_0} (the extra -1 for L_1 takes into account the loss of a 1-resolution from the point of view of L_1). There is a corresponding cofibration sequence of spectra (see Theorem 2 in [LS14a]):

$$\Sigma^a \mathcal{X}^{j+N_{L_0}}(L_0) \hookrightarrow \mathcal{X}^{j+N_L}(L) \twoheadrightarrow \Sigma^b \mathcal{X}^{j-1+N_{L_1}}(L_1) \tag{2.3.2}$$

where the Σ stands for suspensions allowing for shifts in homological degree, with $a = n^-_{L_0} - n^-_L$ and $b = n^-_{L_1} - n^-_L + 1$, the differences in the count of negative crossings n^- for the various diagrams. See Equations 2.2.11 and 2.2.12 to clarify the grading shifts.

Lemma 2.3.7. *With $KC^{j+N_L}(L) = \big(KC^{j+N_{L_0}}(L_0) \longrightarrow KC^{j-1+N_{L_1}}(L_1)\big)$ as above, we have:*

- *If $KC^{j-1+N_{L_1}}(L_1)$ is acyclic, then the induced inclusion $\Sigma^a \mathcal{X}^{j+N_{L_0}}(L_0) \hookrightarrow \mathcal{X}^{j+N_L}(L)$ is a stable homotopy equivalence.*

- *If* $KC^{j+N_{L_0}}(L_0)$ *is acyclic, then the induced surjection* $\mathcal{X}^{j+N_L}(L) \twoheadrightarrow \Sigma^b \mathcal{X}^{j-1+N_{L_1}}(L_1)$ *is a stable homotopy equivalence.*

Proof. Both of these are special cases of Lemma 3.32 in [LS14a], presented as in Theorem 2 from the same paper. A cofibration sequence induces a long exact sequence on cohomology, and if one piece is acyclic, the other two pieces must be isomorphic. Whitehead's theorem for spectra then guarantees that the map involved is a stable homotopy equivalence (there is no π_1 obstruction in the stable homotopy category). □

Lemma 2.3.7 says that we can resolve crossings in a diagram one at a time, and if one resolution of a crossing results in a diagram with an acyclic chain complex in the specified q-degree, this entire part of the full chain complex can be collapsed and we are left with the chain complex using only the other resolution (up to some potential suspensions). We will want to make repeated use of this idea throughout this manuscript.

2.3.2 The Construction (An Overview)

In this section we give a very broad overview of the construction of the L-S-K spectrum $\mathcal{X}(L)$ of a link L. The summary here is based entirely upon [LS14a], to which the reader is referred for a much more complete treatment. We only seek to give the main ideas here. None of the material in this section will be used further in this manuscript.

A *k-manifold with corners* X is a topological space where every point has a neighborhood homeomorphic to some point in the 'cornered' Euclidean space $\mathbb{R}^k_{\geq 0}$, and the transition maps between overlapping neighborhoods give C^∞ diffeomorphisms. The boundary ∂X is made up of points of various co-dimension. A *face* is a union of closures of boundary components of co-dimension 1. A *k-dimensional $\langle n \rangle$-manifold* is a k-manifold with corners X along with a specified arrangement of n faces $\partial_i X$ making up the boundary $\partial X = \partial_1 X \cup \cdots \cup \partial_n X$ so that any two faces intersect in a 'mutual face'. That is, $\partial_i X \cap \partial_j X$ is a face of both $\partial_i X$ and $\partial_j X$ each viewed as their own $(k-1)$-manifolds with corners.

A *flow category* $\mathcal{C}$ is a category where each object x is assigned a single $\mathbb{Z}$-grading $gr(x)$. The objects are to be interpreted as critical points of a Morse function on some space. The morphisms of $\mathcal{C}$ are manifolds with corners of dimensions based on the gradings of the objects, and with composition rules based on faces:

- $\mathrm{Mor}(x, x) = \{id\}$.
- For $x, y \in \mathcal{C}$, $\mathrm{Mor}(x, y)$ is a compact $(gr(x) - gr(y) - 1)$-dimensional $\langle gr(x) - gr(y) - 1 \rangle$-manifold (negative dimensional manifolds are considered empty).
- For $gr(x) > gr(z) > gr(y)$, composition gives an embedding

$$\circ : \mathrm{Mor}(z, y) \times \mathrm{Mor}(x, z) \hookrightarrow \partial_{(gr(z) - gr(y))} \mathrm{Mor}(x, y)$$

  such that $\partial_m \mathrm{Mor}(x, y)$ is given as the union of all of these embeddings over all

objects z with $gr(z) - gr(y) = m$.

The morphisms are to be interpreted as the moduli spaces of flow lines of a Morse function from one critical point to another, after modding out by the 'flowing' action of $\mathbb{R}$. Composition is to be interpreted as giving 'broken flow lines' that pass through a mid-level critical point as the boundary of the full moduli space of flows. A *framed flow category* is a flow category $\mathcal{C}$ together with framed embedding data for all of the morphism spaces into a large multi-faced Euclidean manifold with corners (not necessarily just $\mathbb{R}^k_{\geq 0}$) that all fit together with composition coherently in a specific way.

The relation to Khovanov homology here is based on viewing $KC(L)$ via the cube of resolutions. The generators of $KC(L)$ are decorated diagrams sitting at the vertices of the cube. We would like to have a Morse function for the unit cube where the critical points are precisely the vertices, with grading given by the sum of the coordinates of the vertex. Then the morphism spaces will be based on downward flows of this function from one vertex to another, and these will need to be embedded and framed into some cornered Euclidean space to arrive at a cubical framed flow category $\mathcal{C}_C$. This cubical category will then give rise to a Khovanov flow category $\mathcal{C}_K(L)$ where there are multiple objects 'covering' each critical point (vertex) of the cube, corresponding to the generators of $KC(L)$. The morphism spaces will be (trivial) covering spaces (in the usual topological sense) of the morphism spaces of the cube category, allowing the embeddings of the morphism spaces of $\mathcal{C}_C$ to lift naturally and

make $\mathcal{C}_K(L)$ into a framed flow category. From this point, the general construction of Cohen-Segal-Jones [CJS95] produces a spectrum $\mathcal{X}(L)$ whose cochain complex recovers the complex that $\mathcal{C}_K(L)$ is based on, that is, $KC(L)$.

The process outlined above is carried out in [LS14a], specifically in Sections 4 and 5. We will not go into further detail here, except to mention one important facet of the construction. At one point in order to maintain consistency among the various morphism spaces and composition, a choice needs to be made regarding the 1-dimensional moduli spaces (that is, the morphism spaces coming from decorated resolutions that differ in grading by 2, ie connected by two saddle maps). In the case where either order of taking the two saddle maps would result in first co-multiplication Δ, and then multiplication m (illustrated in Figure 2.8), the 1-dimensional moduli space of the cubical $\mathcal{C}_C$ would be a single interval, while the moduli space starting at v_+ and going down to v_- as in Figure 2.8 should involve two intervals, but there is a choice of what the boundary of each interval should correspond to via composition. Lipshitz-Sarkar refer to this choice as a *ladybug matching*, and provide a consistent rule for doing so, and then go on to show that the eventual invariant $\mathcal{X}(L)$ does not depend on this choice (so long as it is kept consistent throughout the construction). This ladybug matching choice can be regarded as the genuinely new piece of combinatorial data to be extracted from the link diagram D_L that is unseen by the 'despectrified' $KC(L)$ alone.

While constructing $\mathcal{X}(L)$ in this way from the diagram D_L, many choices are

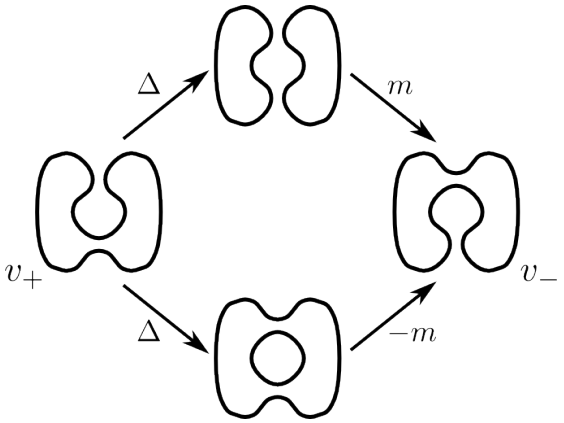

Figure 2.8: A 2-dimensional face of a cube of resolutions illustrating the scenario that requires a choice of ladybug matching. The v_+ term has four choices on how to map down to the v_- term; two choices along the upward path ($\Delta(v_+)$ is a sum of two terms) and likewise two choices along the lower path. The ladybug matching fixes which upward choice corresponds to which downward choice as boundaries of an interval in the 1-dimensional moduli space.

made besides just the ladybug matching and the choice of diagram, including choices of framed embeddings into a (choice of) cornered Euclidean space. The fact that $\mathcal{X}(L)$ is independent of these choices (up to stable homotopy equivalence) is shown in Section 6 of [LS14a].

We end this section with a few simple remarks about the Cohen-Segal-Jones construction as it applies to $\mathcal{C}_K(L)$ and $\mathcal{X}(L)$ specifically. $\mathcal{X}(L)$ is built first as a cell complex, taking a 0-dimensional basepoint, and then adding on one cell per generator (decorated resolution) in the Khovanov chain complex $KC(L)$. The attaching maps for each new cell are based on the framed embeddings of the moduli spaces from the corresponding new object of $\mathcal{C}_K(L)$ to the lower grading objects. The 0-dimensional moduli spaces are single signed points - counting them with sign produces the differential of $KC(L)$, which Defintion 2.2.2 ensures is indeed a sum of maps to different decorated resolutions with coefficient positive or negative 1. Since $KC(L)$ splits over q-degree, this process can also be done one q-degree at a time, ensuring that $\mathcal{X}(L)$ does split as a wedge-sum over q-degree as claimed earlier. Finally, after this cell complex has been constructed, the suspension spectrum is taken (along with possible formal desuspensions to account for proper homological grading) and we have the stable homotopy invariant $\mathcal{X}(L)$.

Chapter 3

SPECTRIFYING THE JONES-WENZL PROJECTOR AND A COLORED LIPSHITZ-SARKAR-KHOVANOV SPECTRUM

The purpose of this chapter is to spectrify the Jones-Wenzl projector P_n and its categorified $\mathbf{P}_n$. Unfortunately, P_n and $\mathbf{P}_n$ are based on TL_n and $\mathbb{TL}_n$ respectively, which are based on tangle diagrams. Since there is no L-S-K spectrum-like invariant for tangles at this time (see Remark 2.3.1), we instead seek to build an L-S-K spectrum for any closed link-like diagram that involves Jones-Wenzl projectors. In particular, this will allow us to build a colored L-S-K spectrum for colored links using the colored diagrams L_γ (see Figure 2.6). In addition, we will prove various properties of our construction that are similar to the axioms of P_n and $\mathbf{P}_n$. Finally, we will also include a small addendum on applying our construction to build an L-S-K spectrum for quantum spin networks.

3.1 Basic Notations and a Key Counting Lemma

We begin with some general notation for use throughout this section.

- $n \in \mathbb{N}$ will always denote a number of strands for various purposes (typically for a given torus braid or, later, for an n-strand cabling of a link diagram).
- Boldface capital letters will refer to braids and/or tangles within a diagram.
- $\mathbf{I}_n$ will denote the identity braid on n strands.
- $\mathbf{T}_n^k$ will denote a torus braid on n strands with k full right-handed (positive) twists (see Equation 2.2.15).
- $\mathbf{T}_n^{-k}$ will denote such a torus braid with k full left-handed (negative) twists.
- $\mathbf{Z}$ will often be used to denote an arbitrary tangle.
- We will use the inner product notation $\langle \mathbf{Z}_1, \mathbf{Z}_2 \rangle$ to indicate connecting two tangles top to top and bottom to bottom. This notation is meant to imitate the inner product in the Temperley-Lieb algebra. See Figure 3.1.
- $\mathbf{Z}^{\cap i}$ will be used to indicate that the i^{th} and $(i+1)^{\text{st}}$ strands at the top of the tangle $\mathbf{Z}$ are being capped off. Similarly, $\mathbf{Z}_{\cup i}$ will indicate capping off the i and $i+1$ strands at the bottom. See Figure 3.1.

In many link diagrams in this manuscript, a single copy of $\mathbf{T}_n^{\pm k}$ will be singled out for consideration, allowing the diagram to be viewed as $\left\langle \mathbf{T}_n^{\pm k}, \mathbf{Z} \right\rangle$ for some tangle $\mathbf{Z}$

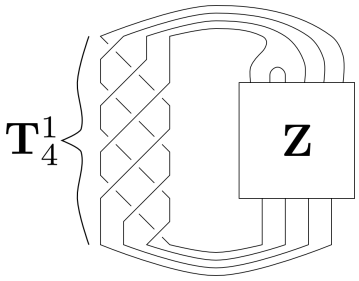

Figure 3.1: The diagram $\langle \mathbf{T}_4^1, \mathbf{Z}^{\cap 2} \rangle$. $\mathbf{T}_4^1$ indicates the full right-handed twist on 4 strands, and $\mathbf{Z}$ is some fixed $(6,4)$-tangle. The $\cap 2$ indicates a cap on the 2nd and 3rd strands above $\mathbf{Z}$.

(similar to Figure 3.1, but without the cap). In these situations, we will also view the normalization shifts of Equations 2.2.11 and 2.2.12 as split into contributions based on the $\mathbf{T}_n$ and the $\mathbf{Z}$ as in the following definition.

Definition 3.1.1. *In a link diagram L viewed as $L = \left\langle \mathbf{T}_n^{\pm k}, \mathbf{Z} \right\rangle$ as above, the symbol τ will be used to denote the q-normalization shift $n^+ - 2n^-$ counting only crossings within* one full twist *of the n strands (that is, within $\mathbf{T}_n^{\pm 1}$). Similarly, the symbol η will be used to denote the homological normalization shift n^- counting only crossings within* one full twist*. The symbol $N_{\mathbf{Z}}$ will be used to denote the q-normalization shift $n^+ - 2n^-$ counting only crossings within the tangle $\mathbf{Z}$. More generally, N_D will denote the shift $n^+ - 2n^-$ counting crossings within a diagram D (whether tangle or otherwise).*

We will have no need for the homological normalization shift n^- counting only crossings in $\mathbf{Z}$.

Remark 3.1.1. *Notice that these shifts τ, η and $N_{\mathbf{Z}}$ depend on the orientation of the strands, and allowable orientations are affected by the* full link diagram involved*, not just the piece being counted. In Figure 3.1 for example, the value of τ depends heavily on the tangle $\mathbf{Z}$, despite the fact that it only counts crossings within the $\mathbf{T}_4^1$. In cases where the tangle $\mathbf{Z}$ is changing, subscripts will be attached to the symbol τ as necessary to indicate which full diagram is being considered. Similarly, if there are multiple $\mathbf{T}_{n_i}$ to consider within some single link diagram, the subscript i will be used for the shifts τ_i and η_i to indicate which twist is being considered.*

In order to illustrate these notations, we prove the following very simple observation about full twists that indicates why they are preferable to work with (as opposed to the fractional twists that will be used later in Chapter 5).

Lemma 3.1.2. *For any (n,n)-tangle $\mathbf{Z}$, consider the diagram $D(k) := \left\langle \mathbf{T}_n^k, \mathbf{Z} \right\rangle$. Then all of the $D(k)$ are links with the same number of strands, which can be oriented equivalently for all k. Thus $N_{D(k)} = k\tau + N_{\mathbf{Z}}$ with $N_{\mathbf{Z}}$ and τ independent of k (in particular, $N_{\mathbf{Z}}$ can be determined by the diagram $D(0) = \langle \mathbf{I}, \mathbf{Z} \rangle$). Similarly for such a diagram, η is also independent of k.*

Proof. In a full twist, any strand takes the i^{th} point at the top to the i^{th} point on the bottom, so for the purposes of counting and orienting the strands, this is equivalent to the identity braid $\mathbf{I}$. The orientations of the strands are all that matters for calculating $N_{\mathbf{Z}}$, and also for calculating τ and η. Since τ counts positive and negative crossings for one full twist, k full twists will contribute $k\tau$. □

Remark 3.1.2. *The previous observation was written and notated for positive full twists, but it is clear that the exact same argument holds for negative full twists as well. This will be typical of several of the arguments later in this section.*

We conclude this section with the key counting lemma which is used essentially throughout the manuscript. This lemma can be viewed as a generalization of Marko Stošić's Lemma 1 in [Sto07].

Lemma 3.1.3. *Fix $n \geq 2$ in $\mathbb{N}$. Then for any $i \in \{1, 2, \ldots, n-1\}$ and for any $(n-2, n)$-tangle $\mathbf{Z}$, consider the link diagram $D_{\pm} = \left\langle (\mathbf{T}_n^{\pm k})^{\cap i}, \mathbf{Z} \right\rangle$. That is, consider any closure of $\mathbf{T}_n^{\pm k}$ involving at least one turnback at the top. Then for any chosen orientation of the strands we have:*

- *This link diagram is isotopic to $D'_{\pm} = \left\langle \mathbf{T}_{n-2}^{\pm k}, \mathbf{Z}_{\cup n-i} \right\rangle$*
- *Letting $\tau_{\pm}$ count $n^+ - 2n^-$ for crossings from $\mathbf{T}_n$ in $D_{\pm}$ and letting $\tau'_{\pm}$ count this shift for crossings from $\mathbf{T}_{n-2}$ in $D'_{\pm}$, we have*

$$\tau'_+ = \tau_+ + 2n \tag{3.1.1}$$

$$\tau'_- = \tau_- + 2n - 6 \tag{3.1.2}$$

Proof. We pull the turnback through the full twists, which corresponds to pulling out two 'parallel' strands wrapping around the cylinder defining the torus braid. As in Lemma 3.1.2, using full twists ensures that the turnback 'exits' the torus braid at the same two points that it entered, which swing around to give the $(n-i)^{\text{th}}$ and

$(n-i+1)^{\text{st}}$ points at the bottom of $\mathbf{Z}$. This leaves us with $n-2$ strands for the torus braid, still with the same amount of twisting. See Figure 3.2. This proves the first point.

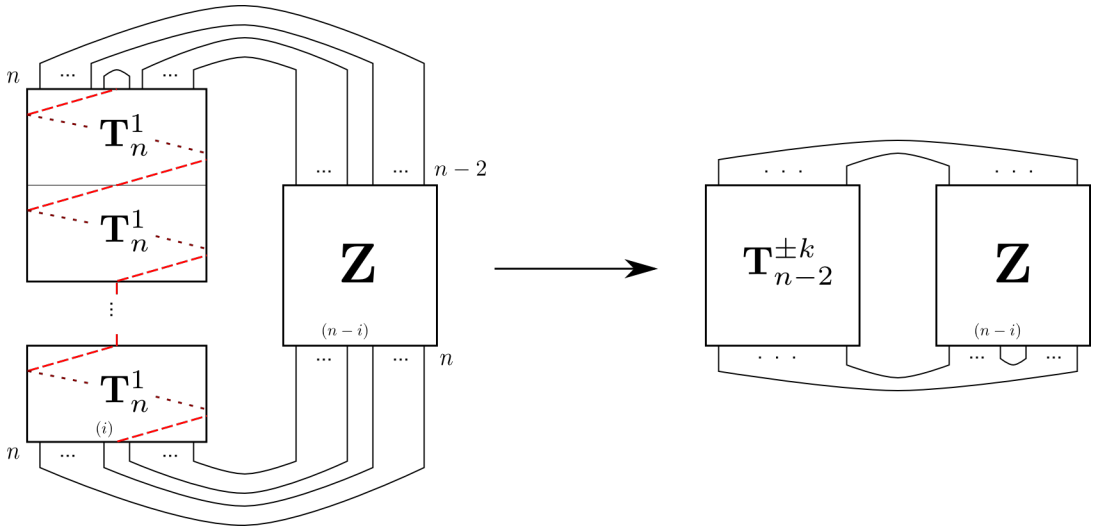

Figure 3.2: The diagram $\left\langle (\mathbf{T}_n^{\pm k})^{\cap i}, \mathbf{Z} \right\rangle$ with the $\mathbf{T}_n^{\pm k}$ drawn as separate $\mathbf{T}_n^1$'s. The cap is pulled through the twists as shown (the dashed red line would be for $+k$; the opposite direction would be taken for $-k$). The n and $n-2$ show the number of strands entering and exiting at various points. The (i) at the bottom of the twisting indicates the i^{th} strand counted from the left, and similarly for the $(n-i)$ at the bottom of $\mathbf{Z}$.

To prove the second point, we first note that the total number of crossings in a full twist on n strands is $n(n-1)$, while the total number for a full twist on $n-2$ strands is $(n-2)(n-3)$. This means that when pulling the turnback through, we managed to eliminate $4n-6$ crossings. One full twist of these two strands corresponds

to two Reidemeister 1 moves; the other $4n-8$ eliminations all must have come from Reidemeister 2 moves. Regardless of the type of twist and the orientation of the strands, all of these Reidemeister 2 moves would have eliminated one positive and one negative crossing each. The two Reidemeister 1 moves would have eliminated negative crossings from a positive twist, or eliminated positive crossings from a negative twist. Again, this is independent of the orientation of the strands. Calculating the effect of these eliminations on the normalization $n^+ - 2n^-$ gives the result. □

Remark 3.1.3. *There is no difference in having the turnback at the bottom of the* $\mathbf{T}_n^{\pm k}$*. The proof makes it clear that it ends up at the top of the* $\mathbf{Z}$ *in that case.*

3.2 Proving Theorem 1.0.2

Let D denote a link diagram involving a finite number of Jones-Wenzl projectors. More precisely, D is obtained from a link diagram by formally replacing a finite number of identity braids $\mathbf{I}_{n_i}$ with Jones-Wenzl projectors P_{n_i}. (Figure 1.3 in the introduction provides clarification). We would like to define $\mathcal{X}^j(D)$ as the homotopy colimit of a sequence of spectra of finite link diagrams that stabilizes as the twisting in the diagram goes to infinity. To do this we focus on a single projector at a time. Towards that end, we combine Lemmas 2.3.7 and 3.1.2 to establish the following two sequences.

Proposition 3.2.1. *Fix* $n \in \mathbb{N}$ *and* $j \in \mathbb{Z}$*. Let* $\mathbf{Z}$ *be an arbitrary* (n,n)*-tangle. Then*

the maps of Lemma 2.3.7 provide the following two sequences (one for right-handed twists, one for left-handed twists):

$$\mathcal{X}^{j+N_{\mathbf{Z}}}\left(\left\langle \mathbf{T}_n^0, \mathbf{Z}\right\rangle\right) \hookrightarrow \Sigma^{\eta}\mathcal{X}^{j+N_{\mathbf{Z}}+\tau}\left(\left\langle \mathbf{T}_n^1, \mathbf{Z}\right\rangle\right) \hookrightarrow \cdots \hookrightarrow \Sigma^{k\eta}\mathcal{X}^{j+N_{\mathbf{Z}}+k\tau}\left(\left\langle \mathbf{T}_n^k, \mathbf{Z}\right\rangle\right) \hookrightarrow \cdots \tag{3.2.1}$$

$$\mathcal{X}^{j+N_{\mathbf{Z}}}\left(\left\langle \mathbf{T}_n^0, \mathbf{Z}\right\rangle\right) \twoheadleftarrow \cdots \twoheadleftarrow \Sigma^{k(\eta-n(n-1))}\mathcal{X}^{j+N_{\mathbf{Z}}+k\tau+kn(n-1)}\left(\left\langle \mathbf{T}_n^{-k}, \mathbf{Z}\right\rangle\right) \twoheadleftarrow \cdots \tag{3.2.2}$$

where the symbols η, τ, and $N_{\mathbf{Z}}$ are as defined in Definition 3.1.1.

Proof. To build the right-handed sequence (3.2.1), we 'start' with the $(k+1)^{\text{st}}$ term and resolve crossings within one of the full twists one at a time until we reach the k^{th} term. Specifically, we consider the diagram $\left\langle \mathbf{T}_n^{k+1}, \mathbf{Z}\right\rangle = \left\langle \mathbf{T}_n^k, \mathbf{T}_n^1 \cdot \mathbf{Z}\right\rangle$ where we use the product notation to indicate concatenation (see Figure 3.3). We number the crossings of the $\mathbf{T}_n^1$ sitting above $\mathbf{Z}$ starting from the 'topmost' such crossing. Then each inclusion in (3.2.1) will be defined as the composition of $n(n-1)$ inclusions coming from (2.3.2) by resolving these numbered crossings as 0-resolutions in this order (note that the all-zero resolution of $\mathbf{T}_n^1$ is precisely $\mathbf{I}_n$).

We now introduce some notation to help keep track of this process. Let $\mathbf{D}_0 := \mathbf{T}_n^1 \cdot \mathbf{Z}$. Then for each $i = 1, 2, \ldots, n(n-1)$, let $\mathbf{D}_i$ denote the diagram obtained from $\mathbf{D}_{i-1}$ by resolving the i^{th} crossing with a 0-resolution, and let $\mathbf{E}_i$ denote the diagram obtained from $\mathbf{D}_{i-1}$ (*not* from $\mathbf{E}_{i-1}$; this will change for the left-handed sequence) by resolving the i^{th} crossing with a 1-resolution. Thus $\mathbf{D}_i$ will have all crossings up to the i^{th} resolved as 0-resolutions, while $\mathbf{E}_i$ will have all crossings up to the $(i-1)^{\text{st}}$

resolved as 0-resolutions, but the i^{th} as a 1-resolution. This arrangement allows us to see, at each step i, the cofibration sequence (ignoring the homological shifts)

$$\begin{array}{ccc} \mathcal{X}^{j+N_{\mathbf{D}_i}+k\tau_{\mathbf{D}_i}}\left(\left\langle \mathbf{T}_n^k, \mathbf{D}_i \right\rangle\right) & \hookrightarrow & \mathcal{X}^{j+N_{\mathbf{D}_{i-1}}+k\tau_{\mathbf{D}_{i-1}}}\left(\left\langle \mathbf{T}_n^k, \mathbf{D}_{i-1} \right\rangle\right) \\ & & \downarrow \\ & & \mathcal{X}^{j+N_{\mathbf{E}_i}+k\tau_{\mathbf{E}_i}-1}\left(\left\langle \mathbf{T}_n^k, \mathbf{E}_i \right\rangle\right). \end{array} \tag{3.2.3}$$

For further clarification, see Figure 3.3. Notice the subscripts on the τ terms - the orientations (and thus positive/negative crossing information) of the strands within $\mathbf{T}_n^k$ may change when resolving crossings (see Remark 3.1.1). However, we also know from Lemma 3.1.2 that all of the τ_* terms and N_* terms are *independent of* k. The final term $\mathbf{D}_{n(n-1)}$ is precisely $\mathbf{Z}$, so Lemma 3.1.2 allows the τ and $N_{\mathbf{Z}}$ terms to be preserved as indicated in the sequence (3.2.1). The suspensions giving the homological shifts are clear: we are counting the number of negative crossings introduced in a new twist.

The left-handed sequence (3.2.2) is built using compositions of the surjections of the cofibration sequence (2.3.2), since the left-handed twist $\mathbf{T}_n^{-1}$ needs an all-one resolution to give the identity braid $\mathbf{I}_n$. For this reason, the roles of the $\mathbf{D}_i$ and $\mathbf{E}_i$ are swapped, and their definitions change slightly. To prevent confusion, we use new names $\mathbf{F}_i$ and $\mathbf{G}_i$ and define $\mathbf{G}_0 := \mathbf{T}_n^{-1} \cdot \mathbf{Z}$, and let $\mathbf{G}_i$ denote the diagram obtained from $\mathbf{G}_{i-1}$ by resolving the i^{th} crossing with a 1-resolution, and let $\mathbf{F}_i$ denote the diagram obtained from $\mathbf{G}_{i-1}$ by resolving the i^{th} crossing with a 0-resolution. Pictorially the $\mathbf{G}_i$ match the $\mathbf{D}_i$ from above, and the $\mathbf{F}_i$ match the $\mathbf{E}_i$,

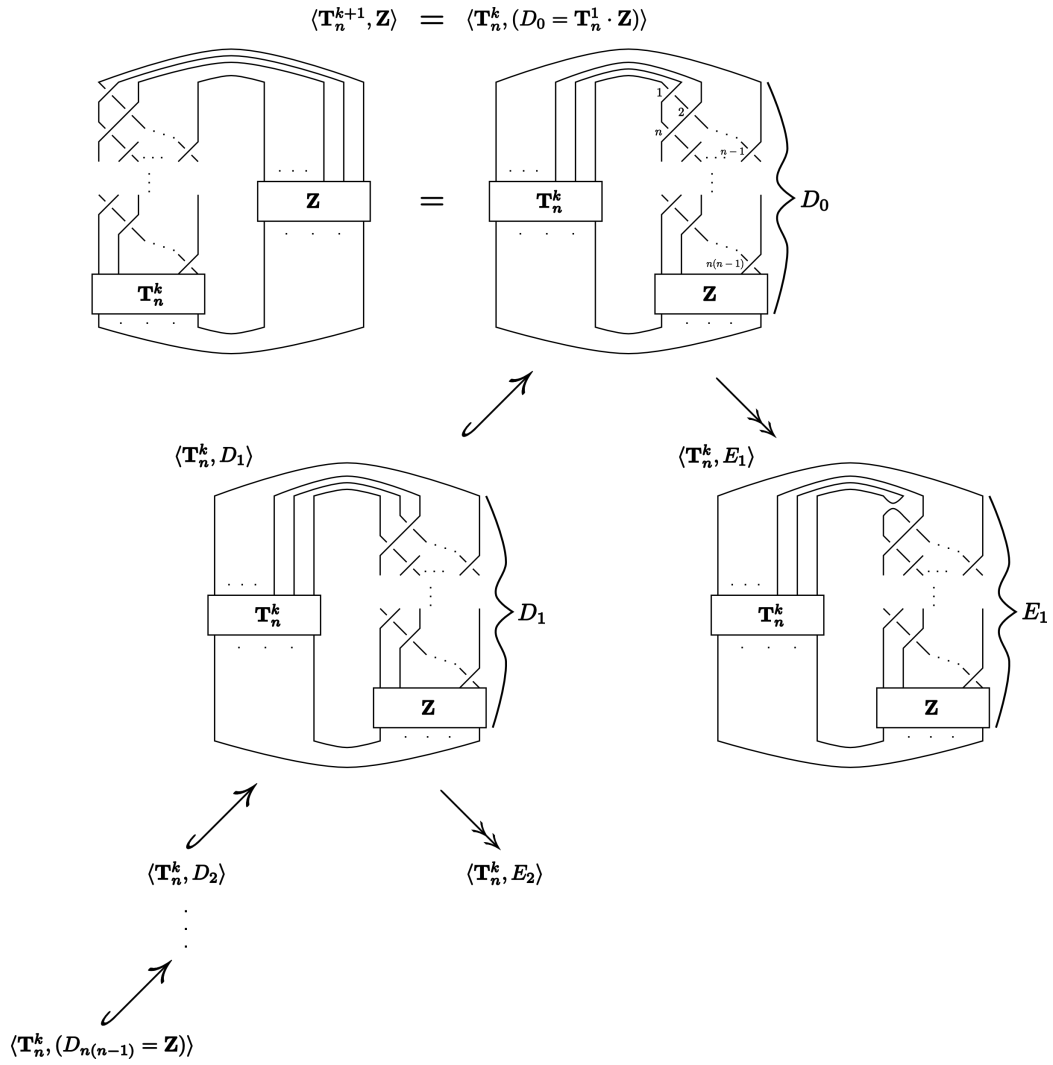

Figure 3.3: Building a single map in the sequence (3.2.1) as a composition of inclusions coming from resolving crossings as in Lemma 2.3.7. The numbering on the crossings in the diagram $\langle \mathbf{T}_n^k, D_0 \rangle$ indicates the order in which we resolve crossings. D_1 and E_1 are illustrated as well, with the first crossing resolved. Note that E_2 is obtained from D_1, not from E_1. Thus any E_i will have precisely one cup/cap.

but in the cofibration sequences we see (again ignoring homological shifts)

$$\begin{aligned}
&\mathcal{X}^{j+(k+1)n(n-1)-(i-1)+N_{\mathbf{F}_i}+k\tau_{\mathbf{F}_i}}\left(\left\langle \mathbf{T}_n^{-k}, \mathbf{F}_i \right\rangle\right) \\
&\qquad \hookrightarrow \mathcal{X}^{j+(k+1)n(n-1)-(i-1)+N_{\mathbf{G}_{i-1}}+k\tau_{\mathbf{G}_{i-1}}}\left(\left\langle \mathbf{T}_n^{-k}, \mathbf{G}_{i-1} \right\rangle\right) \qquad (3.2.4) \\
&\qquad\qquad \twoheadrightarrow \mathcal{X}^{j+(k+1)n(n-1)-i+N_{\mathbf{G}_i}+k\tau_{\mathbf{G}_i}}\left(\left\langle \mathbf{T}_n^{-k}, \mathbf{G}_i \right\rangle\right).
\end{aligned}$$

Notice the extra shifts of $i-1$ and i, which occur because we have been 'losing' 1-resolutions along the way. We can see that, once $i = n(n-1)$, we arrive at $j+kn(n-1)$ together with the normalization terms, as desired for $\left\langle \mathbf{T}_n^{-k}, \mathbf{Z} \right\rangle$ in sequence (3.2.2). We use Lemma 3.1.2 in the same way to guarantee that the $N_{\mathbf{Z}}$ and τ terms don't change, and we also see the extra homological shift due to losing 1-resolutions as we go. □

Proposition 3.2.2. *Fix $j \in \mathbb{Z}$ and $n \geq 2$ in $\mathbb{N}$. Then for any (n,n)-tangle $\mathbf{Z}$, both sequences (3.2.1) and (3.2.2) stabilize. That is, there exist bounds b^+ and b^- such that, for $k \geq b^+$, the maps in (3.2.1) are all stable homotopy equivalences, and similarly for $k \geq b^-$ for the maps in (3.2.2). Furthermore, b^+ depends only on j and the all-zero resolution of $\mathbf{Z}$, while b^- depends on j, the number of crossings in $\mathbf{Z}$, and the all-one resolution of $\mathbf{Z}$.*

Proof. We will prove the stabilization of the two sequences separately to highlight the slight differences between the two. The notations $\mathbf{D}_i$, $\mathbf{E}_i$, $\mathbf{F}_i$ and $\mathbf{G}_i$ introduced in the previous proof will be used throughout.

Focusing first on the right-handed case, we consider the cofibration sequences (3.2.3). According to Lemma 2.3.7, as long as all of the Khovanov chain complexes

$KC^{j+N_{\mathbf{E}_i}+k\tau_{\mathbf{E}_i}-1}\left(\left\langle \mathbf{T}_n^k, \mathbf{E}_i\right\rangle\right)$ are acyclic, the inclusions in Equation 3.2.3 will be stable homotopy equivalences for all $i = 1, \ldots, n(n-1)$, allowing us to conclude that their composition (which is the map in the sequence (3.2.1)) is as well. Let $\min_q(\cdot)$ be the minimal q-degree of non-zero Khovanov homology for a link diagram. Our goal now is to find a bound b^+ so that, for all $i = 1, \ldots, n(n-1)$,

$$j + N_{\mathbf{E}_i} + k\tau_{\mathbf{E}_i} - 1 < \min_q\left(\left\langle \mathbf{T}_n^k, \mathbf{E}_i\right\rangle\right) \qquad \text{for all } k \geq b^+. \tag{3.2.5}$$

Figure 3.4 illustrates the key point of the proof. The diagram $\left\langle \mathbf{T}_n^k, \mathbf{E}_i\right\rangle$ has a turnback at the 'top' of E_i that can be swung around and 'pulled through' the twisting $\mathbf{T}_n^k$ and then back around to the bottom of E_i, just as in Lemma 3.1.3. Let E_i' denote the resulting tangle, so that we have $\left\langle \mathbf{T}_n^k, \mathbf{E}_i\right\rangle$ isotopic to $\left\langle \mathbf{T}_{n-2}^k, \mathbf{E}_i'\right\rangle$. Since Khovanov homology is an isotopy invariant, we must have

$$\min_q\left(\left\langle \mathbf{T}_n^k, \mathbf{E}_i\right\rangle\right) = \min_q\left(\left\langle \mathbf{T}_{n-2}^k, \mathbf{E}_i'\right\rangle\right). \tag{3.2.6}$$

Now the minimal q-degree of non-zero Khovanov homology for a diagram is bounded below by the minimal possible q-degree in the entire Khovanov chain complex, which occurs in the all-zero resolution by decorating all of the circles with v_-. The all-zero resolution of the crossings coming from $\mathbf{T}$'s give identity braids, and so we have

$$\min_q\left(\left\langle \mathbf{T}_{n-2}^k, \mathbf{E}_i'\right\rangle\right) \geq -\#\text{circ}\left(\left\langle \mathbf{I}_{n-2}, \mathbf{Z}_{\cup\iota,\text{all-zero}}^{\cap\iota}\right\rangle\right) + k\tau'_{\mathbf{E}_i'} + N_{\mathbf{E}_i'}. \tag{3.2.7}$$

Here $\#\text{circ}(\cdot)$ indicates the number of circles present in the planar diagram, while $\iota := i \mod (n-1)$. The "all-zero" subscript indicates that all of the crossings in

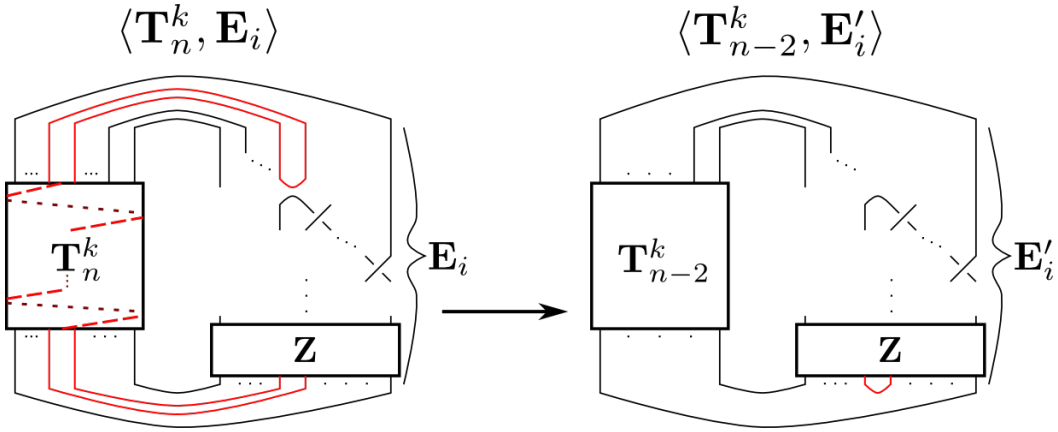

Figure 3.4: Pulling the turnback in $\langle \mathbf{T}_n^k, \mathbf{E}_i \rangle$ through the twists to get $\langle \mathbf{T}_{n-2}^k, \mathbf{E}'_i \rangle$. The turnback and its path are indicated in red. Note that none of the crossings in $\mathbf{E_i}$ (including $\mathbf{Z}$) are affected.

$\mathbf{Z}_{\cup\iota}^{\cap\iota}$ have been resolved into zero-resolutions. The τ' term and the N term are the $n^+ - 2n^-$ normalization terms as usual. The τ' indicates that we are counting positive and negative crossings from $\mathbf{T}_{n-2}$ as opposed to τ that was counting such crossings in $\mathbf{T}_n$ (see the notation used in Lemma 3.1.3).

Now because we performed an isotopy to get from $\mathbf{E}_i$ to $\mathbf{E}'_i$, the orientations of the strands did not change. Furthermore, no crossings were added to or removed from $\mathbf{E}_i$. Thus $N_{\mathbf{E}_i} = N_{\mathbf{E}'_i}$, and $\tau'_{\mathbf{E}'_i}$ can be viewed as $\tau'_{\mathbf{E}_i}$. We then use Equation 3.1.1 from Lemma 3.1.3 to deduce

$$\min_q \left(\left\langle \mathbf{T}_{n-2}^k, \mathbf{E}'_i \right\rangle \right) \geq -\#\text{circ} \left(\left\langle \mathbf{I}_{n-2}, \mathbf{Z}_{\cup\iota,\text{all-zero}}^{\cap\iota} \right\rangle \right) + k(\tau_{\mathbf{E}_i} + 2n) + N_{\mathbf{E}_i}. \tag{3.2.8}$$

Combining Equations 3.2.5, 3.2.6, and 3.2.8 gives us the following new goal for our

bound b^+:

$$j + N_{\mathbf{E}_i} + k\tau_{\mathbf{E}_i} - 1 < -\#\text{circ}\left(\left\langle \mathbf{I}_{n-2}, \mathbf{Z}^{\cap\iota}_{\cup\iota,\text{all-zero}} \right\rangle\right) + k(\tau_{\mathbf{E}_i} + 2n) + N_{\mathbf{E}_i} \quad \text{for all } k \geq b^+ \tag{3.2.9}$$

which is clearly satisfied for all i by choosing

$$b^+ := \max_{\iota=1,\ldots,n-1} \frac{j + \#\text{circ}\left(\left\langle \mathbf{I}_{n-2}, \mathbf{Z}^{\cap\iota}_{\cup\iota,\text{all-zero}} \right\rangle\right)}{2n}. \tag{3.2.10}$$

We see clearly from the definition of b^+ that it depends only on j and the all-zero resolution of $\mathbf{Z}$, as claimed. The final homological shift is clear.

We now turn to the left-handed sequence (3.2.2). The strategy is very similar so we will be brief. This time we consider the cofibration sequence (3.2.4) where our goal is to bound k to ensure that all of the $KC^{j-(i-1)+N_{\mathbf{F}_i}+k\tau_{\mathbf{F}_i}}\left(\left\langle \mathbf{T}^{-k}_n, \mathbf{F}_i \right\rangle\right)$ are acyclic, ensuring that the surjections give stable homotopy equivalences.

Since the $\mathbf{F}_i$ pictorially match the $\mathbf{E}_i$ from before, we can still use Lemma 3.1.3 in the same way to arrive at $\left\langle \mathbf{T}^{-k}_{n-2}, \mathbf{F}'_i \right\rangle$ with corresponding τ'. Now comes the main difference between the left- and right-handed sequences. For the right-handed twist, the all-zero resolution of $\mathbf{T}^k_{n-2}$ is just $\mathbf{I}_n$; in particular, it is independent of k. Taking 0-resolutions motivates bounding based on the minimal q-degree. But for the left-handed twist, it is the all-one resolution of $\mathbf{T}^{-k}_n$ that is just $\mathbf{I}_n$. Taking 1-resolutions motivates bounding based on the maximal q-degree. So we define $\max_q(\cdot)$ to be the maximal q-degree of non-zero Khovanov homology for a given diagram, which is bounded above by the maximal q-degree for the full Khovanov chain complex.

Following the logic of the right-handed case, we get

$$\begin{aligned}
\max_q\left(\left\langle \mathbf{T}_n^{-k}, \mathbf{F}_i\right\rangle\right) &= \max_q\left(\left\langle \mathbf{T}_{n-2}^{-k}, \mathbf{F}_i'\right\rangle\right) \\
&\leq \#\text{cros}\left(\left\langle \mathbf{T}_{n-2}^{-k}, \mathbf{F}_i'\right\rangle\right) + \#\text{circ}\left(\left\langle \mathbf{I}_{n-2}, \mathbf{Z}^{\cap\iota}_{\cup\iota,\text{all-one}}\right\rangle\right) + k(\tau'_{\mathbf{F}_i'}) + N_{\mathbf{F}_i} \\
&= (k(n-2)(n-3) + (n(n-1)-i) + \#\text{cros}(\mathbf{Z})) \\
&\quad + \#\text{circ}\left(\left\langle \mathbf{I}_{n-2}, \mathbf{Z}^{\cap\iota}_{\cup\iota,\text{all-one}}\right\rangle\right) + k(\tau_{\mathbf{F}_i} + 2n - 6) + N_{\mathbf{F}_i} \\
&= k(n^2 - 3n + \tau_{\mathbf{F}_i}) + (n(n-1)-i) + \#\text{cros}(\mathbf{Z}) \\
&\quad + \#\text{circ}\left(\left\langle \mathbf{I}_{n-2}, \mathbf{Z}^{\cap\iota}_{\cup\iota,\text{all-one}}\right\rangle\right) + N_{\mathbf{F}_i}.
\end{aligned}$$

The $\#\text{cros}(\cdot)$ denotes the total number of crossings. This term appears because the q-degree counts the number of 1-resolutions taken (which will be all of the crossings). The third line breaks this term into several self-explanatory pieces; the $n(n-1)-i$ term handles the crossings 'above' the $\mathbf{Z}$ (See Figure 3.4). Meanwhile, the changing of τ' to $\tau + 2n - 6$ in the third line follows from the left-handed version of Lemma 3.1.3.

From the cofibration (3.2.4) above, we see that our goal for the left-handed twists is to ensure that, for all $i = 1, \ldots, n(n-1)$, and for all $k \geq b^-$,

$$\begin{aligned}
&j + (k+1)n(n-1) - (i-1) + N_{\mathbf{F}_i} + k\tau_{\mathbf{F}_i} > \\
&\quad k(n^2 - 3n + \tau_{\mathbf{F}_i}) + (n(n-1)-i) + \#\text{cros}(\mathbf{Z}) + \#\text{circ}\left(\left\langle \mathbf{I}_{n-2}, \mathbf{Z}^{\cap\iota}_{\cup\iota,\text{all-one}}\right\rangle\right) + N_{\mathbf{F}_i}.
\end{aligned}$$

This is clearly achieved by setting

$$b^- := \max_{\iota=1,\ldots,n-1} \frac{-j + \#\text{cros}(\mathbf{Z}) + \#\text{circ}\left(\left\langle \mathbf{I}_{n-2}, \mathbf{Z}^{\cap\iota}_{\cup\iota,\text{all-one}}\right\rangle\right)}{2n} \tag{3.2.11}$$

which clearly depends only on j, the number of crossings in $\mathbf{Z}$, and the all-one resolution of $\mathbf{Z}$ as desired. $\square$

Remark 3.2.1. *Notice the similarity between the bounds b^+ and b^-. In both cases, the bound involves $\frac{\pm j}{2n}$ plus a constant term (independent of j). Thus all of the careful tracking of normalization shifts 'cancel out' in precisely the same way regardless of using right- or left-handed twists. The sign change of j versus $-j$ also makes sense when we recall that the graded Euler characteristic of these spaces is meant to give a power series expansion of the corresponding rational functions coming from the Jones-Wenzl projectors, in q for right-handed twists (so using positive j terms) and in q^{-1} for left-handed twists (so using negative j terms). With this in mind, the only real difference between b^+ and b^- comes from the use of the all-zero resolution of D versus the all-one resolution, and the need to count crossings away from the left-handed twists.*

We are now ready to prove Theorem 1.0.2. Let D denote a diagram obtained from a link diagram by formally replacing a finite number of identity braids $\mathbf{I}_{n_i}$ with Jones-Wenzl projectors P_{n_i}. Let $m \in \mathbb{N}$ denote the total number of projectors in D. For any $(k_1, \ldots, k_m) \in (\mathbb{N} \cup 0)^m$, let $D^{\pm}(k_1, \ldots, k_m)$ denote the diagram D with each P_{n_i} replaced by $T_{n_i}^{\pm k_i}$. Note that it is very important that the diagrams have either all right-handed twists, or all left-handed twists. We do not allow any mixing of the two.

We focus on the right-handed case first. Fixing $j \in \mathbb{Z}$, we consider the infinite

m-dimensional cube of maps built as follows. The vertices of the cube correspond to $(k_1, \ldots, k_m) \in (\mathbb{N} \cup 0)^m$. At each such vertex we place the space

$$\mathcal{X}_+^{j+N_D}(k_1, \ldots, k_m) := \Sigma^{\sum_{i=1}^m k_i \eta_i} \mathcal{X}^{j+N_D+\sum_{i=1}^m k_i \tau_i}(D(k_1, \ldots, k_m)). \tag{3.2.12}$$

Here, the subscripts on the normalization shifts τ and η indicate which $\mathbf{T}_{n_i}$ is being referred to (see Definition 3.1.1 and Remark 3.1.1). Meanwhile, the N_D is referring to the normalization shift $n^+ - 2n^-$ for all crossings totally separate from any of the inserted twists (ie, crossings present in the original diagram D, discounting the Jones-Wenzl projectors). Now between any two adjacent vertices of $(\mathbb{N} \cup 0)^m$, we see all of the k_i remain constant except one of them, say $k_{\hat{i}}$, which differs by one between the two vertices. To this edge we assign the map

$$\mathcal{X}_+^{j+N_D}(k_1, \ldots, k_{\hat{i}}, \ldots, k_m) \hookrightarrow \mathcal{X}_+^{j+N_D}(k_1, \ldots, k_{\hat{i}} + 1, \ldots, k_m) \tag{3.2.13}$$

induced by Lemma 2.3.7 as in Proposition 3.2.1.

Definition 3.2.3. *Given a diagram D involving Jones-Wenzl projectors, the* (right-handed) L-S-K spectrum of D *is defined to be the wedge sum $\mathcal{X}_+(D) := \bigvee_{j \in \mathbf{Z}} \mathcal{X}_+^{j+N_D}(D)$ where for each q-degree $j + N_D$, the spectrum $\mathcal{X}_+^{j+N_D}(D)$ is defined to be the homotopy colimit of the cube of maps described by Equations 3.2.12 and 3.2.13.*

Proof of Theorem 1.0.2 (Right-handed Case). We wish to show that the cube of maps defining $\mathcal{X}_+^{j+N_D}(D)$ 'stabilizes' in a particular sense. To do this we isolate a single projector $P_{n_{\hat{i}}}$ and fix all of the $k_{i \neq \hat{i}}$. This allows us to view the maps (3.2.13) as

(ignoring homological shifts)

$$\mathcal{X}^{j+k_{\hat{i}}\tau_{\hat{i}}+N_D+\sum_{i\neq\hat{i}}k_i\tau_i}\left(\left\langle \mathbf{T}^{k_{\hat{i}}}_{n_{\hat{i}}}, \mathbf{Z}\right\rangle\right) \hookrightarrow \mathcal{X}^{j+(k_{\hat{i}}+1)\tau_{\hat{i}}+N_D+\sum_{i\neq\hat{i}}k_i\tau_i}\left(\left\langle \mathbf{T}^{k_{\hat{i}}+1}_{n_{\hat{i}}}, \mathbf{Z}\right\rangle\right) \quad (3.2.14)$$

where the tangle $\mathbf{Z}$ includes all of the other $\mathbf{T}^{k_i}_{n_i}$. Having fixed j, these maps are all stable homotopy equivalences for $k_{\hat{i}} > b^+_{\hat{i}}$ for some bound $b^+_{\hat{i}}$ that depends only on the all-zero resolution of $\mathbf{Z}$. Since the all-zero resolution of any $\mathbf{T}^{k_i}_{n_i}$ is just $\mathbf{I}_{n_i}$ regardless of k_i, this bound $b^+_{\hat{i}}$ is *independent of the other* k_i (this is the point that requires we do not mix right- and left-handed twists in our construction). Thus we can find the various bounds b^+_i one projector at a time effectively ignoring the rest. Since there are only finitely many projectors, we can find a global bound b^+ which works for all of the k_i at once and declare that the cube is stable for all $k_i > b^+$. This also allows us to use a simpler notation: let $D(k) := D(k, \ldots, k)$, and similarly for $\mathcal{X}^{j+N_D}_+(k) = \mathcal{X}^{j+N_D}_+(k, \ldots, k)$. Our proof then shows that, for any fixed $j \in \mathbf{Z}$, the 'diagonal sequence' $\mathcal{X}^{j+N(D)}_+(k)$ stabilizes as $k \to \infty$, and so the hocolim $\mathcal{X}^{j+N_D}_+(D) \simeq \mathcal{X}^{j+N_D}_+(k)$ for some large enough k depending on j. Since the chain complexes of the twists are known to stabilize to the categorified Jones-Wenzl projectors, the wedge sum $\mathcal{X}_+(D) = \bigvee_{j\in\mathbf{Z}} \mathcal{X}^{j+N_D}_+(D)$ satisfies the requirements of Theorem 1.0.2. □

The left-handed twists work in exactly the same fashion, so we only mention the slight differences. We populate the vertices of the cube by spaces

$$\mathcal{X}^{j+N_D}_-(k_1, \ldots, k_m) := \Sigma^a \mathcal{X}^{j+\sum_{i=1}^m k_i n_i(n_i-1)+N_D+\sum_{i=1}^m k_i\tau_i}(D(k_1, \ldots, k_m)) \quad (3.2.15)$$

where $a := \sum_{i=1}^{m} k_i(\eta_i - n_i(n_i-1))$ gives the homological shift. The edges of the cube are maps

$$\mathcal{X}_-^{j+N(D)}(k_1,\ldots,k_{\hat{i}},\ldots,k_m) \leftarrow \mathcal{X}_-^{j+N_D}(k_1,\ldots,k_i+1,\ldots,k_m) \tag{3.2.16}$$

induced by Lemma 2.3.7 once again. Notice the extra grading shift $\sum_{i=1}^{m} k_i n_i(n_i-1)$, which counts the number of crossings available in all of the $\mathbf{T}_{n_i}^{-k_i}$.

Definition 3.2.4. *Given a diagram D involving Jones-Wenzl projectors, the* (left-handed) L-S-K spectrum of D *is defined to be the wedge sum $\mathcal{X}_-(D) := \bigvee_{j\in\mathbf{Z}} \mathcal{X}_-^{j+N_D}(D)$ where for each q-degree $j+N_D$, the spectrum $\mathcal{X}_-^{j+N_D}(D)$ is defined to be the homotopy limit of the cube of maps described by Equations 3.2.15 and 3.2.16.*

Proof of Theorem 1.0.2 (Left-handed Case). Focusing on one projector $(\hat{i})$ at a time as before, the formula (3.2.11) for $b_{\hat{i}}^-$ does appear to depend on the other k_i since the term $\#\mathrm{cros}(\mathbf{Z})$ will count crossings in the other twists. However, this count is cancelled out precisely by the extra grading shift $\sum_{i=1}^{m} k_i n_i(n_i-1)$, and the bounds b_i^- are again mutually independent allowing the same argument as for the right-handed case to go through. The details here are left to the reader. □

Thus we have two equally eligible candidates, $\mathcal{X}_+(D)$ and $\mathcal{X}_-(D)$, for a spectrum that satisfies the requirements of Theorem 1.0.2, depending on whether we want to view the Euler characteristic as a power series representation of the corresponding rational function in q^{+1} or q^{-1}. In either case, the wedge summand in a specific q-degree can be computed using a finite-twist approximation $D(k)$ where the amount

of twisting k needed depends both on the diagram D and on the q-degree being considered.

Remark 3.2.2. *The independence of the various k_i used in the proofs above has been used to take the homotopy colimit (or limit) 'diagonally', simplifying the notation by tracking only a single value of k. However, this independence can also be viewed as allowing us to take the colimit one projector at a time, in any order we like. This is already implicit in the diagonal version in the passage from $D(k)$ to $D(k+1)$, where it does not matter in what order we treat all of the projectors going from their individual k-twists to their individual $(k+1)$-twists.*

3.3 Properties of $\mathcal{X}(D)$

Before going on to establish the connection to spin networks and colored links, we state and prove some properties for $\mathcal{X}_+(D)$ for diagrams D with Jones-Wenzl projectors as above. The propositions in this section will be stated and proved for right-handed twists only; the left-handed versions for $\mathcal{X}_-(D)$ are proved analogously, using alterations similar to those discussed in the previous section. As such, we drop the + notation for the time being.

Our first property is perhaps the most fundamental one. Recall that the first axiom used to characterize both the Jones-Wenzl projectors and their categorifications is that they are 'killed by turnbacks'. The following proposition gives the analogous

statement for our spectra $\mathcal{X}(D)$.

Proposition 3.3.1. *For any diagram D involving at least one Jones-Wenzl projector that is capped by at least one turnback, $\mathcal{X}(D) \simeq *$.*

Proof. Theorem 1.0.2 ensures that the cohomology of $\mathcal{X}(D)$ matches the homology defined using the categorified Jones-Wenzl projectors, which is known to vanish for such D (see Theorem 2.2.4). As noted in Theorem 2.3.1, $\mathcal{X}(D)$ has the stable homotopy type of the suspension spectrum of a CW complex up to some finite formal de-suspension, and thus Whitehead's theorem implies that the trivial cohomology of $\mathcal{X}(D)$ forces it to be contractible. □

The next proposition ensures that crossings in a diagram involving projectors still give rise to cofibration sequences in the same sense as Equation 2.3.2, leading to a version of Lemma 2.3.7 for our spectra $\mathcal{X}(D)$.

Proposition 3.3.2. *Let D be a diagram involving a finite number of Jones-Wenzl projectors, and consider a specified crossing in D. Let D' and D'' be the corresponding diagrams where the crossing is replaced with its 1-resolution and 0-resolution respectively. Then we have the following cofibration sequence of spectra*

$$\Sigma^a \mathcal{X}^{j+N_{D''}}(D'') \hookrightarrow \mathcal{X}^{j+N_D}(D) \twoheadrightarrow \Sigma^b \mathcal{X}^{j-1+N_{D'}}(D') \tag{3.3.1}$$

where the shifts are precisely the same as those indicated with Equation 2.3.2. In particular, if either of $\Sigma^a \mathcal{X}^{j+N_{D''}}(D'')$ or $\Sigma^b \mathcal{X}^{j-1+N_{D'}}(D')$ is contractible, then the other is stably homotopy equivalent to $\mathcal{X}^{j+N(D)}(D)$.

Proof. In short, the sequence (3.3.1) is built by applying Equation 2.3.2 to a suitably large finite twist approximation $\mathcal{X}(D(k))$ for $\mathcal{X}(D)$. The homological and q-degree shifts coming from Equation 2.3.2 are based on counting positive and negative crossings in the honest link diagram $D(k)$. The crossings away from the twists account for the shifts in Equation 3.3.1, while the crossings within the twisting contribute only to renormalizing the diagonal sequences used for D' and D''. The final statement is then clear (see Lemma 2.3.7).

In more detail, we consider the term $\Sigma^{\sum_{i=1}^m k\eta_i}\mathcal{X}^{j+N_D+\sum_{i=1}^m k\tau_i}(D(k))$ in the diagonal sequence used to build $\mathcal{X}^{j+N_D}(D)$ (continuing to use the notation of earlier in this section). Resolving the specified crossing in the diagram $D(k)$ results in the diagrams $D'(k)$ and $D''(k)$ which would be used to approximate $\mathcal{X}(D')$ and $\mathcal{X}(D'')$. The key point to notice is that for the honest link diagram $D(k)$, the shift $N_D + \sum_{i=1}^m k\tau_i$ is the same as $N_{D(k)}$, and similarly for $D'(k)$ and $D''(k)$. Thus we can use Equation 2.3.2 to build a cofibration sequence

$$\begin{array}{ccc} \Sigma^A\Sigma^{\sum k\eta_i}\mathcal{X}^{j+N_{D''(k)}}(D''(k)) & \hookrightarrow & \Sigma^{\sum k\eta_i}\mathcal{X}^{j+N_{D(k)}}(D(k)) \\ & & \downarrow \\ & & \Sigma^B\Sigma^{\sum k\eta_i}\mathcal{X}^{j-1+N_{D'(k)}}(D'(k)). \end{array}$$

The homological shifts A and B are differences in total counts of negative crossings. Since a and b account for these differences away from the twisting, the reader can easily verify that $A = a + \sum k(\eta_i'' - \eta_i)$ and $B = b + \sum k(\eta_i' - \eta_i)$. Putting these in

place we see the sequence

$$\begin{array}{ccc} \Sigma^a\Sigma^{\sum k\eta_i''}\mathcal{X}^{j+N_{D''(k)}}(D''(k)) & \hookrightarrow & \Sigma^{\sum k\eta_i}\mathcal{X}^{j+N_{D(k)}}(D(k)) \\ & & \downarrow \\ & & \Sigma^b\Sigma^{\sum k\eta_i'}\mathcal{X}^{j-1+N_{D'(k)}}(D'(k)). \end{array}$$

Since all of these spectra stabilize as $k \to \infty$, we can take k large enough so that each term in this sequence is stably homotopy equivalent to the corresponding spectrum in Equation 3.3.1. □

Corollary 3.3.3. *For any diagram D involving an n-strand Jones-Wenzl projector P_n concatenated with a braid β on those n strands, $\mathcal{X}^{j+N_D}(D) \simeq \Sigma^{a+\beta^-}\mathcal{X}^{j+N_{D\setminus\beta}-\beta^-}(D\backslash\beta)$ where $D \setminus \beta$ is used to denote the diagram created by replacing β with $\mathbf{I}_n$, the identity braid on those same n strands (this replacement is referred to as* straightening the braid *β), and β^- is the number of crossings of the form $\diagup\!\!\!\diagdown$ in β viewed vertically (ie the number of crossings that require 1-resolutions to transform β into $\mathbf{I}_n$). The homological shift a is the difference between the number of negative crossings in the two diagrams, as in Lemma 2.3.7.*

Proof. Let P_{n_1} be the projector with β concatenated. Since any braid β is a product of elementary generators $\sigma_\iota^{\pm 1}$ in the braid group B_{n_1} (so $\iota \in \{1, \ldots, n_1 - 1\}$), it is enough to prove the statement for such generators (ie, for a single crossing above the P_{n_1}). For each $j \in \mathbb{Z}$, Proposition 3.3.2 allows us to build a cofibration sequence (3.3.1) using this crossing. One of the two resolutions will lead to a diagram involving a turnback above P_{n_1}, forcing the corresponding spectrum to be contractible via Proposition

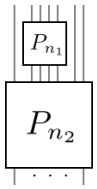

Figure 3.5: An example of two concatenated projectors $P_{n_1} \cdot P_{n_2}$ with $n_1 \leq n_2$, for which Corollary 3.3.4 allows us to absorb P_{n_1} into P_{n_2} on the level of the spectra.

3.3.1. Thus the other resolution, corresponding to 'straightening' the crossing $\sigma_\iota^{\pm 1}$, will give a spectrum stably homotopy equivalent to the original. The $-\beta^-$ shift comes from the -1 term for the 1-resolution in Equation 3.3.1 needed to 'straighten' any σ_ι^{-1} in β. The homological shift is determined similarly. □

The next corollary can be viewed as lifting the idempotency of the Jones-Wenzl projectors and their categorifications to the realm of spectra.

Corollary 3.3.4. *Let D be a diagram involving two concatenated projectors of possibly different sizes, say $P_{n_1} \cdot P_{n_2}$ with $n_1 \leq n_2$ (see Figure 3.5 for clarification on this notion). Let D' be obtained from D by replacing the smaller projector P_{n_1} with an identity braid $\mathbf{I}_{n_1}$. Then $\mathcal{X}(D) \simeq \mathcal{X}(D')$.*

Proof. We fix $j \in \mathbb{Z}$ and replace D by $D(k)$ for $k > b^+$ as in the proof of Theorem 1.0.2. Here we make stronger use of the independence of the various k_i to fix $k_1 > b_1^+$, while still allowing the other k_i to limit towards infinity together. In symbols, we are considering $\mathcal{X}^{j+N(D)+k_1\tau_1+k\sum_{i=2}^m \tau_i}(D(k_1, k, \ldots, k))$. Having fixed k_1 in this way, we

can view the $\mathbf{T}_{n_1}^{k_1}$ as a braid that is allowed to be straightened as in Corollary 3.3.3. When doing this, the grading shift effectively removes the $k_1\tau_1$, and there is no $-\beta^-$ term because all of the crossings are of the form $\diagup\!\!\diagdown$. This leaves us with precisely

$$\mathcal{X}^{j+N(D)+k_1\tau_1+k\sum_{i=2}^m \tau_i}(D(k_1,k,\ldots,k)) \simeq \mathcal{X}^{j+N(D)+k\sum_{i=2}^m \tau_i}(D'(k))$$

and since the $\mathbf{T}_{n_1}^{k_1}$ contributed only full twists to the diagram, the strand orientations before and after the straightening can be the same so that $N(D) = N(D')$. Thus we are left with $\mathcal{X}^{j+N(D')+k\sum_{i=2}^m \tau_i}(D'(k))$ which is precisely the sequence needed to build $\mathcal{X}(D')$. Any homological shifts that are needed along the way cancel precisely; we leave these details to the reader. □

3.4 An L-S-K Spectrum for Colored Links

Recall that, given a colored link L_γ with colored diagram D_{L_γ}, the colored Jones polynomial of L_γ is calculated by taking the usual Jones polynomial of the diagram D_{L_γ}. Using categorified Jones-Wenzl projectors as in [Roz14a] or [CK12], we can build a colored chain complex for L_γ in the same way, whose homology groups are referred to as the colored Khovanov homology of L_γ (see [CK12] and [Roz14b]). Using Rozansky's version of the categorified projectors allows us to prove Theorem 1.0.1.

Definition 3.4.1. *Given a colored link L_γ, we define the* colored L-S-K spectrum of L_γ *to be $\mathcal{X}_c(L_\gamma) := \mathcal{X}(D_{L_\gamma})$ as defined by Theorem 1.0.2 for the diagram D_{L_γ}.*

Proof of Theorem 1.0.1. As indicated above, the colored Khovanov homology groups for a colored link L_γ are defined by a link diagram D_{L_γ} involving Jones-Wenzl projectors. Therefore Theorem 1.0.2 gives the existence of a colored L-S-K spectrum that properly recovers the colored homology. There is a choice of where to place the projector on each cabled component when creating D_{L_γ}. The invariance of $\mathcal{X}_c$ with respect to such a choice is proved one q-degree at a time. Since each $\mathcal{X}_c^j(L_\gamma)$ is equivalent to $\mathcal{X}^j(D_{L_\gamma}(k))$ for some large enough k, and $D_{L_\gamma}(k)$ is just an honest link diagram with $\mathbf{T}^k_{n_h}$ in place of the P_{n_h}, we see that these twists $\mathbf{T}^k_{n_h}$ can be slid up and down along the cablings, including above or below other cablings, as desired. Similarly invariance under Reidemeister moves II and III is proved by considering the finite approximation for each j, where such moves give clear isotopies of honest link diagrams. Meanwhile, Reidemeister I moves give framing shifts as expected, since undoing a kink corresponds to adding a full twist on a cable. □

We end this short section with a quick property of the colored L-S-K spectra inspired by the discussion in section 3.8 of [Hoga], which illustrates the use of Proposition 3.3.2 and Corollary 3.3.3 in dealing with the colored spectra.

Definition 3.4.2. *Let L_γ denote a colored link with ℓ components, and let α_h denote the component of L_γ colored with n_h. Define $L_\gamma^{o(h)}$ to be the colored link obtained from L_γ by introducing a new unknotted, 1-colored component $\alpha_{\ell+1}$ that links positively once around the component α_h as in Figure 3.6.*

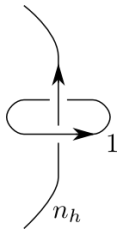

Figure 3.6: The new unknotted, 1-colored component $\alpha_{\ell+1}$ linking positively once around the component α_h (colored with n_h), forming $L_\gamma^{o(h)}$

Proposition 3.4.3. *For any colored link L_γ with ℓ components as above, the colored spectra of L_γ and $L_\gamma^{o(h)}$ for any $h \in \{1, \ldots, \ell\}$ fit in the following cofibration sequence:*

$$\mathcal{X}_c^{j+1-2n_h}(L_\gamma) \hookrightarrow \mathcal{X}_c^j(L_\gamma^{o(h)}) \twoheadrightarrow \Sigma^{2n_h}\mathcal{X}_c^{j-1-4n_h}(L_\gamma). \tag{3.4.1}$$

Proof. We focus on $\mathcal{X}_c^j(L_\gamma^{o(h)})$, built via the diagram $D_{L_\gamma^{o(h)}}$. In this diagram we slide the specified P_{n_h} along the cabling to be drawn directly below the 'new' unknot $\alpha_{\ell+1}$, which is colored by 1 so that we need no cabling for this component (note that P_1 is just the identity strand). We then construct the cofibration sequence of Proposition 3.3.2 by resolving the 'upper-left' crossing (see Figure 3.7).

As illustrated in Figure 3.7, we denote the resulting diagrams D_0 and D_1 for the 0-resolution and 1-resolution respectively. The 0-resolution is also the oriented one, and so the resulting shift in q-degree is only -1 for the loss of a positive crossing. The 1-resolution allows for an orientation as shown in the diagram, where all of the previously positive crossings (there were originally $2n_h$ of them, but one was resolved) become negative. Thus we have a q-degree shift of -1 for the loss of the resolved

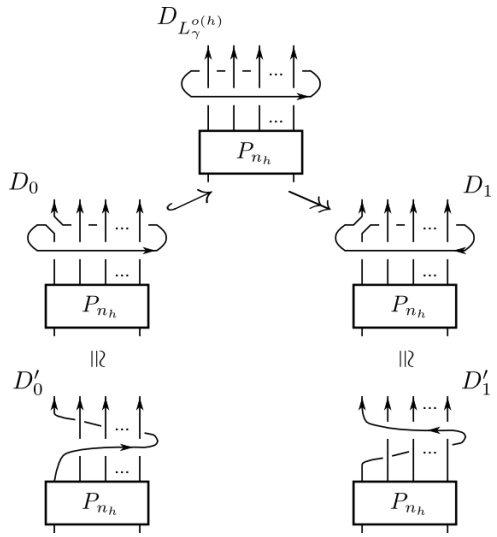

Figure 3.7: Resolving the upper-left crossing in $D_{L_\gamma^{o(h)}}$ to create a cofibration sequence. The resulting diagrams D_0 and D_1 are isotopic to D_0' and D_1' which allow the use of Corollary 3.3.3.

positive crossing, -1 for the loss of a 1-resolution, and $-3(2n_h - 1)$ for the positive crossings becoming negative (-1 each for losing a positive crossing, and -2 each for adding a negative crossing). We also have a homological shift of $-2n_h$ given the loss of a 1-resolution and the addition of $2n_h - 1$ negative crossings, which is offset by the $2n_h$ suspension. The diagrams also make it clear that crossings away from this area retain their sign, so that these shifts are the only shifts present and we see:

$$\mathcal{X}^{j-1}(D_0) \hookrightarrow \mathcal{X}^j(D_{L_\gamma^{o(h)}}) \twoheadrightarrow \Sigma^{2n_h}\mathcal{X}^{j+1-6n_h}(D_1). \tag{3.4.2}$$

At this point, we first use an isotopy (Reidemeister moves) to rearrange D_0 and D_1 into D_0' and D_1' respectively (also shown in the diagram). The D_0' and D_1' are

then diagrams with braids above the P_{n_h}. The shifts in Equation 3.4.1 are obtained from those in Equation 3.4.2 by straightening these braids (all positive crossings for D'_0, and all negative for D'_1) as in Corollary 3.3.3. □

Remark 3.4.1. *There are similar cofibration sequences for a* (-1)*-linking unknot (ie switching the orientation of the unknot* $\alpha_{\ell+1}$ *in Figures 3.6 and 3.7). The details of the resulting degree shifts are left to the reader.*

3.5 An L-S-K Spectrum for Quantum Spin Networks

We include this final section to introduce another application of our construction. This section is largely separate from the remainder of this manuscript, and can be skipped with no loss to the other chapters.

A *(closed) quantum spin network* (the notion dates back to Roger Penrose in [Pen71]) consists of a trivalent graph where each edge has been labelled with a natural number. The labels are not entirely independent: for each vertex where three edges labelled n_1, n_2, n_3 meet, we must have

$$\begin{gathered} n_i \leq n_j + n_k \ \forall \ \{i,j,k\} = \{1,2,3\} \\ n_1 + n_2 + n_3 \equiv 0 \mod 2. \end{gathered} \tag{3.5.1}$$

From such a spin network G, a q-deformed quantum invariant can be defined as follows (see chapter 4 in [KL94]). First we replace each n-labelled edge by a cable

of n parallel strands together with a copy of the Jones-Wenzl projector P_n. Then we replace each vertex having edge labels n_1, n_2, n_3 with a 'balanced splitting' of the cables as in Figure 3.8. Call the resulting diagram $D(G)$. The final step is to evaluate the Jones polynomial of $D(G)$, using the rational expressions for the Jones-Wenzl projectors present.

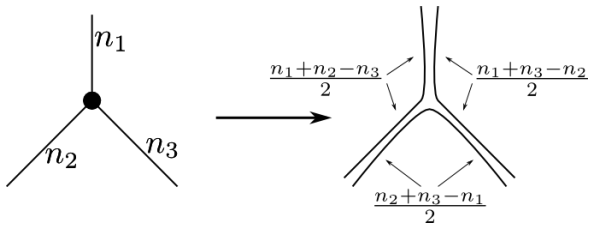

Figure 3.8: Building the q-deformed invariant of a quantum spin network; the n_i are labels in the original network, and the fractions on the right hand side tell how many parallel strands to send each direction from the vertex

In [CK12], Cooper and Krushkal replace the projectors in $D(G)$ with their own categorified projectors, thus defining a categorified spin network. If instead of this we replace the projectors with Rozansky's categorifications using infinite twists, we see a diagram of the form covered by Theorem 1.0.2.

Definition 3.5.1. *Given a quantum spin network G, we define the* L-S-K spectrum of the spin network G *to be* $\mathcal{X}(G) := \mathcal{X}(D(G))$ *as defined in Theorem 1.0.2 for the diagram $D(G)$.*

Theorem 3.5.2. *There exists an L-S-K spectrum for any $\mathfrak{sl}_2(\mathcal{C})$ quantum spin net-*

work. Its reduced cohomology is isomorphic to the homology of the categorified spin networks defined in [CK12].

Proof. $\mathcal{X}(G)$ as defined using Theorem 1.0.2 is clearly well-defined with regards to isotopies of the graph of G, which induce isotopies of $D(G)$. There is also a 'twist' move at a vertex, shown in Figure 3.9. This move is accomplished by a framing twist on the strand labelled n_1, which would result in a shift of q-degree for the spectrum (a framing twist creates a torus braid on the relevant cable, which can be straightened at the cost of such a shift using Corollary 3.3.3). This corresponds to the shift described in section 4.2 of [KL94]. □

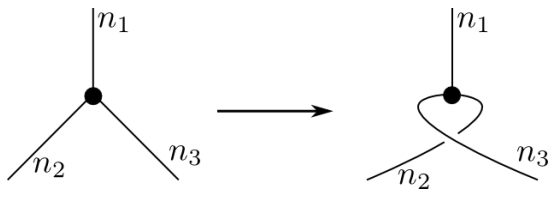

Figure 3.9: A twist move on a spin network coming from a framing twist on the strand labelled n_1

Chapter 4

A TAIL FOR THE COLORED L-S-K SPECTRUM OF A B-ADEQUATE LINK

In this chapter the main goal is to establish the stabilization of the uni-colored L-S-K spectra of B-adequate links as the coloring $n \to \infty$, generalizing the work of [Arm13, GL15] for the colored Jones polynomial and [Roz14b] for the colored Khovanov homology. The first three sections will be devoted to proving Theorem 1.0.3. These sections will make heavy use of the definitions and notations from Chapter 3. In the final section, we also provide a largely separate (and simpler) proof for Theorem 1.0.4 for the case of the unknot, which also provides a sharper bound on the amount of twisting needed.

4.1 Discussion and Strategy

Before investigating the details of the proof of Theorem 1.0.3, we outline the general strategy and logic, expanding on the summary given in the introduction. The goal is

to adapt Rozansky's proof in [Roz14b] of the fact that the colored Khovanov homology groups of B-adequate links stabilize as the color goes to infinity. The proof in that paper builds maps f_n that give isomorphisms of colored homology groups between the n-colored and $(n+1)$-colored link L, but only within a certain homological range. In order to prove Theorem 1.0.3 then, it is enough to show that

- The maps f_n in [Roz14b] are induced by maps F_n between colored spectra, at least within the homological range of isomorphism.

- If n is large enough, the homological range of isomorphism guaranteed by Rozansky is enough to cover all non-zero homology of the corresponding colored spectra (and thus the F_n induce isomorphisms on all homology, and so give stable homotopy equivalences by Whitehead's theorem).

Neither of these statements is difficult to prove conceptually, but the notation involved becomes somewhat cumbersome. The reason is that, on the one hand, the colored spectrum is a homotopy limit, and in order to build maps we resort to finite approximations (ie the corresponding diagram with high twisting of the cables). This requires q-degree shifts depending on k. On the other hand, the maps f_n built by Rozansky are compositions of a large number of simpler maps, many of which themselves shift the q-degree which will lead to separate q-degree shifts depending on n. In addition, the maps were built with the use of the categorified Jones-Wenzl projectors rather than finite-twist approximations of them. Thus some care will be

needed.

Throughout this section, following [Roz14b], all of the twisting will be *left-handed* (ie, using $\mathcal{X}_{-}(D)$ from the proof of Theorem 1.0.2). We recall here that, in addition to shifts of the form $k\tau$ for the normalization shift $n^{+}-2n^{-}$, the left-handed sequence also requires shifts of the form $kn(n-1)$ for counting the total number of crossings within the twist, accounting for 1-resolutions needed to move backward in the sequence. See Equation 3.2.2.

4.2 Definitions, Notation, and a Restatement of Theorem 1.0.3

We begin with the deifnition of B-adequacy, as well as some notation. Some of this is repeated from previous sections but is recalled here for convenience. Note that, since the colored L-S-K spectrum of a link requires a specified framing, B-adequacy will be stated in terms of a blackboard framed diagram.

Definition 4.2.1. *A link diagram L is called* B-adequate *if the all-one resolution of L contains precisely one more circle than any resolution of L which contains precisely one 0-resolution.*

- L denotes a framed, oriented link having a blackboard framed diagram which is B-adequate (the diagram will also be denoted L).

- χ will denote the total number of crossings in the diagram L.
- π will denote the total number of positive crossings in the diagram L (only important for the homological shift, which will be ignored as often as possible).
- $\chi^!$ will denote the total number of crossings in a minimal B-adequate diagram for L, ignoring framing (only important for one key bound).
- ζ will denote the total number of circles present in the all-1 resolution of the diagram L.
- $\mathcal{X}_c^j(L_n)$ will denote the colored L-S-K spectrum, in q-degree j, of the link L with all of its components colored with the natural number n; see Definition 3.4.1.
- For each $(n,k) \in \mathbb{N}^2$, $L(n,k)$ will denote the diagram obtained from L by cabling all components with n parallel strands, and adding a twist of $\mathbf{T}_n^{-k}$ to each cabling between *every crossing*. That is, if we replace the diagram L with the graph with vertices at crossings and edges for strands between them, then each edge would be assigned a $\mathbf{T}_n^{-k}$ (see the beginning of section 4 in [Roz14b]).
- m will denote the total number of twistings $\mathbf{T}_n^{-k}$ coming from Jones-Wenzl projectors in the diagram $L(n,k)$. This plays a similar role to ℓ, the number of components of the link L, in Chapter 3. However, as the previous item suggests, $m > \ell$ for our diagrams since we will be placing many such twistings on each component.

- For any oriented diagram (link or tangle) D, N_D will denote the normalization shift $n^+ - 2n^-$ counting all crossings in D.

The following notation is important enough to warrant its own definition.

Definition 4.2.2. *For a given diagram L as above, the* Colored q-degree Shift *is the integer function $s(n,k)$ that counts the normalization shift, the number of crossings, and the number of circles in the all-1 resolution of the link $L(n,k)$. That is, with notation as above,*

$$s(n,k) := N_{L(n,k)} + kmn(n-1) + n^2\chi + n\zeta. \tag{4.2.1}$$

Remark 4.2.1. *Note that $n\zeta$ is the proper count for the number of circles in the all-1 resolution of $L(n,k)$, since the $\mathbf{T}_n^{-k}$'s present will become $\mathbf{I}_n$'s, and the all-1 resolution of a crossing coming from the original diagram gives a cabled version of the same resolution as in Figure 4.1.*

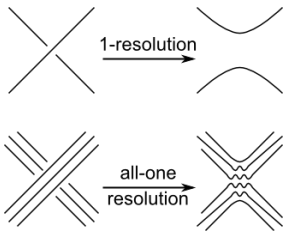

Figure 4.1: Illustration of the all-1 resolution of a crossing in a cabled diagram

Before moving forward, we illustrate the use of these notations to restate the result of Theorem 1.0.1:

Theorem 4.2.3 (Theorem 1.0.1 Restated For Uni-Colored Links)**.** *For any colored link L_n with the coloring n on every component, there exists a colored L-S-K spectrum $\mathcal{X}_c(L_n) := \bigvee_{j\in\mathbb{Z}} \mathcal{X}_c^{j+s(n,0)}(L_n)$ with wedge summands defined to be the homotopy limits of the following sequences*

$$\mathcal{X}^{j+s(n,0)}(L(n,0)) \twoheadleftarrow \cdots \twoheadleftarrow \mathcal{X}^{j+s(n,k)}(L(n,k)) \twoheadleftarrow \cdots \tag{4.2.2}$$

which stabilize for large enough k. In particular, for large enough k we have a finite-twist approximation for $\mathcal{X}_c^{j+s(n,0)}(L_n)$ as

$$\mathcal{X}_c^{j+s(n,0)}(L_n) \simeq \mathcal{X}^{j+s(n,k)}(L(n,k)) \tag{4.2.3}$$

Remark 4.2.2. *The term $s(n,0)$ is included in the original wedge summand for $\mathcal{X}_c(L_n)$ for convenience moving forward; note that the terms $n^2\chi$ and $n\zeta$ in Equation 4.2.1 are independent of k, and simply persist throughout the sequence (4.2.2).*

Proof. This is essentially the sequence built in the proof of Theorem 1.0.2 for $\mathcal{X}_-(D)$ as applied to Theorem 1.0.1, except that extra projectors (and thus extra copies of $\mathbf{T}_n^{-k}$) are present. These extra projectors cause no issues, however, thanks to Corollary 3.3.4. In the proof of Theorem 1.0.2, the shift in the sequence includes a normalization term $-\sum k_i\tau_i$ and a crossing counting term $\sum k_i n_i(n_i-1)$. Here the k_i and n_i are all equal, and both terms are then absorbed into the shift $s(n,k)$. Meanwhile, the left-handed twisting of a cabling where all strands are oriented the same way (in accordance with the orientation of L) means that all of the crossings involved are negative. This ensures that the homological shifts cancel out (we lose

negative crossings at the same rate that we lose 1-resolutions), so no suspensions are necessary. □

We now restate Theorem 1.0.3 in a more precise fashion.

Theorem 4.2.4. *Fix a framed, oriented B-adequate link with blackboard framed diagram L. With notation as above, there exist sequences of maps for each $j \in \mathbb{Z}$*

$$\mathcal{X}_c^{j+s(1,0)}(L_1) \twoheadleftarrow \Sigma^{-3\pi}\mathcal{X}_c^{j+s(2,0)}(L_2) \twoheadleftarrow \cdots \Sigma^{-(n^2-1)\pi}\mathcal{X}_c^{j+s(n,0)}(L_n) \twoheadleftarrow \cdots \tag{4.2.4}$$

that become stable homotopy equivalences for $n > \chi^! - 2j + 1$.

This version of Theorem 1.0.3 is the desired final result. However, as indicated in the previous section, we actually build the required maps by taking finite-twist approximations for the various $\mathcal{X}_c(L_n)$. With the help of Equation 4.2.3 we translate Theorem 4.2.4 into the following:

Theorem 4.2.5. *Fix a framed, oriented B-adequate link with blackboard framed diagram L. With notation as above, for each $j \in \mathbb{Z}$ and for each $(n,k) \in \mathbb{N}^2$, there exists a map denoted $F_{n,k,j}$ as shown below:*

$$F_{n,k,j} : \Sigma^{-((n+1)^2-1)\pi}\mathcal{X}^{j+s(n+1,k)}(L(n+1,k)) \twoheadrightarrow \Sigma^{-(n^2-1)\pi}\mathcal{X}^{j+s(n,k)}(L(n,k)) \tag{4.2.5}$$

such that, for large enough k, the following properties both hold:

1. *Both the $\mathcal{X}(L(n,k))$ and $\mathcal{X}(L(n+1,k))$ terms are stably homotopy equivalent to their respective colored L-S-K spectra, so that $F_{n,k,j}$ provides the map $F_{n,j}$*

below:

$$\begin{array}{c} \Sigma^{-((n+1)^2-1)\pi}\mathcal{X}_c^{j+s(n+1,0)}(L_{n+1}) \\ \wr \\ \Sigma^{-((n+1)^2-1)\pi}\mathcal{X}^{j+s(n+1,k)}(L(n+1,k)) \\ \downarrow \\ \Sigma^{-(n^2-1)\pi}\mathcal{X}^{j+s(n,k)}(L(n,k)) \\ \wr \\ \Sigma^{-(n^2-1)\pi}\mathcal{X}_c^{j+s(n,0)}(L_n) \end{array} \tag{4.2.6}$$

which is used to construct the sequence (4.2.4).

2. *For $n > \chi^! - 2j + 1$, the map $F_{n,k,j}$ (and thus, $F_{n,j}$) is a stable homotopy equivalence.*

Before discussing the proof of this theorem, we provide a table and example to illustrate the statement of Theorem 4.2.4. The following lemma and corollary are provided to avoid useless clutter.

Lemma 4.2.6. *For any link L, and for any $n \in \mathbb{N}$, we have that $j = 0$ gives the maximal possible q-degree for non-zero colored spectrum $\mathcal{X}_c^{j+s(n,0)}(L_n)$.*

Proof. By the finite-twist approximation (4.2.3), we have that

$$\mathcal{X}_c^{j+s(n,0)}(L_n) \simeq \mathcal{X}^{j+s(n,k)}(L(n,k))$$

for some large enough k. The link $L(n,k)$ has Khovanov chain complex generator z with maximal possible q-degree occurring in the all-one resolution, assigning v^+ to

all of the circles. Since the all-one resolution of the left-handed twists give identity braids, this generator z has q-degree equal to:

$$\begin{aligned}\deg_q(z) &= \#(\text{1-resolutions}) + (\#(v_+) - \#(v_-)) + (n^+ - 2n^-) \\ &= \#(\text{crossings}) + \#(\text{circles}) + N_{L(n,k)} \\ &= s(n,k).\end{aligned}$$

which corresponds to $j = 0$. □

Corollary 4.2.7. *For any link L, and for any $n \in \mathbb{N}$, we have that $\mathcal{X}_c^{j+s(n,0)}(L_n)$ is trivial for odd j.*

Proof. We see from the proof of Lemma 4.2.6 that in any finite approximation for $\mathcal{X}_c^{j+s(n,0)}(L_n)$, there is a generator in q-degree corresponding to $j = 0$. The parity of q-degree is constant throughout the Khovanov chain complex, so we must have j even. □

Remark 4.2.3. *Lemma 4.2.6 can be regarded as giving an alternative meaning for what the grading j, and the shift $s(n,k)$, are describing. We see that $s(n,k)$ is precisely the maximum possible q-grading for the Khovanov chain complex of $L(n,k)$, and then j is a measure of how far from that maximum we are. This means $j \leq 0$, which correctly corresponds to building a power series in q^{-1} for the rational terms in the decategorified setting of the projectors.*

We now present the general table of colored spectra for any link L arranged to take advantage of Theorem 4.2.4.

	$j=0$		$j=-2$		$j=-4$		$j=-6$		$\dots$
$\mathcal{X}_c(L_1)$	$\mathcal{X}_c^{s(1,0)}(L_1)$	$\vee$	$\mathcal{X}_c^{s(1,0)-2}(L_1)$	$\vee$	$\mathcal{X}_c^{s(1,0)-4}(L_1)$	$\vee$	$\mathcal{X}_c^{s(1,0)-6}(L_1)$	$\vee$	$\cdots$
$\mathcal{X}_c(L_2)$	$\mathcal{X}_c^{s(2,0)}(L_2)$	$\vee$	$\mathcal{X}_c^{s(2,0)-2}(L_2)$	$\vee$	$\mathcal{X}_c^{s(2,0)-4}(L_2)$	$\vee$	$\mathcal{X}_c^{s(2,0)-6}(L_2)$	$\vee$	$\cdots$
$\mathcal{X}_c(L_3)$	$\mathcal{X}_c^{s(3,0)}(L_3)$	$\vee$	$\mathcal{X}_c^{s(3,0)-2}(L_3)$	$\vee$	$\mathcal{X}_c^{s(3,0)-4}(L_3)$	$\vee$	$\mathcal{X}_c^{s(3,0)-6}(L_3)$	$\vee$	$\cdots$
$\vdots$	$\vdots$		$\vdots$		$\vdots$		$\vdots$		

Table 4.1: The table of uni-colored L-S-K spectra for a link L, with the vertical axis indicating color via subscript on L and the horizontal axis indicating the suitably normalized q-degree; stabilization occurs vertically starting at a color that depends on both j (the column) and L.

With Table 4.1 in mind, we can reinterpret some of the theorems stated above.

- Theorem 4.2.3 guarantees that all of the colored L-S-K spectra in Table 4.1 exist, and Equation 4.2.3 guarantees that any one of them is stably homotopy equivalent to the spectrum of a finite-twist approximation $L(n,k)$. Note that there is no single bound for k that approximates all of the spectra in the table at once, since the bound would depend on both j and n.

- Theorem 4.2.4 asserts that there are 'vertical' maps connecting all of the terms in any column of Table 4.1, and furthermore that these maps are stable homotopy equivalences for $n > \chi^! - 2j + 1$. Thus in any given column (fixed j) we see that the spectra are all stably equivalent for large enough n. This is the general statement of Theorem 1.0.3.

- Theorem 4.2.5 is the stepping stone to proving Theorem 4.2.4. It asserts the existence of the vertical maps *after* replacing each entry in Table 4.1 by its corresponding finite-twist approximation as guaranteed by Equation 4.2.3. Since we build the maps one at a time, we can focus on two adjacent entries in one column of the table (fix j and focus on n and $n+1$ for some n) and take k to be larger than both stability bounds for these two entries. Then this vertical map composes with the finite-twist approximation equivalences as in Equation 4.2.6 to give the maps asserted by Theorem 4.2.4.

To illustrate the stabilization as $n \to \infty$, we build the table for L being the

simplest non-trivial link, that is, the positive Hopf link.

Example 4.2.8. Let L be the positive Hopf link. The reader can quickly verify that

$$\chi = \chi^! = 2$$

$$\zeta = 2$$

$$N_L = 2$$

$$\begin{aligned} s(n,0) &= N_{L(n,0)} + 0 + n^2\chi + n\zeta \\ &= n^2 N_L + n^2\chi + n\zeta \\ &= 4n^2 + 2n \end{aligned}$$

which means that the bound $n > \chi^! - 2j + 1$ for stabilization becomes

$$n > 3 - 2j.$$

Thus we have Table 4.2 for the Hopf link.

Notice that in the second column of Table 4.2, stabilization begins after $n = 8$ ($n > 3-2(-2) = 7$). Also, note the absence of horizontal dots in the first row. When $n = 1$, the colored Khovanov homology (and spectrum) is just the usual Khovanov homology (and spectrum), which we know only exists in these 4 q-degrees for the positive Hopf link L.

4.3 The Proof

As mentioned in the discussion on strategy above, the maps $F_{n,k,j}$ will be lifts of the maps f_n defined in Theorem 2.12 of [Roz14b]. In that paper, Rozansky considers these

	$j=0$		$j=-2$		$j=-4$		$j=-6$		$\dots$
$\mathcal{X}_c(L_1)$	$\mathcal{X}_c^{6}(L_1)$	$\vee$	$\mathcal{X}_c^{4}(L_1)$	$\vee$	$\mathcal{X}_c^{2}(L_1)$	$\vee$	$\mathcal{X}_c^{0}(L_1)$		
$\mathcal{X}_c(L_2)$	$\mathcal{X}_c^{20}(L_2)$	$\vee$	$\mathcal{X}_c^{18}(L_2)$	$\vee$	$\mathcal{X}_c^{16}(L_2)$	$\vee$	$\mathcal{X}_c^{14}(L_2)$	$\vee$	$\cdots$
$\mathcal{X}_c(L_3)$	$\mathcal{X}_c^{42}(L_3)$	$\vee$	$\mathcal{X}_c^{40}(L_3)$	$\vee$	$\mathcal{X}_c^{38}(L_3)$	$\vee$	$\mathcal{X}_c^{36}(L_3)$	$\vee$	$\cdots$
$\mathcal{X}_c(L_4)$	$\mathcal{X}_c^{72}(L_4)$	$\vee$	$\mathcal{X}_c^{70}(L_4)$	$\vee$	$\mathcal{X}_c^{68}(L_4)$	$\vee$	$\mathcal{X}_c^{66}(L_4)$	$\vee$	$\cdots$
	$\wr$								
$\mathcal{X}_c(L_5)$	$\mathcal{X}_c^{110}(L_5)$	$\vee$	$\mathcal{X}_c^{108}(L_5)$	$\vee$	$\mathcal{X}_c^{106}(L_5)$	$\vee$	$\mathcal{X}_c^{104}(L_5)$	$\vee$	$\cdots$
	$\wr$								
$\mathcal{X}_c(L_6)$	$\mathcal{X}_c^{156}(L_6)$	$\vee$	$\mathcal{X}_c^{154}(L_6)$	$\vee$	$\mathcal{X}_c^{152}(L_6)$	$\vee$	$\mathcal{X}_c^{150}(L_6)$	$\vee$	$\cdots$
	$\wr$								
$\mathcal{X}_c(L_7)$	$\mathcal{X}_c^{210}(L_7)$	$\vee$	$\mathcal{X}_c^{208}(L_7)$	$\vee$	$\mathcal{X}_c^{206}(L_7)$	$\vee$	$\mathcal{X}_c^{204}(L_7)$	$\vee$	$\cdots$
	$\wr$								
$\mathcal{X}_c(L_8)$	$\mathcal{X}_c^{272}(L_8)$	$\vee$	$\mathcal{X}_c^{270}(L_8)$	$\vee$	$\mathcal{X}_c^{268}(L_8)$	$\vee$	$\mathcal{X}_c^{266}(L_8)$	$\vee$	$\cdots$
	$\wr$		$\wr$						
$\vdots$	$\vdots$		$\vdots$		$\vdots$		$\vdots$		

Table 4.2: The table of uni-colored L-S-K spectra for the positive Hopf link L; the vertical stable homotopy equivalences begin when $n > 3 - 2j$, illustrated in the first two columns.

as grading-preserving maps between 'shifted colored Khovanov homology groups':

$$f_n : \tilde{H}^{i_R,j_R}(L_n) \longrightarrow \tilde{H}^{i_R,j_R}(L_{n+1}) \tag{4.3.1}$$

where we have used i_R and j_R to denote Rozansky's grading conventions. [Roz14b] asserts the existence of these maps, and the fact that they are isomorphisms so long as $i_R \leq n-1$.

Here, we first provide the translation between Rozansky's grading conventions and our own. The reader can verify from [Roz14b] that

$$i_R = \#\text{cros} - \#\text{1-resolutions} = \#\text{0-resolutions} \tag{4.3.2}$$

$$j_R = -\left(\#(v_+) - \#(v_-)\right) + n\zeta \tag{4.3.3}$$

where the #cros term refers to the total number of crossings in the diagram D_{L_n} (see Figure 2.6 in Section 4). From this and Equations 2.2.11 and 2.2.12 we see that

$$i = -i_R + n^+ \tag{4.3.4}$$

$$j = (-i_R - j_R) + (n^+ - 2n^-) + \#\text{cros} + n\zeta \tag{4.3.5}$$

where the n^+ and n^- are counting positive and negative crossings in the diagram D_{L_n}. Although some further simplifications are possible, this format most clearly matches the format seen in the sequence (4.2.4) of Theorem 4.2.4 involving the $s(n,k)$ shift.

Now these colored homology groups use the diagrams D_{L_n} containing the categorified Jones-Wenzl projectors. In [Roz14a] these categorified projectors are defined as stable limits of complexes using $\mathbf{T}_n^{-k}$ in place of the projectors, as in the proof of

Theorem 1.0.1. This means that for large enough k the following homology groups match:

$$\tilde{H}^{i_R,j_R}(L_n) \cong \tilde{H}^{i_R,j_R}(D_{L_n}(k))$$

$$\tilde{H}^{i_R,j_R}(L_{n+1}) \cong \tilde{H}^{i_R,j_R}(D_{L_{n+1}}(k))$$

so long as $i_R \leq n-1$, the homological range which we are interested in. Thus we may focus on these finite-twist approximations of the colored links L_n, and the maps f_n in this context will give rise to the maps $F_{n,k,j}$ we seek. The reader may check that the grading shifts now correspond to those present in Equation 4.2.5.

Now we prove the two lemmas that correspond to the two points discussed in the beginning of this section. For the first lemma, we avoid going into detail about the precise definition of the maps f_n; the interested reader should consult sections 3 and 4 of [Roz14b].

Lemma 4.3.1. *The maps f_n of Rozansky can be lifted to maps $F_{n,k,j}$ as in Equation 4.2.5.*

Proof. The maps f_n are built out of several sorts of maps corresponding to local transformations as in Section 4 of [Roz14b]:

1. Reidemeister moves involving strands away from the projectors.

2. Short exact sequences of complexes arising from resolving a crossing away from the projectors.

3. 'Straightening braids' via resolving crossings adjacent to projectors.

4. Adding new P_n projectors adjacent to an existing P_{n+1} projector, and other similar uses of the idempotent-like behavior of the categorified projectors.

5. 'Sliding' projectors above and below other strands.

6. Viewing the categorified P_{n+1} as a cone of a map $C \to \mathbf{I}_{n+1}$ where the complex C involves no identity braid diagrams (there are further grading conditions; see both [Roz14a] and [Roz14b]). This allow a short exact sequence roughly of the form $KC(\langle C, \mathbf{Z}\rangle) \hookrightarrow KC(\langle P_{n+1}, \mathbf{Z}\rangle) \twoheadrightarrow KC(\langle \mathbf{I}_{n+1}, \mathbf{Z}\rangle)$.

The first two types of maps clearly extend first to the finite-twist approximations, then to the corresponding spectra (type 1 can be viewed as the content of Section 6 of [LS14a], while type 2 is Lemma 2.3.7 also based on [LS14a]). Types 3 and 4 lift in a manner corresponding to Corollaries 3.3.3 and 3.3.4 respectively, giving stable homotopy equivalences for large enough k. Type 5 is just a combination of Reidemeister moves on the level of the finite-twist approximation, as in the proof of well-definedness of the colored spectrum (proof of Theorem 1.0.1 in Section 4.2).

For type 6, we return to [Roz14a] where the cone format of the categorified P_{n+1} is derived based on the finite-twist approximations, which exhibit this cone structure via resolving all of the crossings in the twisting. And so this map lifts to a long composition of maps of spectra coming from the cofibrations (2.3.2) which, on the level of homology, is precisely the desired map.

We note here that some of these maps giving stable homotopy equivalences (especially types 3 and 4) rely not just on Rozansky's bounds, but in the new setting on a proper lower bound for k. Since there are only finitely many such moves used to build the map f_n, we can always force k to be large enough to satisfy all of these lower bounds before we begin. □

The second lemma requires the following theorem from [Roz14b].

Theorem 4.3.2 ([Roz14b] Theorem 2.1)**.** *Using the notation of Equation 4.3.1, we have that* $\tilde{H}^{i_R,j_R}(L_n) = 0$ *for* $j_R < -\frac{1}{2}(i_R + \chi^!)$.

Proof. This is one of several bounds on non-zero shifted colored Khovanov homology provided by Theorem 2.1 in [Roz14b]. It is treated as a corollary of Theorem 2.11 which is proved with a spectral sequence built from the multicone presentation of the colored Khovanov chain complex resulting from resolving crossings away from the projectors. See Section 5 of that paper. □

Using this result we can prove the following.

Lemma 4.3.3. *Fix* $j \in \mathbb{Z}$. *Then for* $n > \chi^! - 2j + 1$, *we have (for large enough* k*)*

$$H^i(\Sigma^{-(n^2-1)\pi}\mathcal{X}^{j+s(n,k)}(L(n,k))) = 0$$

for all $i < \pi - n + 1$, *which is equivalent to all* $i_R > n - 1$ *for* $\tilde{H}^{i_R,j_R}(L_n)$.

Proof. For large enough k we have

$$H^i(\Sigma^{-(n^2-1)\pi}\mathcal{X}^{j+s(n,k)}(L(n,k))) \cong H^{i+(n^2-1)\pi}\mathcal{X}_c^{j+s(n,0)}(L_n)) \cong \tilde{H}^{i_R,j_R}(L_n)$$

Definition 4.2.2 describes $s(n,k)$ as a count of normalizations, crossings, and circles. This allows us to use Equations 2.2.12 and 4.3.2 to convert:

$$\begin{aligned} j + s(n,k) &= j + N_{L(n,k)} + \#\text{crossings}(L(n,k)) + n\zeta \\ &= \#(\text{1-resolutions}) + (\#(v_+) - \#(v_-)) + N_{L(n,k)} \\ j + \#\text{0-resolutions} + n\zeta &= (\#(v_+) - \#(v_-)) \end{aligned}$$

so that

$$\begin{aligned} j_R &= -\#(v_+ - v_-) + n\zeta \\ &= -j - \#\text{0-resolutions} \\ &= -j - i_R. \end{aligned}$$

The last line follows from the fact that the suspensions are designed to ensure that i_R counting 0-resolutions in L_n is the same as counting 0-resolutions in the finite-twist approximation $L(n,k)$. A similar (and simpler) conversion ensures that the bound $i < \pi - n + 1$ is equivalent to $i_R > n - 1$. Meanwhile, the bound $n > \chi^! - 2j + 1$ quickly yields

$$j > \frac{1}{2}(\chi^! - n + 1).$$

Combining all of these gives, for $n > \chi^! - 2j + 1$ and $i < \pi - n + 1$ ($i_R > n - 1$),

$$\begin{aligned} j_R &= -j - i_R \\ &< -\frac{1}{2}(\chi^! - n + 1) - i_R \\ &< -\frac{1}{2}(\chi^! + i_R) \end{aligned}$$

which is precisely the bound of Theorem 4.3.2 for zero homology as desired. □

Proof of Theorem 4.2.5. From Lemma 4.3.1, we have the existence of the required maps $F_{n,k,j}$ that induce isomorphisms on homology for all homological gradings corresponding to $i_R \leq n-1$. From Lemma 4.3.3, once $n > \chi^! - 2j + 1$ all of the spaces involved have zero homology in all homological gradings corresponding to $i_R > n-1$. Therefore for $n > \chi^! - 2j + 1$ the maps $F_{n,k,j}$ induce isomorphisms on all homology groups, and so by Whitehead's theorem they are stable homotopy equivalences as desired. □

As noted above, this provides the proof of Theorem 1.0.3.

4.4 A More Explicit Tail for the Colored L-S-K Spectrum of the Unknot

In this final section we prove Theorem 1.0.4 by giving an alternative, more explicit proof showing the tail behavior for the colored L-S-K spectrum of the unknot. Since cabling an unknot with a torus braid twist simply produces the torus links $T(n,m)$, we use the notation $\mathcal{X}(T(n,\infty))$ for the spectrum of the n-colored unknot. Along the way, we will also be able to prove Corollary 1.0.5.

Remark 4.4.1. *There is an important distinction to be made here. Earlier, the notation* $\mathbf{T}_n^k$ *was used to denote a torus* braid *consisting of* k full (right-handed)

twists. *Now we use the notation* $T(n,m)$ *to denote a torus* link *with* m fractional $\frac{1}{n}^{\text{th}}$ (right-handed) twists. *The reasons for this change will be made clear moving forward.*

To begin with, we give our precise limiting definition in this setting of fractionally twisting torus links.

Definition 4.4.1.

$\mathcal{X}(T(n,\infty)) = \bigvee_{j\in\mathbb{Z}} \mathcal{X}^{j-n}(T(n,\infty))$*, where for each* $j \in \mathbb{Z}$*,*

$$\mathcal{X}^{j-n}(T(n,\infty)) := \text{hocolim}\left[\mathcal{X}^{j-n}(T(n,0)) \hookrightarrow \cdots \hookrightarrow \mathcal{X}^{(j-n)+m(n-1)}(T(n,m)) \hookrightarrow \cdots\right] \tag{4.4.1}$$

Note that the q-degree shift of $-n$ in this definition plays a role similar to that of the term $s(n,0)$ in Sections 4.2 and 4.3. (Indeed, since the unknot has no crossings and one circle in any resolution, this term is precisely $s(n,0)$; the negation is because we will be considering right-handed twisting rather than left-handed). The maps in this sequence come from resolving crossings, precisely as in Proposition 3.2.1.

Before going into the details of the proof, we provide Table 4.3 to illustrate the goal of the construction, similar to Table 4.1 for the general case. As in Lemma 4.2.6 and Corollary 4.2.7, we have only even values for the q-degree j starting at $j = 0$.

The goal of this section will be to construct the 'vertical' stable homotopy equivalences already presented in Table 4.3. Note that, like in the general case (Table 4.1), the j terms are arranged to 'start' at zero, but now *increase* in the positive direction. This stems from the fact that we will be using right-handed twists rather than the

	$j=0$		$j=2$		$j=4$		$j=6$		$\dots$
$\mathcal{X}(1,\infty)$	$\mathcal{X}^{-1}(1,\infty)$	$\vee$	$\mathcal{X}^{1}(1,\infty)$						
	$\wr$		$\wr$						
$\mathcal{X}(2,\infty)$	$\mathcal{X}^{-2}(2,\infty)$	$\vee$	$\mathcal{X}^{0}(2,\infty)$	$\vee$	$\mathcal{X}^{2}(2,\infty)$	$\vee$	$\mathcal{X}^{4}(2,\infty)$	$\vee$	$\cdots$
	$\wr$		$\wr$		$\wr$				
$\mathcal{X}(3,\infty)$	$\mathcal{X}^{-3}(3,\infty)$	$\vee$	$\mathcal{X}^{-1}(3,\infty)$	$\vee$	$\mathcal{X}^{1}(3,\infty)$	$\vee$	$\mathcal{X}^{3}(3,\infty)$	$\vee$	$\cdots$
	$\wr$		$\wr$		$\wr$		$\wr$		
$\mathcal{X}(4,\infty)$	$\mathcal{X}^{-4}(4,\infty)$	$\vee$	$\mathcal{X}^{-2}(4,\infty)$	$\vee$	$\mathcal{X}^{0}(4,\infty)$	$\vee$	$\mathcal{X}^{2}(4,\infty)$	$\vee$	$\cdots$
	$\wr$		$\wr$		$\wr$		$\wr$		
$\vdots$	$\vdots$		$\vdots$		$\vdots$		$\vdots$		

Table 4.3: The table of colored L-S-K spectra for the unknot, notated as spectra of torus links (the T is dropped from the notation), with the horizontal axis indicating suitably normalized q-degree; the vertical stabilizations in each column besides the first begin along the diagonal $n = j/2$.

left-handed twists considered in the previous section. Also, since $T(1,\infty)$ is just an unknot, there is no need for an infinite wedge sum in the first row (similar to the first row in Table 4.2 for the Hopf link; see Example 4.2.8).

The construction of these vertical maps follows a simple observation. It is well known that the torus links satisfy $T(n,n+1) \cong T(n+1,n)$. The sequences used to build $\mathcal{X}(T(n,\infty))$ in Definition 4.4.1 are based on going from $\mathcal{X}(T(n,m)) \hookrightarrow \mathcal{X}(T(n,m+1))$. We can combine these two ideas to see a 'diagonal' sequence of the form (omitting the T from the notation):

$$\begin{array}{ccccccccc}
\mathcal{X}(n,n-1) & \hookrightarrow & \mathcal{X}(n,n) & \hookrightarrow & \mathcal{X}(n,n+1) & \hookrightarrow & \cdots & & \\
 & & & & \wr & & & & \\
 & & & & \mathcal{X}(n+1,n) & \hookrightarrow & \mathcal{X}(n+1,n+1) & \hookrightarrow & \mathcal{X}(n+1,n+2) \\
 & & & & & & & & \wr \\
 & & & & & & & & \mathcal{X}(n+2,n+1)
\end{array}
\begin{array}{l}
\\
\\
\hookrightarrow \cdots \\
\\
\hookrightarrow \cdots \\
\\
\hookrightarrow \cdots \\
\ddots
\end{array}
\tag{4.4.2}$$

If we can find a lower bound on n so that all of these maps are stable homotopy equivalences, including the horizontal dots (indicating that in fact $\mathcal{X}(n,n-1) \simeq \mathcal{X}(n,\infty)$, and similarly for the other rows), we would have stable equivalences between spectra $\mathcal{X}(n,\infty)$ as $n \to \infty$ as desired. Of course, this cannot be done once and for all; instead, it is done one (shifting) q-degree at a time. The vertical equivalences in Table 4.3 will be precisely the resulting maps.

We begin with the horizontal maps.

Theorem 4.4.2. *Fix $j \in \mathbb{Z}$ and $n \in \mathbb{N}$. Then for $m \geq \max(j-n, n-1)$, the sequence (4.4.1) stabilizes. That is, the maps*

$$\mathcal{X}^{(j-n)+m(n-1)}(T(n,m)) \hookrightarrow \mathcal{X}^{(j-n)+(m+1)(n-1)}(T(n,m+1)) \tag{4.4.3}$$

are stable homotopy equivalences.

Proof. Since this proof requires updating all of the notation and bounds of Proposition 3.2.2, we relegate this to an appendix (Subsection 4.4.1) at the end of the chapter. □

Proof of Corollary 1.0.5. For the case when $n = 3$ and $j = 6$, we have

$$\mathcal{X}^3(T(3,\infty)) \simeq \mathcal{X}^9(T(3,3)) \simeq \mathcal{X}^{11}(T(3,4)) \simeq \mathcal{X}^{13}(T(3,5)) \simeq \cdots \tag{4.4.4}$$

and it is shown in [LS14c] that $\mathcal{X}^{11}(T(3,4))$ has non-trivial Sq^2 action. □

With the bounds of Theorem 4.4.2 in place, we are ready to provide the vertical equivalences of Table 4.3 via the idea of Equation 4.4.2.

Lemma 4.4.3. *Fix $j \in (2\mathbb{N} \cup 0)$. Then for $n \geq \frac{j}{2}$, we have*

$$\mathcal{X}^{j-n}(T(n,\infty)) \simeq \begin{cases} \mathcal{X}^{(j/2)^2}(T(\frac{j}{2},\frac{j}{2})) & n = \frac{j}{2} \\ \mathcal{X}^{j-n+(n-1)^2}(T(n,n-1)) & n > \frac{j}{2} \end{cases} \tag{4.4.5}$$

$$\mathcal{X}^{j-(n+1)}(T(n+1,\infty)) \simeq \mathcal{X}^{j-(n+1)+n^2}(T(n+1,n)) \tag{4.4.6}$$

Proof. This follows directly from Theorem 4.4.2. When $n = \frac{j}{2}$, the $j - n$ term dominates in the bound $m \geq \max(j-n, n-1)$, and the sequence (4.4.1) stabilizes

once $m = j - n = \frac{j}{2}$. If $n > \frac{j}{2}$, the $n-1$ term dominates and the sequence stablizes as soon as $m = n-1$. Note that if $j = 0$, then for any n we are automatically in this second case. Meanwhile, if $n \geq \frac{j}{2}$, then $n+1 > \frac{j}{2}$ and this gives Equation 4.4.6. $\square$

Lemma 4.4.4. *For $n \geq \frac{j}{2}$ as above, define the map $\phi_{n,j}$ to be the composition below (we omit the first term and first map if $n = \frac{j}{2}$)*

$$\begin{array}{c} \mathcal{X}^{j-n+(n-1)^2}(T(n,n-1)) \\ \downarrow \\ \mathcal{X}^{j-n+n(n-1)}(T(n,n)) \\ \downarrow \\ \mathcal{X}^{j-n+(n+1)(n-1)}(T(n,n+1)) \\ \wr \\ \mathcal{X}^{j-(n+1)+n^2}(T(n+1,n)) \end{array}$$

where the first two maps are the same maps appearing in the sequence (4.4.1), and the final equivalence comes from the isotopy $T(n,m) \cong T(m,n)$. Then $\phi_{n,j}$ defines a stable homotopy equivalence

$$\phi_{n,j} : \mathcal{X}^{j-n+(n-1)^2}(T(n,n-1)) \xrightarrow{\simeq} \mathcal{X}^{j-(n+1)+n^2}(T(n+1,n)).$$

Proof. As in the previous lemma, the first two maps are stable homotopy equivalences due to the bound in Theorem 4.4.2. $\square$

Remark 4.4.2. *We see that this map $\phi_{n,j}$ plays a role similar to that of the $F_{n,j}$ of*

the previous section, but is much easier to define than the maps f_n in [Roz14b] that lead to $F_{n,j}$.

Proof of Theorem 1.0.4. Combining Lemmas 4.4.3 and 4.4.4 gives stable homotopy equivalences

$$\begin{array}{c} \mathcal{X}^{j-n}(T(n,\infty)) \\ \text{Lemma 4.4.3} \quad \wr \\ \mathcal{X}^{j-n+(n-1)^2}(T(n,n-1)) \\ \text{Lemma 4.4.4} \quad \wr \\ \mathcal{X}^{j-(n+1)+n^2}(T(n+1,n)) \\ \text{Lemma 4.4.3} \quad \wr \\ \mathcal{X}^{j-(n+1)}(T(n+1,\infty)) \end{array}$$

for arbitrary $n > \frac{j}{2}$, which gives all of the necessary stable homotopy equivalences as indicated in Table 4.3 but for the initial ones in each column. The calculations presented in Theorem 1.0.4 refer to these initial equivalences that mark the beginning of the stabilization, that is when $n = \frac{j}{2}$ so that we are considering $\mathcal{X}^{j/2}(T(\frac{j}{2},\infty))$. In this case, Lemma 4.4.3 shows that $\mathcal{X}^{j/2}(T(\frac{j}{2},\infty)) \simeq \mathcal{X}^{(j/2)^2}(T(\frac{j}{2},\frac{j}{2}))$ so long as $j > 0$, from which point the same construction gives the initial stable homotopy equivalence. Meanwhile the $j = 0$ case stabilizes immediately (ie for $n = 1$) giving the spectrum of an unknot, which is known to be the sphere spectrum in q-degrees ± 1. $\square$

Remark 4.4.3. *It is clear that a similar argument could be used to define $\mathcal{X}(U_\gamma)$ for an unlink U allowing the colors on each component to tend to infinity. We do not go through the calculation here.*

We conclude with a brief discussion on the differences between the new approach of this section and the general approach of the previous one. One difference is that we use right-handed twisting in this new approach, but this is of no consequence and a left-handed version of the new approach could easily be derived. The important difference is that, in the general case, the stable homotopy equivalences required are based on Rozansky's maps f_n which are very complicated, requiring multiple properties of the categorified projectors (idempotency, straightening adjacent braids, a careful multi-cone presentation). Even with no crossings (as in the unknot or unlink), the passage from cabling with n strands to cabling with $n+1$ requires extra projectors and clever manipulations between them. In our new approach for the unknot, the only maps required are those that already arise in the stable sequence (4.4.1) based on resolving crossings, and maps derived from Reidemeister moves providing the isotopy between $T(n, n+1)$ and $T(n+1, n)$. In fact this new approach views the tail of the colored L-S-K spectra of the unknot as a stabilization (one q-degree at a time) of the sequence $\mathcal{X}(T(n+1, n))$ as $n \to \infty$, rather than as a statement about categorified projectors and colored spectra in the usual sense.

The simple form of the maps used in this approach also gives an improvement on the bound on n for stabilization. In Rozansky's approach, the bound grows like $2j$,

while here the bound grows like $\frac{j}{2}$. Compare Table 4.3 to Table 4.2 to see the gap between beginning of stabilization for adjacent columns in the two cases.

4.4.1 Proof of Theorem 4.4.2

The map of Equation 4.4.3 is built in the same way as the maps of Proposition 3.2.1. We have cofibration sequences similar to those in Figure 3.3 where the tangle $\mathbf{Z}$ is now just the vertical identity tangle $\mathbf{I}$, and the full twists on the left are now allowed to be fractional twists. In a slight abuse of notation, we set $D_0 := T(n, m)$ and D_i to be the link obtained from D_{i-1} by resolving the 'topmost' crossing of D_i as a 0-resolution, and E_i obtained from D_{i-1} by resolving the topmost crossing as a 1-resolution. Note that these symbols are links now, not tangles, since we do not need to keep track of the extra tangle $\mathbf{Z}$. See Figure 4.2.

The concept of this proof is the same as that of Proposition 3.2.2. That is, we write out a cofibration sequence for each $i = 1, \ldots, n-1$

$$\mathcal{X}^{(j-n)+N_{D_i}}(D_i) \hookrightarrow \mathcal{X}^{(j-n)+N_{D_{i-1}}}(D_{i-1}) \twoheadrightarrow \mathcal{X}^{(j-n)-1+N_{E_i}}(E_i) \tag{4.4.7}$$

and try to show that all of the terms $\mathcal{X}^{(j-n)+N_{E_i}}(E_i)$ are homologically trivial. The only ingredient from before that is missing here is a counting lemma similar to Lemma 3.1.3 for the E_i that are encountered here (in particular, these E_i involve fractional twists instead of full twists). Thus, our main goal is to prove

Lemma 4.4.5. *Any diagram E_i coming from $T(n, m+1)$ as above can be simplified*

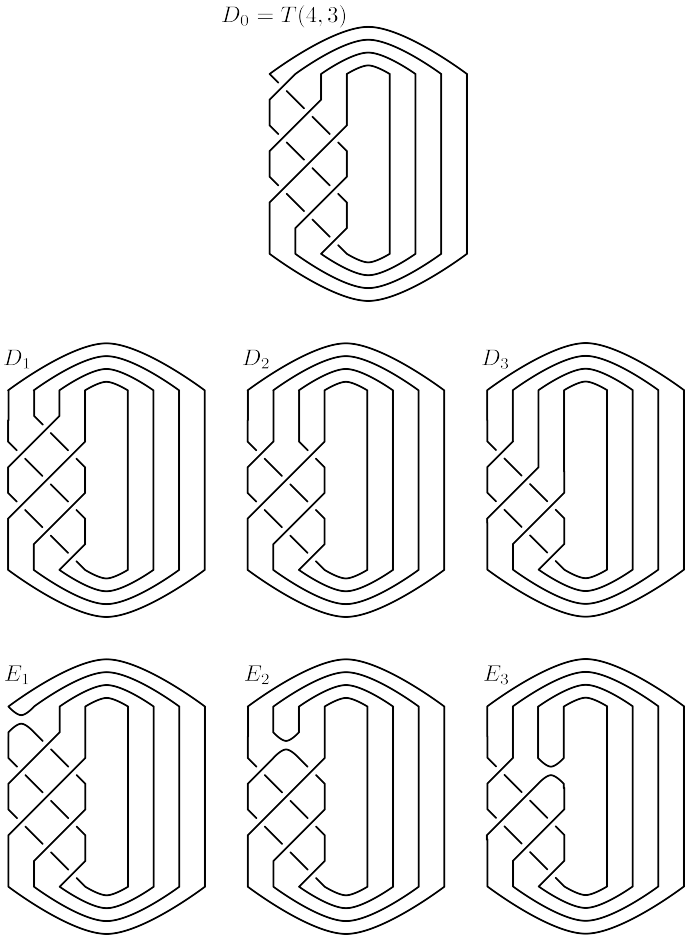

Figure 4.2: The new definition for D_i and E_i, illustrated for the case $n = 4$, $m = 2$. In this case, $D_0 = T(4,3)$, while $D_3 = D_{n-1} = T(4,2)$.

by Reidemeister moves to a new positive link diagram E_i' by pulling the turnbacks through the twisting. Letting N_{E_i} and $N_{E_i'}$ denote the normalization shifts $n^+ - 2n^-$ for each of these diagrams, we have for $m \geq n-1$

$$N_{E_i'} > N_{E_i} + n + m - 2 \tag{4.4.8}$$

Proof. For $m \geq n$, this bound follows from Lemma 1 in [Sto07]. The count $n+m-2$

is a direct translation of Stošić's count of negative crossings in the diagram E_i, and each negative crossing gets removed by either a Reidemeister 1 or Reidemeister 2 move as we pull the turnback through the diagram to arrive at E_i'. Reidemeister 2 moves shift the normalization by precisely 1 (loss of one positive and one negative crossings affecting $N = n^+ - 2n^-$), while the Reidemeister 1 moves will clearly be for negative crossings giving a shift of 2. Because $m \geq n$, we have at least one full twist to pull through which guarantees at least 2 Reidemeister 1 moves, which accounts for the strict inequality. Indeed in this case, we are guaranteed $N_{E_i'} > N_{E_i} + n + m - 1$ because we have at least 2 such moves.

When $m = n - 1$, we treat E_1 separately from the other E_i. For E_1 we see the diagram illustrated in Figure 4.3, where the strands are closed up outside of the picture in the usual way. The red circles clearly indicate that the turnback can be pulled through via $n-2$ Reidemeister 2 moves, then a negative Reidemeister 1 move, then another $n-2$ Reidemeister 2 moves. The shifts above quickly show that

$$N_{E_i'} = N_{E_i} + 2n - 2 = N_{E_i} + n + m - 1$$

indicating that we do need the precise form of Equation 4.4.8.

For $E_{i>1}$, we see that the turnback can be pulled through the torus braid $\mathcal{T}(n, n-1)$ leaving us with a copy of $\mathcal{T}(n-2, n-3)$ as in Figure 4.4 (note that we use the notation $\mathcal{T}$ to indicate the fractionally twisting torus braid rather than the complete torus link). Now we count crossings similarly to the proof of Lemma 3.1.3. The initial braid $\mathcal{T}(n, n-1)$ had $(n-1)^2$ crossings, while the new $\mathcal{T}(n-2, n-3)$ has $(n-3)^2$

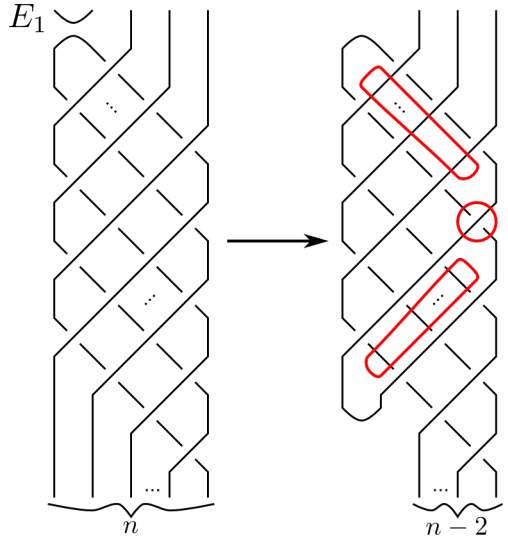

Figure 4.3: The picture for E_1, where the topmost turnback is pulled around the cabling allowing for the diagram on the right; the red circles indicate Reidemeister moves that will occur while pulling the turnback through the twisting.

crossings. The crossings 'above' the braid remain unchanged, so the total change in the number of crossings is $(n-1)^2 - (n-3)^2 = 4n - 8$. Since the turnback was able to swing completely around the entire torus braid (see the red dashed line in Figure 4.4), it must have accomplished precisely two (negative) Reidemeister 1 moves (ie a shift of 4). This leaves $4n - 10$ crossings eliminated by Reidemeister 2 moves (see Figure 4.3 to see that these are the only moves involved), ie a shift of $2n - 5$. We compute a total shift of $2n - 1 = m + n$, again verifying the inequality. □

The bound $m \geq n-1$ contributes the $(n-1)$ term in the bound given in Theorem 4.4.2. Meanwhile, we also need a bound on the minimal q-degree of our E_i' similar to

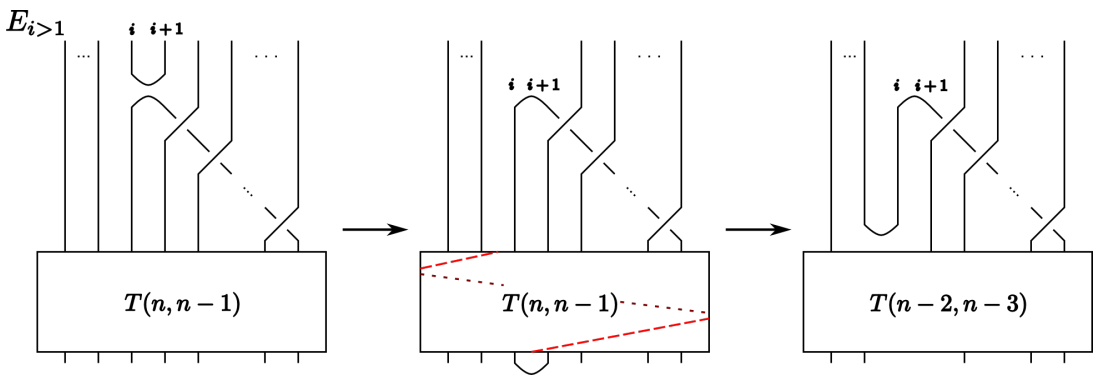

Figure 4.4: The picture for $E_{i>1}$; the topmost turnback is pulled around the cabling and then through the torus braid $\mathcal{T}(n, n-1)$ along the indicated dashed line, eliminating two strands from the braid but keeping the twisting at one strand less than a full twist, leaving us with $\mathcal{T}(n-2, n-3)$.

Equation 3.2.7.

Lemma 4.4.6. *For each $i = 1, \ldots, n-1$, the diagram E_i' coming from Lemma 4.4.5 has minimal q-degree bound*

$$\min_q(E_i') \geq N_{E_i'} - (n-1). \tag{4.4.9}$$

Proof. Using the same logic as Equation 3.2.7, we have

$$\begin{aligned} \min_q(E_i') &\geq N_{E_i'} - \#\text{circ}(E'_{i,\text{all-zero}}) \\ &\geq N_{E_i'} - (n-1) \end{aligned}$$

where we bound the number of circles $\#\text{circ}(E'_{i,\text{all-zero}}) \leq n-1$ as follows. Each disjoint circle must have at least one local max. The diagram $T(n,m)$ begins with n

local maxima. When we resolve one (and only one) crossing as a 1-resolution ($\asymp$) to create E_i, this pushes us to $n+1$ local maxima. However, since we pull the upper turnback around the diagram down to the bottom, we lose two local maxima, putting us at $n-1$. None of the moves during the simplification from E_i to E_i' introduce any new maxima. Thus we have the necessary bound. □

We now prove Theorem 4.4.2 by appealing to the logic of the proof of Proposition 3.2.2. For any $i = 1, \ldots, n-1$, we have that $\mathcal{X}^{(n-j)-1+N_{E_i}}(E_i) \simeq \mathcal{X}^{(n-j)-1+N_{E_i}}(E_i')$. But using Lemmas 4.4.5 and 4.4.6 (valid since we assume $m \geq n-1$), our assumption that $m \geq (j-n)$ implies

$$\begin{aligned}(j-n)-1+N_{E_i} &\leq m-1+N_{E_i} \\ &< N_{E_i'}-n+1 \\ &\leq \min_q(E_i')\end{aligned}$$

And thus $\mathcal{X}^{(n-j)-1+N_{E_i}}(E_i)$ is trivial for all i, and so all of the $\mathcal{X}^{(j-n)+N_{D_i}}(D_i)$ are stably homotopy equivalent, and since $D_0 = T(n, m+1)$ and $D_{n-1} = T(n,m)$, we are done.

Chapter 5

THE KHOVANOV HOMOLOGY AND L-S-K SPECTRUM FOR MORE GENERAL INFINITE BRAIDS

The purpose of this chapter is to prove Theorem 1.0.6, and then to state and prove a similar theorem for L-S-K spectra. All of the work in this chapter was done in collaboration with Gabriel Islambouli. We will begin by reviewing some homological algebra necessary for handling the limits of complexes arising from our infinite braids, mostly borrowed from the groundwork in [Roz14a] used to prove Theorem 2.2.4. Throughout this chapter, the notations h and q will be used to denote shifts in homological grading and q-grading, respectively, of Khovanov chain complexes (see Remark 5.1.1 to avoid potential confusion with the shifts involved in earlier notation).

5.1 Homological Algebra and Rozansky's Infinite Twist

5.1.1 A Closer Look at the Khovanov Chain Complex

We begin by recalling Equation 2.3.1 as it applies to a tangle $\mathbf{Z}$. We will be handling this cone construction more carefully moving forward, so we restate it here as a lemma.

Lemma 5.1.1. *Let $\mathbf{Z}$ be an oriented tangle, with a specified crossing* . *Let $\mathbf{Z}_0$ denote the same tangle with the crossing replaced by its 0-resolution* , *and let $\mathbf{Z}_1$ denote the same with the 1-resolution*  . *Then the shifted Khovanov complex of $\mathbf{Z}$ can be viewed as a mapping cone:*

$$\mathrm{h}^{n^-}\mathrm{q}^{-N}KC(\mathbf{Z}) = Cone\left(\mathrm{h}^{n_0^-}\mathrm{q}^{-N_0}KC(\mathbf{Z}_0) \longrightarrow \mathrm{h}^{n_1^-}\mathrm{q}^{-N_1+1}KC(\mathbf{Z}_1)\right). \tag{5.1.1}$$

Here n^- indicates the number of negative crossings in $\mathbf{Z}$, while N indicates $n^+ - 2n^-$, the number of positive crossings minus twice the number of negative crossings in $\mathbf{Z}$. The subscripts n_i^- and N_i indicate the same counts of crossings in $\mathbf{Z}_i$ for $i = 0, 1$.

The main arguments of this chapter will use this construction in an iterated fashion over many crossings. As such, the Cone() notation and the subscripts for the grading shifts quickly become unwieldy. For this reason, we drop the word Cone from the notation and adopt the following convention:

Definition 5.1.2. *The symbols n^- and $N := n^+ - 2n^-$ will count positive and negative*

crossings in whatever tangle they appear with. Thus Equation 5.1.1 will be written as

$$\mathrm{h}^{n^-}\mathrm{q}^{-N}KC(\mathbf{Z}) = \left(\mathrm{h}^{n^-}\mathrm{q}^{-N}KC(\mathbf{Z}_0) \longrightarrow \mathrm{h}^{n^-}\mathrm{q}^{-N+1}KC(\mathbf{Z}_1)\right) \tag{5.1.2}$$

and it will be understood that the various n^- and N are actually different numbers within this mapping cone.

Corollary 5.1.3. *Given tangles $\mathbf{Z}, \mathbf{Z}_0$, and $\mathbf{Z}_1$ as in Lemma 5.1.1, there is a chain map $\mathrm{h}^{n^-}\mathrm{q}^{-N}KC(\mathbf{Z}) \to \mathrm{h}^{n^-}\mathrm{q}^{-N}KC(\mathbf{Z}_0)$ with mapping cone that is chain homotopy equivalent to $\mathrm{h}^{n^-+1}\mathrm{q}^{-N+1}KC(\mathbf{Z}_1)$.*

Now in our normalization, KC itself is invariant under all Reidemeister moves. Combining this with the notational convention of Definition 5.1.2 gives the following shifts for the (negative) Reidemeister I and Reidemeister II moves that we shall need later.

$$\mathrm{h}^{n^-}\mathrm{q}^{-N}KC\left(\right) \simeq \mathrm{h}^{n^-+1}\mathrm{q}^{-N+2}KC\left(\right) \tag{5.1.3}$$

$$\mathrm{h}^{n^-}\mathrm{q}^{-N}KC\left(\right) \simeq \mathrm{h}^{n^-+1}\mathrm{q}^{-N+1}KC\left(\right) \simeq \mathrm{h}^{n^-}\mathrm{q}^{-N}KC\left(\right) \tag{5.1.4}$$

Compare these shifts to those that occur using the grading conventions in [Roz14a], and to the counting arguments used in the earlier chapters (particularly Lemma 4.4.5). Meanwhile, since Reidemeister III moves only change the arrangement of crossings rather than their number or orientation, we see that Reidemeister III moves incur no shifts to either homological or q-grading even within this renormalized setting.

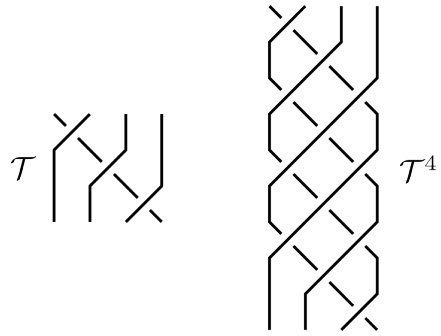

Figure 5.1: The fractional twist $\mathcal{T}$ and the full twist $\mathbf{T} = \mathcal{T}^n$ in the case $n = 4$.

Remark 5.1.1. *There is a potential for confusion in the shifting notation used here. The shifting functors* h *(or* Σ*) and* q *indicate a shift in homological and q-degrees for* KC *and* $\mathcal{X}$*. However, a superscript on* KC *or* $\mathcal{X}$ *indicates a specified degree, and this specification is taken to occur* after *any indicated shifts. For example, for any given* $j \in \mathbb{Z}$*, we have that* $\mathrm{q}^{-N}KC^j(L) = (\mathrm{q}^{-N}KC)^j(L) = KC^{j+N}(L)$.

5.1.2 Limits of Chain Complexes and Rozansky's Infinite Twist

Definition 5.1.4. *In the braid group* $\mathfrak{B}_n$ *on* n *strands, the symbol* $\mathcal{T}$ *will denote the* fractional (right-handed) twist $\mathcal{T} := \sigma_1\sigma_2\cdots\sigma_{n-1}$*. We will continue to use the notation* $\mathbf{T}$ *for the full twist* $\mathbf{T} = \mathcal{T}^n$.

In [Roz14a] Lev Rozansky provided a notion of a system of chain complexes stabilizing to some limiting complex, and proved Theorem 2.2.4 stating that $\lim_{k\to\infty} \mathrm{h}^{n^-}\mathrm{q}^{-N}KC(\mathbf{T}_n^k) \cong \mathbf{P}_n$.

Remark 5.1.2. *In fact Rozansky's original result concerned left-handed rather than right-handed twisting, but the methods clearly translate to the right handed case with no trouble. The left-handed version recovers a power series expansion of P_n in the variable q^{-1}; see Remark 2.2.6.*

For a full account of the notions involved with such limiting complexes, see [Roz14a]. Here we recall only the material most helpful for our current purposes, translated to right-handed twisting.

Definition 5.1.5. *Given a chain map $\mathbf{A} \xrightarrow{f} \mathbf{B}$ between chain complexes, let $|f|_h$ denote the maximal degree d for which the complex $Cone(f)$ is chain homotopy equivalent to a complex $\mathbf{C}$ that is trivial below homological degree d.*

In essence, $|f|_h$ denotes the maximal homological degree through which the map f gives a chain homotopy equivalence between $\mathbf{A}$ and $\mathbf{B}$. Note that all of the chain complexes being discussed here have differential *increasing* homological degree by 1 (as in the Khovanov chain complex).

Definition 5.1.6. *An* inverse system *of chain complexes is a sequence of chain maps*

$$\{\mathbf{A_k}, f_k\} := \mathbf{A_1} \xleftarrow{f_1} \mathbf{A_2} \xleftarrow{f_2} \cdots \tag{5.1.5}$$

Such a system is called Cauchy *if the maps f_k satisfy $|f_k|_h \to \infty$ as $k \to \infty$.*

Definition 5.1.7. *An inverse system $\{\mathbf{A_k}, f_k\}$ has a* (inverse) limit $\mathbf{A}_\infty := \lim_{k\to\infty} \mathbf{A_k}$ *if there exist maps $\tilde{f}_k : \mathbf{A}_\infty \to \mathbf{A_k}$ that commute with the system maps f_k such that $|\tilde{f}_k|_h \to \infty$ as $k \to \infty$.*

Theorem 5.1.8 (Theorem 2.5 in [Roz14a]). *An inverse system of chain complexes* $\{\mathbf{A_k}, f_k\}$ *has a limit* $\mathbf{A}_\infty$ *if and only if it is Cauchy.*

Unwinding the definitions and results in [Roz14a], we see that the limiting complex $\mathbf{A}_\infty$ of Theorem 5.1.8 is, up through homological degree d, chain homotopy equivalent to the corresponding $\mathbf{A_{k_0}}$ beyond which all of the maps $f_{k\geq k_0}$ satisfy $|f_{k\geq k_0}|_h \geq d$. In this sense the chain complexes $\mathbf{A_k}$ stabilize to give the limiting complex $\mathbf{A}_\infty$ "one homological degree at a time". Thus if we have a second inverse system of $\mathbf{B}_\ell$'s with homotopy equivalences to the $\mathbf{A_k}$'s up through ever-increasing homological degrees, we should be able to conclude that $\mathbf{B}_\infty \simeq \mathbf{A}_\infty$. The following proposition clarifies this idea.

Proposition 5.1.9. *Suppose* $\{\mathbf{A_k}, f_k\}$ *and* $\{\mathbf{B}_\ell, g_\ell\}$ *are Cauchy inverse systems with limits* $\mathbf{A}_\infty = \lim_{k\to\infty} \mathbf{A_k}$ *and* $\mathbf{B}_\infty = \lim_{\ell\to\infty} \mathbf{B}_\ell$ *respectively. Suppose there are maps*

$$F_\ell : \mathbf{B}_\ell \to \mathbf{A_{k=z(\ell)}}$$

($z(\ell)$ *is an increasing function of* ℓ*, not necessarily strict, such that* $z(\ell) \to \infty$ *as* $\ell \to \infty$*) forming a commuting diagram with the system maps* f_k *and* g_ℓ*. If* $|F_\ell|_h \to \infty$ *as* $\ell \to \infty$*, then* $\mathbf{B}_\infty \simeq \mathbf{A}_\infty$*.*

Proof. Similar to the proof of Proposition 3.13 in [Roz14a], the definition of the limit provides maps that compose with the maps F_ℓ to give maps from $\mathbf{B}_\infty$ to all of the $\mathbf{A_k}$ (this may require composing with some of the maps f_k). Thus there is a map $F_\infty : \mathbf{B}_\infty \to \mathbf{A}_\infty$ making commutative diagrams with all of the $\tilde{f}_k$ (see Theorem 3.9

in [Roz14a]). All of the other maps have homological order going to infinity as ℓ and k go to infinity, forcing $|F_\infty|_h = \infty$ and thus $\mathbf{B}_\infty \simeq \mathbf{A}_\infty$. Figure 5.2 illustrates the situation that will occur within this chapter. □

5.2 Proving Theorem 1.0.6

5.2.1 An Overview

Definition 5.2.1. *A* semi-infinite right-handed braid $\mathcal{B}$ *on* n *strands is a semi-infinite word in the standard generators* σ_i *of the braid group* $\mathfrak{B}_n$

$$\mathcal{B} := \sigma_{j_1}\sigma_{j_2}\cdots \tag{5.2.1}$$

Such a braid is called complete *if each* σ_i *for* $i = 1, 2, \ldots, n-1$ *occurs infinitely often in the word for* $\mathcal{B}$.

Such an infinite braid $\mathcal{B}$ is called right-handed because there are no left-handed crossings (σ_i^{-1}) allowed.

Definition 5.2.2. *Given a semi-infinite right-handed braid* $\mathcal{B} = \sigma_{j_1}\sigma_{j_2}\cdots$, *the* ℓ^{th} partial braid of $\mathcal{B}$ *shall be the braid* $\mathcal{B}_\ell := \sigma_{j_1}\sigma_{j_2}\cdots\sigma_{j_\ell}$.

The proof of Theorem 1.0.6 will be based upon Proposition 5.1.9 and, in particular, Figure 5.2. With that diagram in mind, we have the following correspondences.

1. The chain complexes $\mathrm{h}^{n^-}\mathrm{q}^{-N}KC(\mathcal{T}^{kn})$ will play the role of the $\mathbf{A_k}$.

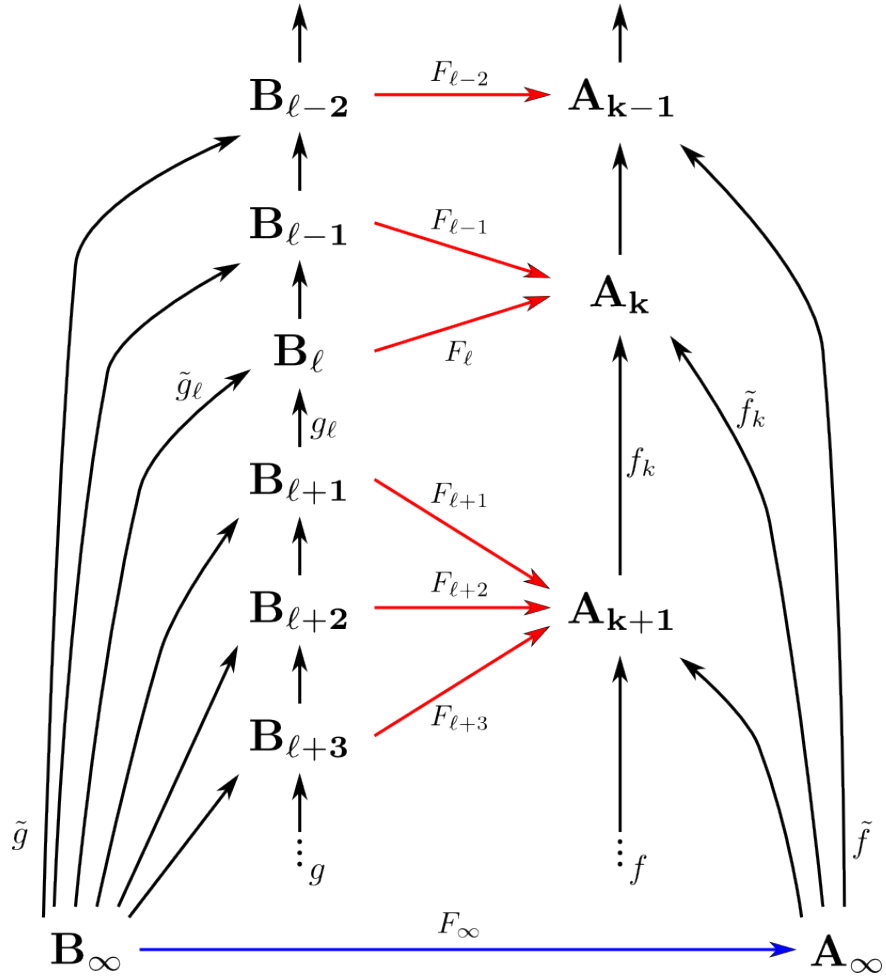

Figure 5.2: The diagram for Proposition 5.1.9. Given the two Cauchy systems $\{\mathbf{A_k}, f_k\}$ and $\{\mathbf{B}_\ell, g_\ell\}$, [Roz14a] provides the complexes $\mathbf{A}_\infty, \mathbf{B}_\infty$ and the maps $\tilde{f}, \tilde{g}$. If we can find maps F (shown in red), then [Roz14a] also provides the map F_∞ (blue). If we can show $|F_\ell|_h \to \infty$ as $\ell \to \infty$, then F_∞ is a chain homotopy equivalence.

2. Theorem 2.2.4 then guarantees that $\mathbf{A}_\infty \simeq \mathbf{P}_n$.

3. Given a semi-infinite right-handed braid $\mathcal{B} := \sigma_{j_1}\sigma_{j_2}\cdots$, the chain complexes $\mathrm{h}^{n^-}\mathrm{q}^{-N}KC(\mathcal{B}_\ell)$ will play the role of the $\mathbf{B}_\ell$.

4. Each map g_ℓ will be precisely the map of Corollary 5.1.3 obtained by resolving the crossing $\sigma_{j_{\ell+1}}$. The maps f_k are just compositions of such maps, as in [Roz14a].

5. The maps F_ℓ will be constructed via iterating Corollary 5.1.3 over a careful choice of crossings to resolve.

6. The function $k = z(\ell)$ will be based upon how far along the infinite braid $\mathcal{B}$ we must look before we can "see" the braid $\mathcal{T}^{kn}$ sitting within $\mathcal{B}_\ell$.

7. The estimates on $|F_\ell|_h$ will be based upon Corollary 5.1.3 together with careful use of Equations 5.1.3 and 5.1.4. Similar arguments will estimate $|g_\ell|_h$ to guarantee that $\{\mathbf{B}_\ell, g_\ell\}$ was indeed Cauchy.

5.2.2 The Details

Fix the number of strands n. We begin with a semi-infinite, right-handed, complete braid $\mathcal{B}$ and set out to prove Theorem 1.0.6 via Proposition 5.1.9 using the list of the overview. The points 1-4 of the overview require no further explanation. We begin

with points 5 and 6, that is, the construction of the map

$$F_\ell : \mathrm{h}^{n^-}\mathrm{q}^{-N}KC(\mathcal{B}_\ell) \to \mathrm{h}^{n^-}\mathrm{q}^{-N}KC(\mathcal{T}^{kn})$$

where $k = z(\ell)$ must be determined.

Given the braid $\mathcal{B}_\ell$, we start at the top of the braid (beginning of the braid word) and seek the first occurrence of generator σ_1. From that point we go downward and find the first occurrence of σ_2, and so forth until we reach σ_{n-1}. In this way we have found crossings within $\mathcal{B}_\ell$ that would, in the absence of the crossings we "skipped", give a single copy of $\mathcal{T}^1$. We connect these crossings with a dashed line going rightward then downward as in Figure 5.3, and we call such a set of crossings a *diagonal*. The crossings involved are called *diagonal crossings*. Having found such a diagonal within $\mathcal{B}_\ell$, we work our way back *up* the braid $\mathcal{B}_\ell$ in the same way going from the diagonal σ_{n-1} to the previous (not necessarily diagonal) σ_{n-2} and so forth until we reach another σ_1 (if there were no skipped crossings, we are now back at the σ_1 we started with). We begin the second diagonal from the first σ_1 that is *below* this σ_1 we found at the end of our upward journey. In this way we find disjoint diagonals with as few "skipped" crossings between them as possible. See Figure 5.3 for clarification.

Let $y(\ell)$ denote the number of diagonals that can be completed within $\mathcal{B}_\ell$ in this way. The function $z(\ell)$ determining the destination of the map F_ℓ is

$$z(\ell) := \left\lfloor \frac{y(\ell)}{n} \right\rfloor \tag{5.2.2}$$

where $\lfloor \cdot \rfloor$ denotes the integer floor function. Thus $z(\ell)$ gives the number of *full*

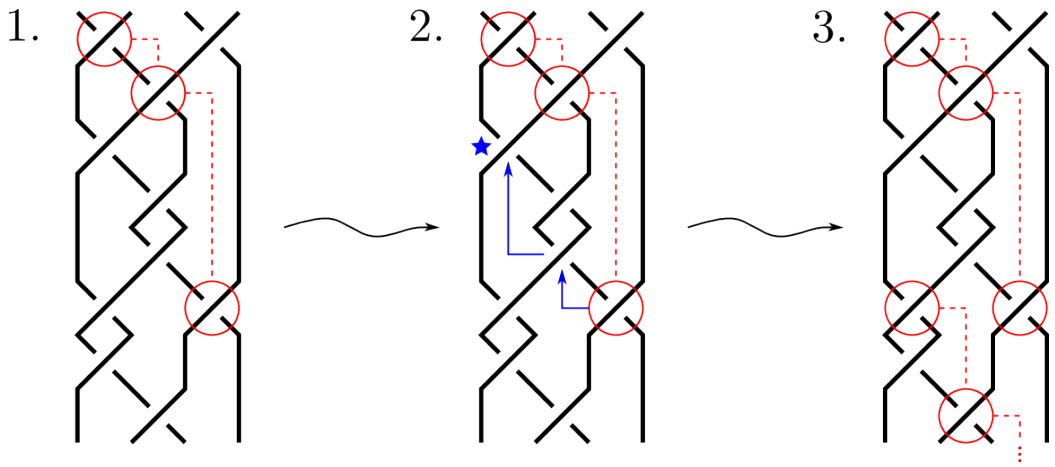

Figure 5.3: An illustration of finding diagonals within some $\mathcal{B}_\ell$. In step 1, we find the first diagonal illustrated in red. In step 2, we work our way back up from the diagonal σ_{n-1} as in the blue arrows until we arrive at the σ_1 marked by a blue star. In step 3, we begin forming the second diagonal starting from the first σ_1 below the starred crossing from step 2.

twists that can be seen within $\mathcal{B}_\ell$. The map F_ℓ is then the composition of maps coming from Corollary 5.1.3 where we are resolving all non-diagonal crossings in $\mathcal{B}_\ell$. Note that the order in which we resolve the crossings is irrelevant, and in fact the map F_ℓ can be viewed as a projection from the single mapping cone of the direct sum of the Khovanov maps assigned to each non-diagonal crossing. However in this chapter we shall consider F_ℓ as a large composition starting from resolving the bottom-most (non-diagonal) crossing. From this consideration it should be clear that the maps F_ℓ commute with the maps f_k and g_ℓ of the two systems $\mathrm{h}^{n^-}\mathrm{q}^{-N}KC(\mathcal{T}^{kn})$ and $\mathrm{h}^{n^-}\mathrm{q}^{-N}KC(\mathcal{B}_\ell)$, which are also just maps based on resolving bottom-most crossings.

We now move on to point 7 from the overview. We wish to estimate $|F_\ell|_h$. Viewing F_ℓ as a composition of projections from crossing resolutions as above, we estimate the homological order of the cone of the i^{th} such projection with the help of Corollary 5.1.3. That is, we view $\mathrm{h}^{n^-}\mathrm{q}^{-N}KC(\mathcal{B}_\ell)$ as an iterated mapping cone

$$\mathrm{h}^{n^-}\mathrm{q}^{-N}KC(\mathcal{B}_\ell) =$$
$$\Big(\Big(\Big(\cdots \to \mathrm{h}^{n^-}\mathrm{q}^{-N+1}KC(\mathbf{Z}_3)\Big) \to \mathrm{h}^{n^-}\mathrm{q}^{-N+1}KC(\mathbf{Z}_2)\Big) \to \mathrm{h}^{n^-}\mathrm{q}^{-N+1}KC(\mathbf{Z}_1)\Big)$$

and we consider the minimum homological order of

$$\mathrm{h}^{n^-+1}\mathrm{q}^{-N+1}KC(\mathbf{Z}_i)$$

where $\mathbf{Z}_i$ is a tangle that is obtained from $\mathcal{B}_\ell$ by resolving the first $i-1$ non-diagonal crossings (starting from the bottom of the braid) as 0-resolutions, and then resolving the i^{th} non-diagonal crossing as a 1-resolution. Iterating Lemma 5.1.1 over all of the

remaining non-diagonal crossings, we can see $\mathrm{h}^{n^-+1}\mathrm{q}^{-N+1}KC(\mathbf{Z}_i)$ as a large multi-cone as illustrated in Figure 5.4.

Note that every diagram within the large multi-cone for $\mathrm{h}^{n^-+1}\mathrm{q}^{-N+1}KC(\mathbf{Z}_i)$ is made up of diagonal crossings and possible turnbacks from 1-resolutions ($\asymp$) between the diagonals. Indeed we are guaranteed at least the one turnback pair ($\asymp$) already present within $\mathbf{Z}_i$, but there may be many more. Now we turn to the key lemma that produces the required estimate on $|F_\ell|_h$. This lemma can be seen as a generalization of the counting lemmas 3.1.3 and 4.4.5 used in previous chapters.

Lemma 5.2.3. *Let $\mathcal{D}$ be any (n,n) tangle diagram involving precisely y diagonals of crossings, no other crossings, and at least one pair of turnbacks between the diagonals (see the diagrams in Figure 5.4). Then $\mathcal{D}$ can be simplified to a new diagram $\mathcal{D}'$ via Reidemeister 3, Reidemeister 2, and negative Reidemeister 1 moves. During this process, all of the Reidemeister 2 and negative Reidemeister 1 moves remove crossings, and the total number of such moves is at least y.*

Proof. We view the y diagonals as partitioning the diagram $\mathcal{D}$ into $y+1$ *zones*, and we call such a zone *empty* if there are no turnbacks ($\asymp$) within it. By assumption there is at least one non-empty zone. We start from the topmost non-empty zone, and choose the 'bottommost' such pair in this zone (ie, the last σ_{j_m} within the given zone where a 1-resolution occurred). The lower turnback can then be passed through the diagonals below it one at a time via Reidemeister II moves (Figure 5.5) and negative Reidemeister I moves (first step of Figure 5.6) until the turnback reaches the next non-

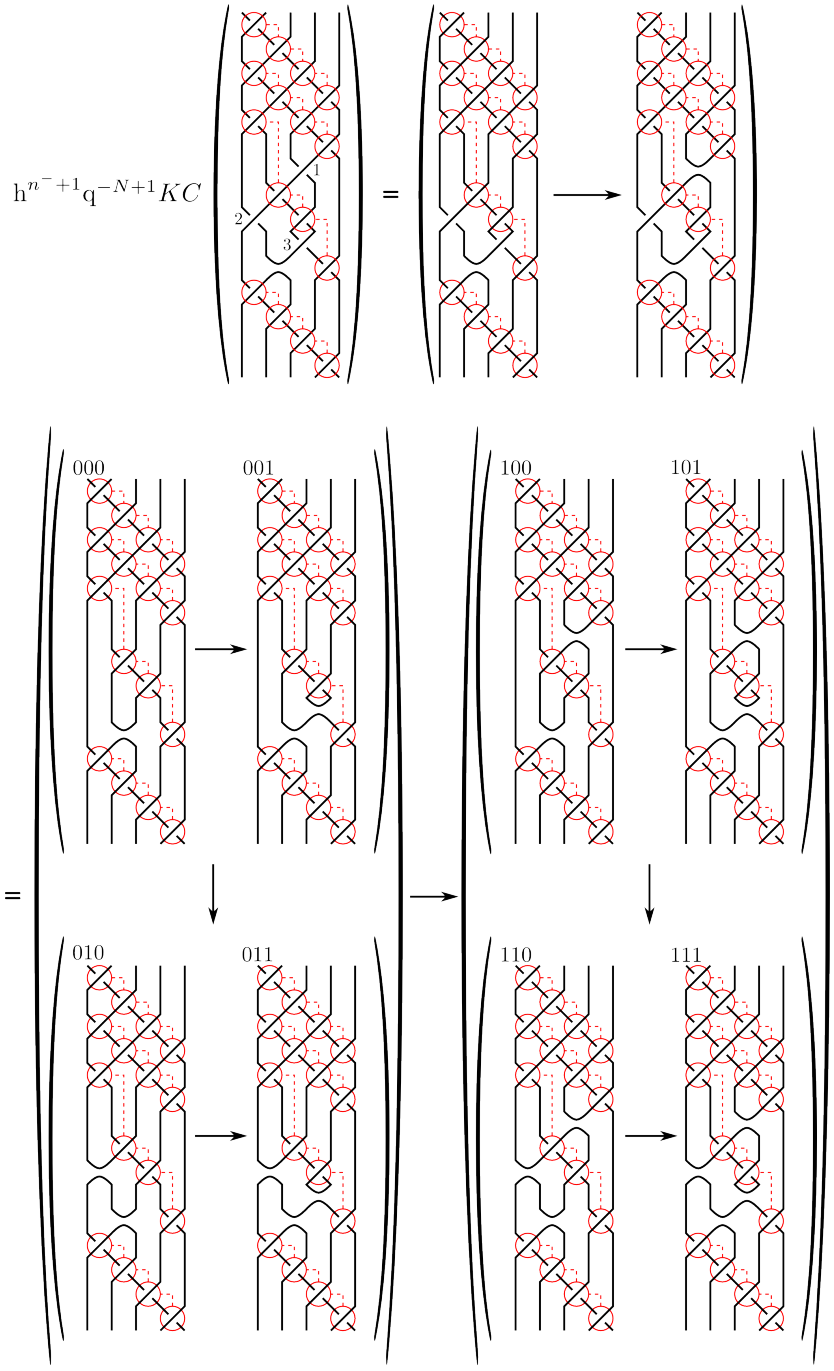

Figure 5.4: A multicone presentation for an example $\mathrm{h}^{n^-+1}\mathrm{q}^{-N+1}KC(\mathbf{Z}_i)$. The KC notation and the shifts $\mathrm{h}^{n^-+1}\mathrm{q}^{-N+1+r}$ on each term are suppressed. Here r is the sum of the three resolution numbers above each diagram.

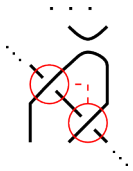

Figure 5.5: Pulling a turnback downward through a diagonal via Reidemeister II.

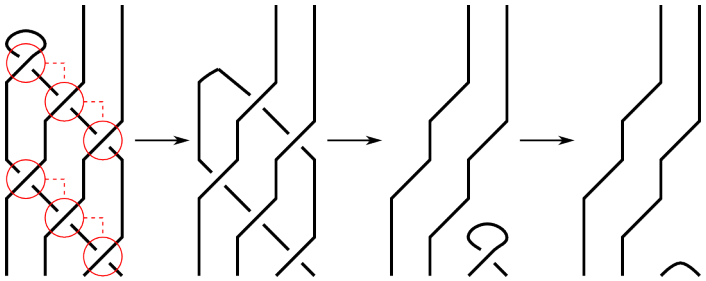

Figure 5.6: An example of pulling a turnback downward through two diagonals via negative Reidemeister I and Reidemeister II moves.

empty zone. Note that, following a Reidemeister I move into an empty zone, multiple moves are required to pass through the next diagonal (also illustrated in Figure 5.6). Nevertheless, it is clear that during this process, the number of such Reidemeister moves will be at least the same as the number of diagonals passed through.

Having now reached the second non-empty zone, we find the bottommost turnback within this zone and continue the process until the final zone is reached. This accounts for passing through all the diagonals below the topmost non-empty zone. Finally, we return to that starting zone and choose the 'topmost' turnback within that zone (ie the first σ_{j_m} within that zone where a 1-resolution occurred) and pass this turnback through all of the diagonals above it. If the first move required is a Reidemeister II

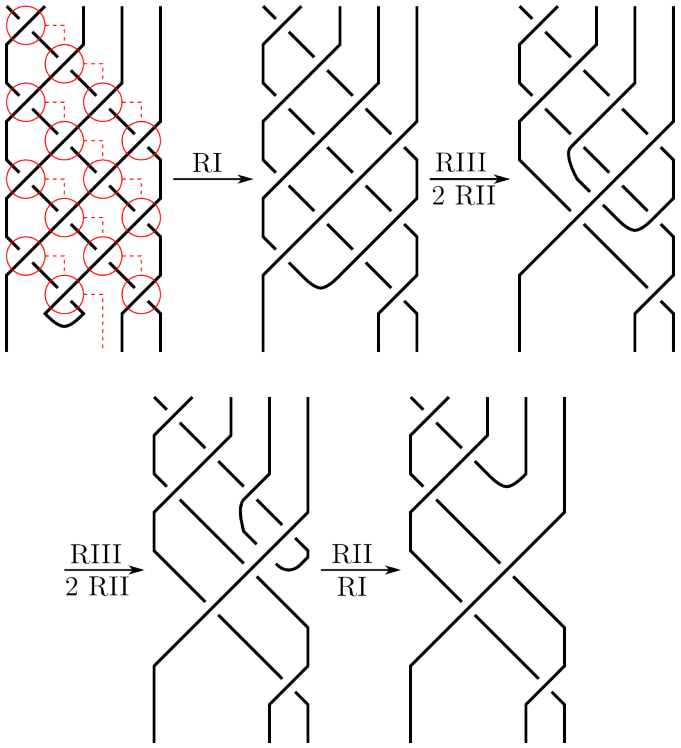

Figure 5.7: An example of pulling a turnback upward through diagonals. Each step indicates passing through one diagonal, so that the total number of negative Reidemeister I and Reidemeister II moves is clearly at least the number of such diagonals.

move (ie the two strands connected by the turnback are adjacent on the defining torus of the twist), this process will be the same as the downward one. If the first move is a (negative) Reidemeister I move, this process may require some Reidemeister III moves as illustrated in Figure 5.7. However it is clear that there will still be at least as many Reidemeister II and negative Reidemeister I moves as there are diagonals, and thus the total number of such moves is at least y as desired.

More conceptually, a sequence of diagonals with empty zones between them cor-

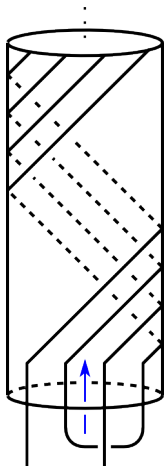

Figure 5.8: A topmost turnback entering a set of diagonals corresponds to a turnback being pulled through the center of a torus braid as shown here. The blue arrow indicates the direction of the pulling.

responds to a torus braid. A topmost turnback below this (or bottommost turnback above this) corresponds to connecting two strands of the torus braid. The simpler cases above correspond to these two strands being adjacent, while the more complex case of Figure 5.7 corresponds to connecting two non-adjacent strands. Either way, the turnback can be pulled up (or down) through the center of the torus as in Figure 5.8. Passing through diagonals corresponds to passing by other strands, which must eliminate crossings, thus necessitating at least one Reidemesiter I or II move. The Reidemeister I moves must be negative because they are undoing right-handed twisting. □

Corollary 5.2.4. *Every term* $\mathrm{h}^{n^-+1}\mathrm{q}^{-N+1+r}KC(\mathcal{D})$ *in the multicone expansion of any* $\mathrm{h}^{n^-+1}\mathrm{q}^{-N+1}KC(\mathbf{Z}_i)$ *(see Figure 5.4) is chain homotopy equivalent to a complex*

of the form $\mathrm{h}^{n^-+1+s_h}\mathrm{q}^{-N+1+r+s_q}KC(\mathcal{D}')$ *where* s_h *and* s_q *are homological and* q*-degree shifts depending on the expansion term, and* r *is the number of 1-resolutions taken to arrive at* $\mathcal{D}$ *from* $\mathbf{T_i}$*. Moreover, for any term in the expansion,* $s_q \geq s_h \geq y$*.*

Proof. The shifts come from Equations 5.1.3 and 5.1.4. □

As an example of Corollary 5.2.4, consider the (111)-entry from Figure 5.4. We illustrate the process of Lemma 5.2.3, keeping track of the shifts, for this entry in Figure 5.9. In this case we get $s_h = 4 = y$, while $s_q = 5$. As an illustration of the case where Reidemeister III moves are also required, we show the process for the (001)-entry in Figure 5.10 where $s_h = 8 > y$ and $s_q = 10$. Notice that further simplifications are possible in the first case, indicating that our given bounds will rarely be sharp.

Proof of Theorem 1.0.6. We build a commuting diagram as in Figure 5.2 using the listed points of the overview. The construction of F_ℓ as a composition of mapping cone projections p ensures $|F_\ell|_h$ is at least as large as the minimum $|p|_h$ amongst all such p. As described above, this is precisely the minimum homological order amongst all the $\mathrm{h}^{n^-+1}\mathrm{q}^{-N+1}KC(\mathbf{Z}_i)$ via Corollary 5.1.3. Corollary 5.2.4 guarantees that the minimal homological degree of any term in the multicone expansion of such a complex (and thus for the entire complex) is at least y, the number of diagonals found in $\mathcal{B}_\ell$. Thus we have

$$|F_\ell|_h \geq y.$$

The assumption that the semi-infinite braid $\mathcal{B}$ is complete ensures that $y \to \infty$ as

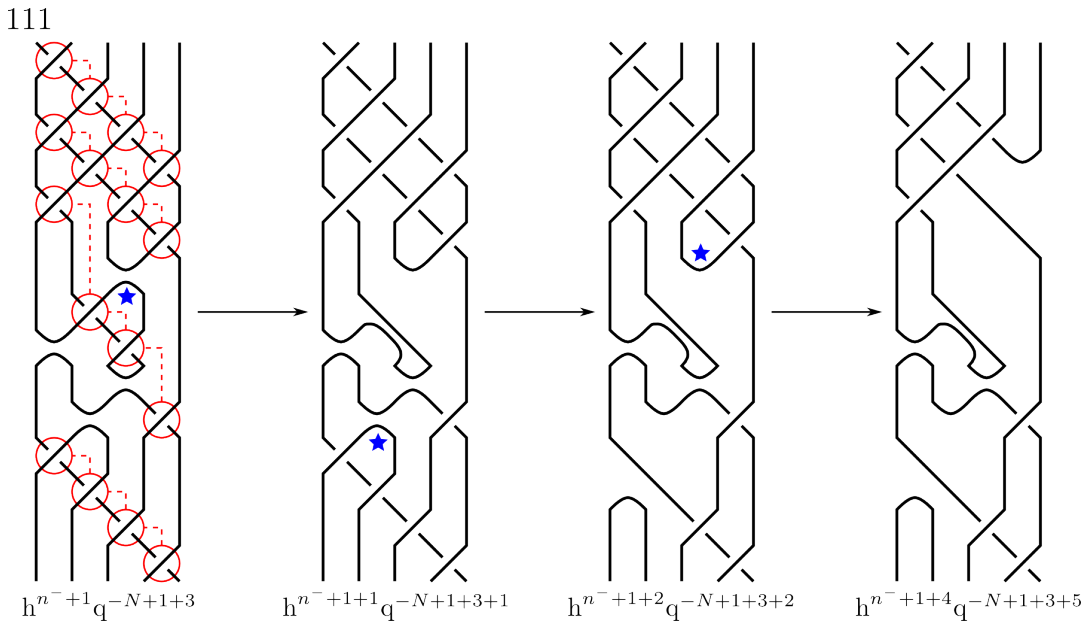

Figure 5.9: The process of Lemma 5.2.3 shown for the (111)-entry from Figure 5.4, illustrating the degree shifts of Corollary 5.2.4. The turnback that is about to be 'pulled' is indicated by a blue star.

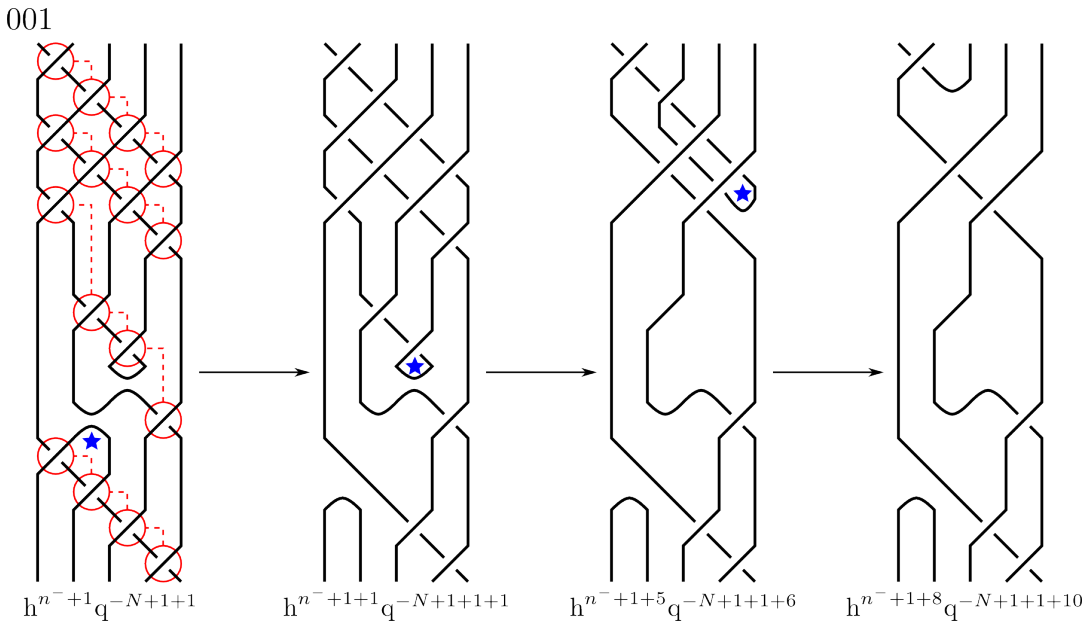

Figure 5.10: The process of Lemma 5.2.3 shown for the (001)-entry from Figure 5.4, illustrating the degree shifts of Corollary 5.2.4. The turnback that is about to be 'pulled' is indicated by a blue star.

$\ell \to \infty$. The mapping cones of the maps g_ℓ also involve diagrams with turnbacks, so that a similar (and simpler) argument also ensures $|g_\ell|_h \to \infty$ as $\ell \to \infty$, verifying that this system is Cauchy and has a limit. Thus we may use Proposition 5.1.9 to conclude the proof. □

5.3 A Similar Theorem for L-S-K Spectra

In this section we seek to generalize the work of the previous section into the realm of the L-S-K spectra built with infinite twists in Chapter 3. The precise statement is provided below.

Theorem 5.3.1. *Let $\overline{\mathcal{B}}$ denote any closure of a complete semi-infinite positive braid $\mathcal{B}$ as in Theorem 1.0.6. Let $\overline{\mathcal{T}^\infty}$ denote the corresponding closure of the infinite twist. Then*

$$\mathcal{X}(\overline{\mathcal{B}}) := \lim_{\ell \to \infty} \Sigma^a \mathrm{q}^b \mathcal{X}(\overline{\sigma_{j_1}\sigma_{j_2}\cdots\sigma_{j_\ell}}) \simeq \mathcal{X}(\overline{\mathcal{T}^\infty}) \tag{5.3.1}$$

where a and b stand for homological shifts (via suspensions Σ) and q-degree shifts.

Figure 5.11 illustrates a closure of $\mathcal{B}$ and the corresponding closure of $\mathcal{T}^\infty$. As noted earlier (see Remark 2.3.1), the L-S-K spectrum for braids and/or tangles has not yet been defined; as such, Theorem 5.3.1 is the closest notion available to a lifting of Theorem 1.0.6 to the stable homotopy category.

The proof of Theorem 5.3.1 is a very simple generalization of the proof of Theorem 1.0.6 to the setting of the L-S-K spectra. In short, we build a diagram similar to

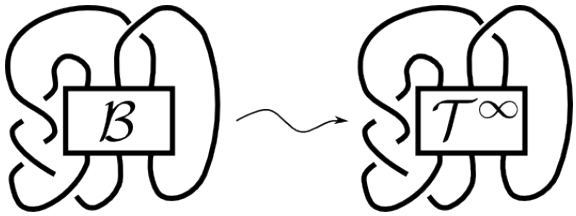

Figure 5.11: A possible closure $\overline{\mathcal{B}}$ of the infinite braid $\mathcal{B}$, and the corresponding closure $\overline{\mathcal{T}^\infty}$ of the infinite twist.

Figure 5.2 out of spectra instead of chain complexes. Then instead of tracking the homological order below which the maps are chain homotopy equivalences, we track the q-degree below which the maps are stable homotopy equivalences. Corollary 5.2.4 ensures that this maximal q-degree of equivalence goes to infinity as the sequence of maps goes to infinity.

We begin by recalling the cofibration sequence of Equation 2.3.2, repeated below for convenience.

$$\Sigma^a \mathcal{X}^{j+N_{L_0}}(L_0) \hookrightarrow \mathcal{X}^{j+N_L}(L) \twoheadrightarrow \Sigma^b \mathcal{X}^{j-1+N_{L_1}}(L_1)$$

Then if we continue to use the convention of Definition 5.1.2, the version of Lemma 2.3.7 we will use is restated as a corollary here.

Corollary 5.3.2. *If for some q-degree $j \in \mathbb{Z}$ we have $\mathrm{q}^{-N+1}KC^j(L_1)$ homologically trivial, then the inclusion map*

$$\Sigma^{n^-} \mathcal{X}^{j+N}(L_0) \hookrightarrow \Sigma^{n^-} \mathcal{X}^{j+N}(L) \tag{5.3.2}$$

is a stable homotopy equivalence.

We now generalize the definitions needed to discuss stable limits of infinite sequences of L-S-K spectra, as in Definition 5.1.6 and Theorem 5.1.8. We do not need a notion of sequences of spectra being 'Cauchy', but we do need some notion of stability.

Definition 5.3.3. *A map between L-S-K spectra* $f : \Sigma^{n^-}\mathrm{q}^{-N}\mathcal{X}(L) \to \Sigma^{n^-}\mathrm{q}^{-N}\mathcal{X}(L')$ *is called* q-homogeneous *if* f *preserves normalized* q*-degrees between wedge summands. That is,*

$$f = \vee_{j\in\mathbb{Z}} f^j \tag{5.3.3}$$

for q*-preserving maps*

$$f^j : \mathcal{X}^{j+N}(L) \to \mathcal{X}^{j+N}(L').$$

In this case, we let $|f|_q$ *denote the maximal* q*-degree* d *for which* f^j *is a stable homotopy equivalence for all* $j \leq d$*.*

It is clear from the definitions that the maps of Equation 2.3.2 are q-homogeneous.

Definition 5.3.4. *An infinite sequence of* q*-homogeneous maps*

$$\Sigma^{n^-}\mathrm{q}^{-N}\mathcal{X}(L_0) \xrightarrow{f_0} \Sigma^{n^-}\mathrm{q}^{-N}\mathcal{X}(L_1) \xrightarrow{f_1} \Sigma^{n^-}\mathrm{q}^{-N}\mathcal{X}(L_2) \xrightarrow{\cdots} \tag{5.3.4}$$

will be called a direct q-system *of L-S-K spectra, denoted* $\{\mathcal{X}(L_k), f_k\}$*. Such a system is called* q-stable *if* $|f_k|_q \to \infty$ *as* $k \to \infty$*.*

Theorem 5.3.5. *A* q*-stable direct* q*-system* $\{\mathcal{X}(L_k), f_k\}$ *has homotopy colimit*

$$\mathcal{X}(L_\infty) := hocolim\left(\Sigma^{n^-}\mathrm{q}^{-N}\mathcal{X}(L_0) \xrightarrow{f_0} \Sigma^{n^-}\mathrm{q}^{-N}\mathcal{X}(L_1) \xrightarrow{f_1} \Sigma^{n^-}\mathrm{q}^{-N}\mathcal{X}(L_2) \xrightarrow{\cdots}\right) \tag{5.3.5}$$

$$= \bigvee_{j\in\mathbb{Z}} \mathcal{X}^j(L_\infty) \tag{5.3.6}$$

where

$$\mathcal{X}^j(L_\infty) := hocolim\left(\mathcal{X}^{j-N}(L_0) \xrightarrow{f_0} \mathcal{X}^{j-N}(L_1) \xrightarrow{f_1} \mathcal{X}^{j-N}(L_2) \xrightarrow{\cdots}\right)$$

and for each j, there exists lower bound k_j such that

$$\mathcal{X}^j(L_\infty) \simeq \mathcal{X}^{j-N}(L_k) \ \ \forall k \geq k_j.$$

Proof. This is clear from the properties of a homotopy colimit after unwinding the definitions. □

Remark 5.3.1. *Notice that the maps of the sequence (5.3.4) go in the opposite direction as those of Equation 5.1.5 considered earlier for chain complexes. This is to be expected, since the inverse system of Equation 5.1.5 should be recovered by the singular cochain functor C^* which is* contravariant*. Similarly, our limits here are homotopy* co*limits, as opposed to the inverse limits considered in the previous section.*

With these ideas in place, we can state and prove the stable homotopy version of Proposition 5.1.9 providing the diagram corresponding to Figure 5.2.

Proposition 5.3.6. *Suppose $\{\mathcal{X}(L_k), f_k\}$ and $\{\mathcal{X}(M_\ell), g_\ell\}$ are q-stable direct q-systems with homotopy colimits $\mathcal{X}(L_\infty)$ and $\mathcal{X}(M_\infty)$ respectively, as in Equation 5.3.5. Suppose there are q-homogeneous maps*

$$F_\ell : \Sigma^{n^-}\mathrm{q}^{-N}\mathcal{X}(L_{z(\ell)}) \to \Sigma^{n^-}\mathrm{q}^{-N}\mathcal{X}(M_\ell)$$

($z(\ell)$ is an increasing function of ℓ, not necessarily strict, such that $z(\ell) \to \infty$ as $\ell \to \infty$) forming a commuting diagram with the system maps f_k and g_ℓ. If $|F_\ell|_q \to \infty$

as $\ell \to \infty$, then we have

$$\mathcal{X}(L_\infty) \simeq \mathcal{X}(M_\infty).$$

Proof. The proof is very similar to that of Proposition 5.1.9. See Figure 5.12. The properties of homotopy colimits provide the existence of q-homogeneous maps $\tilde{f}_k : \Sigma^{n^-}\mathrm{q}^{-N}\mathcal{X}(L_k) \to \mathcal{X}(L_\infty)$ and $\tilde{g}_\ell : \Sigma^{n^-}\mathrm{q}^{-N}\mathcal{X}(M_\ell) \to \mathcal{X}(M_\infty)$ as well as the map $F_\infty : \mathcal{X}(L_\infty) \to \mathcal{X}(M_\infty)$ which must commute with all of the other maps. Fixing some q-degree j, Theorem 5.3.5 and the assumption on the maps F_ℓ guarantee that the wedge summand maps $\tilde{f}_k^j$, $\tilde{g}_\ell^j$ and F_ℓ^j all become stable homotopy equivalences once k and ℓ are large enough. Thus F_∞ must also provide a stable homotopy equivalence $F_\infty^j : \mathcal{X}^j(L_\infty) \xrightarrow{\simeq} \mathcal{X}^j(M_\infty)$. This happens for all j, so in fact F_∞ is the desired (q-homogeneous) stable homotopy equivalence. □

Proof of Theorem 5.3.1. Given a specified closure $\overline{\mathcal{B}}$ of a complete semi-infinite right-handed braid $\mathcal{B}$ on n strands, we build the diagram of Figure 5.12 in a manner completely analogous the building of the diagram of Figure 5.2.

- The links L_k are the corresponding closures of the full twists $L_k := \overline{\mathcal{T}^{nk}}$.
- The maps f_k are compositions of the cofibration maps of Equation 5.3.2 coming from resolving the crossings of the last full twist in $\overline{\mathcal{T}^{n(k+1)}}$ as 0-resolutions (our convention will now be to resolve the bottom-most twist, rather than the top-most as in Chapter 3, since this aligns most closely with drawing braids downwards as we have done).

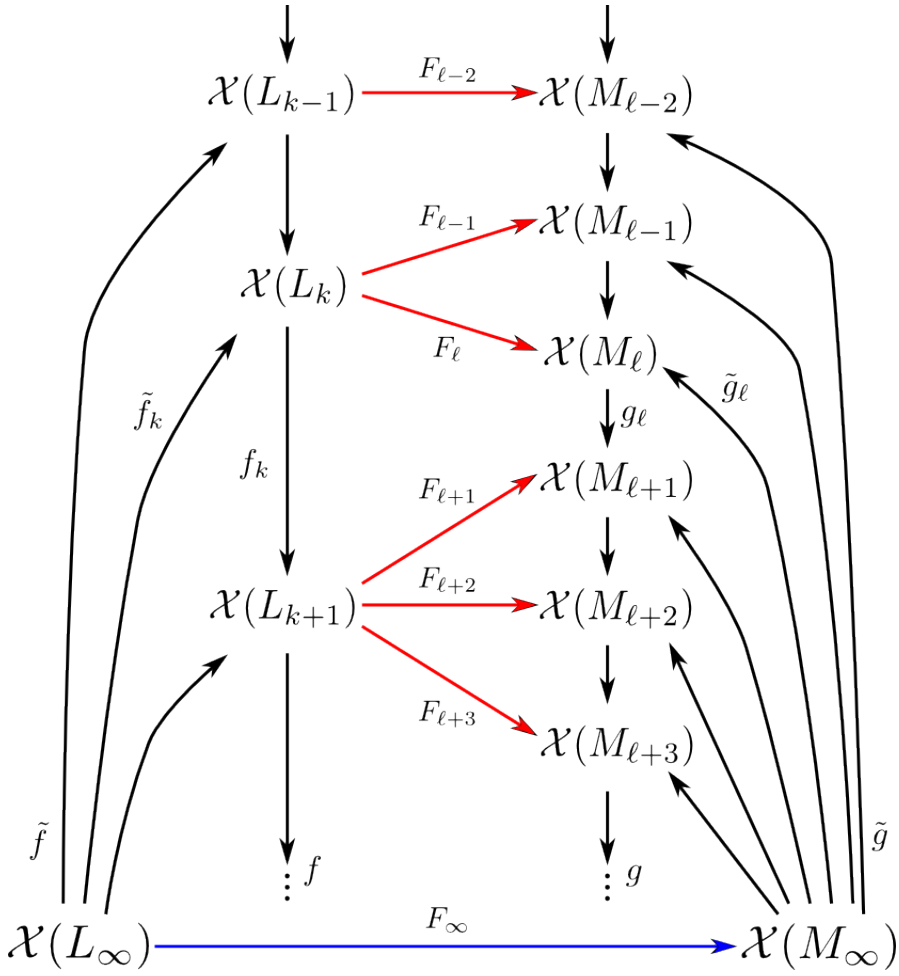

Figure 5.12: The diagram for Proposition 5.3.6, omitting the normalization shifts $\Sigma^{n^-}\mathrm{q}^{-N}$ on each term. Compare to Figure 5.2. Given the two q-stable systems $\{\mathcal{X}(L_k), f_k\}$ and $\{\mathcal{X}(M_\ell), g_\ell\}$, the homotopy colimits $\mathcal{X}(L_\infty)$ and $\mathcal{X}(M_\infty)$ come with maps $\tilde{f}$ and $\tilde{g}$. If we find the q-homogeneous maps F (red) and show that $|F_\ell|_q \to \infty$ as $\ell \to \infty$, then the map F_∞ on the colimits (blue) is a stable homotopy equivalence.

- The links M_ℓ are the corresponding closures of the partial braids $\mathcal{B}_\ell$, that is, $M_\ell := \overline{\mathcal{B}_\ell}$.

- The maps g_ℓ are the inclusion maps of Equation 2.3.2 coming from resolving the last crossing of $\mathcal{B}_{\ell+1}$ as a 0-resolution.

- The maps F_ℓ are compositions of inclusions coming from resolving non-diagonal crossings as 0-resolutions precisely as in the proof of Theorem 1.0.6.

See Figure 5.11 for the notion of corresponding closures of braids. In this language, Chapter 3 shows that the direct system $\{\mathcal{X}(\overline{\mathcal{T}^{nk}}), f_k\}$ is q-stable, with homotopy colimit $\mathcal{X}(\overline{\mathcal{T}^{\infty}})$ satisfying many properties similar to closures of the Jones-Wenzl projectors $\mathbf{P}_n$. The proof that $|F_\ell|_q$ and $|g_\ell|_q$ go to infinity with ℓ is analogous to the similar statement about $|F_\ell|_h$ and $|g_\ell|_h$ in the proof of Theorem 1.0.6. In short, we use Corollary 5.3.2 to change the question to one of homological triviality of $\mathrm{q}^{-N+1}KC^j(\overline{\mathbf{Z}_i})$ for closures of braids $\mathbf{Z}_i$ involving diagonals and turnbacks, as before. The estimate of Corollary 5.2.4 still holds, but now we are concerned with the minimum q-value (rather than minimum homological value) of a complex of the form $\mathrm{h}^{n^-+1+s_h}\mathrm{q}^{-N+1+r+s_q}KC(\overline{\mathcal{D}'})$ (where again $\mathcal{D}'$ came from a partial resolution $\mathcal{D}$ of $\mathbf{Z}_i$ by pulling turnbacks through diagonals). As in Chapters 3 and 4 we let $\#\mathrm{circ}(D_{\text{all-zero}})$ denote the number of circles present in the all-zero resolution of the diagram D. Then the minimum q-degree for generators of the complex $\mathrm{h}^{n^-+1+s_h}\mathrm{q}^{-N+1+r+s_q}KC(\overline{\mathcal{D}'})$ is

precisely

$$\min_q \left(\mathrm{h}^{n^- + 1 + s_h} \mathrm{q}^{-N+1+r+s_q} KC(\overline{\mathcal{D}'}) \right) = 1 + r + s_q - \#\mathrm{circ}(\overline{\mathcal{D}'}_{\text{all-zero}}) \tag{5.3.7}$$

since each circle in the all-zero resolution of the link can contribute a generator v_- with q-degree -1.

Now the number of circles in a resolution is bounded above by the number of local maxima present in the diagram. The number of such maxima in the all-zero resolution of any $\overline{\mathcal{D}'}$ is comprised of two parts, those within the tangle $\mathcal{D}'$ and those without (so those due to the specified closure). The second category will contribute some constant c that is independent of the tangle $\mathcal{D}'$, and indeed independent of the infinite braid $\mathcal{B}$ at all. The first category will be bounded above by the number of 1-resolutions that were taken to arrive at $\mathcal{D}$ from $\mathcal{B}_\ell$ (note that the process of pulling turnbacks through diagonals does not create maxima). But this number is precisely $1 + r$. Thus we have

$$\begin{aligned} \min_q \left(\mathrm{h}^{n^- + 1 + s_h} \mathrm{q}^{-N+1+r+s_q} KC(\overline{\mathcal{D}'}) \right) &= 1 + r + s_q - \#\mathrm{circ}(\overline{\mathcal{D}'}_{\text{all-zero}}) \\ &\geq 1 + r + s_q - (1 + r + c) \\ &\geq y - c \end{aligned}$$

which certainly goes to infinity as y does. The assumption of completeness ensures $y \to \infty$ as $\ell \to \infty$, and so we have $|F_\ell|_q \to \infty$ as $\ell \to \infty$. As in the proof of Theorem 1.0.6, the argument for $|g_\ell|_q$ is a simpler version of this, and so we are done. $\square$

5.4 More General Infinite Braids

In this section we collect a handful of corollaries of Theorems 1.0.6 and 5.3.1 for dealing with other types of infinite braids.

Corollary 5.4.1. *Let $\mathcal{B}$ be a complete semi-infinite braid containing only finitely many left-handed crossings* ($\diagup\!\!\!\!\diagdown$)*. Then $KC(\mathcal{B})$ is chain homotopy equivalent to a shifted categorified Jones-Wenzl projector $\mathrm{h}^a\mathrm{q}^b\mathbf{P}_n$, and similarly for the L-S-K spectra $\mathcal{X}(\overline{\mathcal{B}}) \simeq \Sigma^a\mathrm{q}^b\mathcal{X}(\overline{\mathcal{T}^\infty})$.*

Proof. If there are only finitely many left-handed crossings, we can view $\mathcal{B}$ as the product of the finite partial braid $\mathcal{B}_m$ which contains all of these crossings, and the infinite braid $\mathcal{B}'$ which consists of the rest of $\mathcal{B}$. Then the result follows from the similar properties of $\mathbf{P}_n$ (see [Roz14a]) and $\mathcal{X}(\overline{\mathcal{T}^\infty})$ (see Corollary 3.3.3). The shifts a and b will depend on the orientations of the crossings in the finite $\mathcal{B}_m$. □

To give the most general possible statement, we start with a definition.

Definition 5.4.2. *A* tangle involving semi-infinite braids *is a tangle diagram $\mathbf{Z}$ where any finite number of interior discs $\mathcal{D}^i$ containing only the identity tangles I_{n_i} are formally replaced by complete semi-infinite right-handed braids $\mathcal{B}^i$ (see Figure 5.13).*

Theorem 5.4.3. *For any tangle $\mathbf{Z}$ involving finitely many complete semi-infinite right-handed braids $\mathcal{B}^i$ on n_i strands, the Khovanov chain complex $KC(\mathbf{Z})$ (defined in a limiting sense analogous to that of $KC(\mathcal{B})$ in Theorem 1.0.6) is chain homotopy*

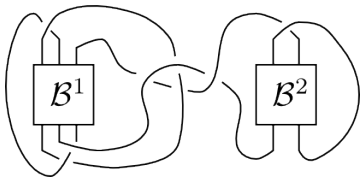

Figure 5.13: An example of a closed tangle involving semi-infinite braids $\mathcal{B}^1$ and $\mathcal{B}^2$. As long as both are right-handed and complete, the resulting Khovanov chain complex and L-S-K spectrum will match those of the same diagram with infinite twists in place of the $\mathcal{B}^1$ and $\mathcal{B}^2$.

equivalent to the Khovanov complex of the same tangle where the $\mathcal{B}^i$ have been replaced with the corresponding $\mathbf{P}_{n_i}$. Similarly, if the tangle $\mathbf{Z}$ is closed, then $\mathcal{X}(\mathbf{Z})$ is stably homotopy equivalent to the same tangle where the $\mathcal{B}^i$ have been replaced with the corresponding infinite twist $\mathcal{T}^{\infty}_{n_i}$.

Proof. This is an immediate generalization of the work presented in this chapter. □

Theorem 5.4.3 allows us to consider many sorts of infinite (right-handed) braids by breaking them up into complete semi-infinite (right-handed) braids. For instance, a non-complete semi-infinite braid is equivalent to a tangle involving a finite braid and two or more complete semi-infinite braids below it (see Figure 5.14). As another example, a bi-infinite braid $\mathcal{B} = \cdots \sigma_{j_{-2}}\sigma_{j_{-1}}\sigma_{j_0}\sigma_{j_1}\sigma_{j_2}\cdots$ can be viewed as the composition of two semi-infinite braids $\mathcal{B} = \mathcal{B}^- \cdot \mathcal{B}^+$ (see Figure 5.15). In this way we see that many different notions of infinite braids have limiting Khovanov complex (and L-S-K spectrum, if closed) made up of combinations of Jones-Wenzl projectors (or

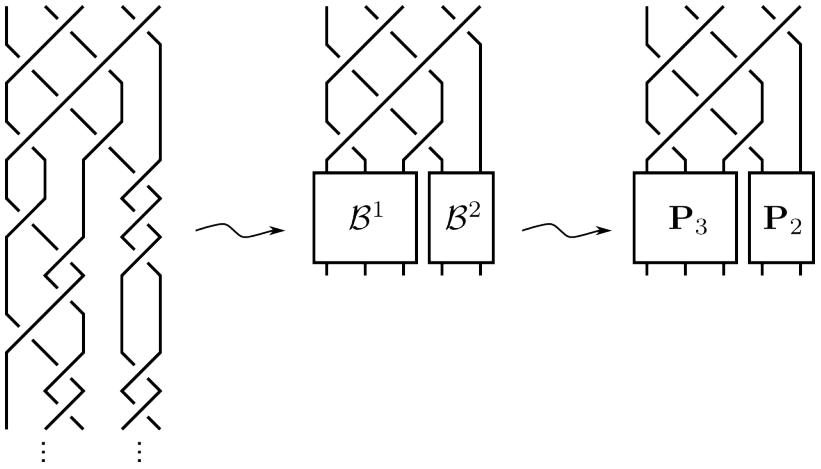

Figure 5.14: Viewing a non-complete infinite braid as a combination of two complete ones, which limit to their respective $\mathbf{P}_{n_i}$.

spectra involving closures of infinite twists). Choices of how to arrange the diagrams (for instance, where to begin the semi-infinite complete braid in Figure 5.14) lead to normalization shifts within the resulting complex or spectrum similar to those in Corollary 5.4.1.

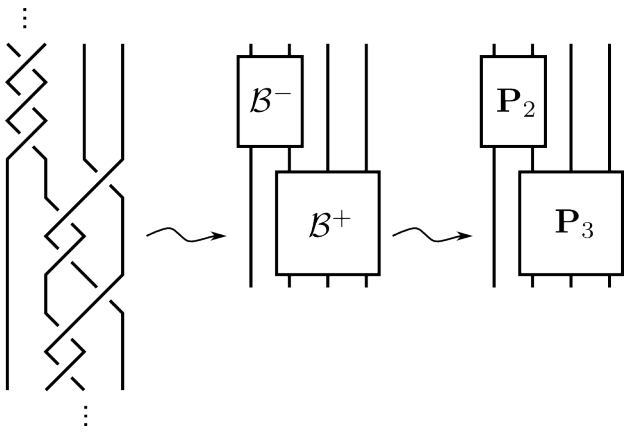

Figure 5.15: Viewing a bi-infinite braid as a combination of two semi-infinite ones, which limit to their respective $\mathbf{P}_{n_i}$.

Bibliography

[Arm13] Cody Armond. The head and tail conjecture for alternating knots. *Algebr. Geom. Topol.*, 13(5):2809–2826, 2013.

[BN05] Dror Bar-Natan. Khovanov's homology for tangles and cobordisms. *Geom. Topol.*, 9:1443–1499, 2005.

[BN07] Dror Bar-Natan. Fast Khovanov homology computations. *J. Knot Theory Ramifications*, 16(3):243–255, 2007.

[Cha56] S. C. Chang. On algebraic structures and homotopy invariants. *Bull. Acad. Polon. Sci. Cl. III.*, 4:797–800, 1956.

[CJS95] R. L. Cohen, J. D. S. Jones, and G. B. Segal. Floer's infinite-dimensional Morse theory and homotopy theory. In *The Floer memorial volume*, volume 133 of *Progr. Math.*, pages 297–325. Birkhäuser, Basel, 1995.

[CK12] Benjamin Cooper and Vyacheslav Krushkal. Categorification of the Jones-Wenzl projectors. *Quantum Topol.*, 3(2):139–180, 2012.

[GL15] Stavros Garoufalidis and Thang T. Q. Lê. Nahm sums, stability and the colored Jones polynomial. *Res. Math. Sci.*, 2:Art. 1, 55, 2015.

[GOR13] Eugene Gorsky, Alexei Oblomkov, and Jacob Rasmussen. On stable Khovanov homology of torus knots. *Exp. Math.*, 22(3):265–281, 2013.

[GORS14] Eugene Gorsky, Alexei Oblomkov, Jacob Rasmussen, and Vivek Shende. Torus knots and the rational DAHA. *Duke Math. J.*, 163(14):2709–2794, 2014.

[Hoga] Matt Hogancamp. A polynomial action on colored $sl(2)$ link homology. arXiv:1405.2574.

[Hogb] Matthew Hogancamp. Stable homology of torus links via categorified Young symmetrizers I: one-row partitions. arXiv:1505.08148.

[IW17] Gabriel Islambouli and Michael Willis. The Khovanov homology of infinite braids. To appear in *Quantum Topol.*, 2017. arXiv:1610.04582.

[Jon97] Vaughan F. R. Jones. A polynomial invariant for knots via von Neumann algebras [MR0766964 (86e:57006)]. In *Fields Medallists' lectures*, volume 5 of *World Sci. Ser. 20th Century Math.*, pages 448–458. World Sci. Publ., River Edge, NJ, 1997.

[Kas97] R. M. Kashaev. The hyperbolic volume of knots from the quantum dilogarithm. *Lett. Math. Phys.*, 39(3):269–275, 1997.

[Kau88] Louis H. Kauffman. New invariants in the theory of knots. *Amer. Math. Monthly*, 95(3):195–242, 1988.

[Kho00] Mikhail Khovanov. A categorification of the Jones polynomial. *Duke Math. J.*, 101(3):359–426, 2000.

[Kho02] Mikhail Khovanov. A functor-valued invariant of tangles. *Algebr. Geom. Topol.*, 2:665–741, 2002.

[KL94] Louis H. Kauffman and Sóstenes L. Lins. *Temperley-Lieb recoupling theory and invariants of* 3*-manifolds*, volume 134 of *Annals of Mathematics Studies*. Princeton University Press, Princeton, NJ, 1994.

[KM11] P. B. Kronheimer and T. S. Mrowka. Khovanov homology is an unknot-detector. *Publ. Math. Inst. Hautes Études Sci.*, (113):97–208, 2011.

[KR00] Ilya Kofman and Yongwu Rong. Approximating Jones coefficients and other link invariants by Vassiliev invariants. *J. Knot Theory Ramifications*, 9(7):955–966, 2000.

[LOS] Andrew Lobb, Patrick Orson, and Dirk Schuetz. A Khovanov stable homotopy type for colored links. arXiv:1602.01386.

[LS14a] Robert Lipshitz and Sucharit Sarkar. A Khovanov stable homotopy type. *J. Amer. Math. Soc.*, 27(4):983–1042, 2014.

[LS14b] Robert Lipshitz and Sucharit Sarkar. A refinement of Rasmussen's S-invariant. *Duke Math. J.*, 163(5):923–952, 2014.

[LS14c] Robert Lipshitz and Sucharit Sarkar. A Steenrod square on Khovanov homology. *J. Topol.*, 7(3):817–848, 2014.

[Pen71] Roger Penrose. Applications of negative dimensional tensors. In *Combinatorial Mathematics and its Applications (Proc. Conf., Oxford, 1969)*, pages 221–244. Academic Press, London, 1971.

[Ras10] Jacob Rasmussen. Khovanov homology and the slice genus. *Invent. Math.*, 182(2):419–447, 2010.

[Roz14a] Lev Rozansky. An infinite torus braid yields a categorified Jones-Wenzl projector. *Fund. Math.*, 225(1):305–326, 2014.

[Roz14b] Lev Rozansky. Khovanov homology of a unicolored B-adequate link has a tail. *Quantum Topol.*, 5(4):541–579, 2014.

[Sto07] Marko Stošić. Homological thickness and stability of torus knots. *Algebr. Geom. Topol.*, 7:261–284, 2007.

[Thi87] Morwen B. Thistlethwaite. A spanning tree expansion of the Jones polynomial. *Topology*, 26(3):297–309, 1987.

[Wen87] Hans Wenzl. On sequences of projections. *C. R. Math. Rep. Acad. Sci. Canada*, 9(1):5–9, 1987.

[Whi50] J. H. C. Whitehead. A certain exact sequence. *Ann. of Math. (2)*, 52:51–110, 1950.

[Wil] Michael Willis. A colored Khovanov homotopy type and its tail for B-adequate links. To appear in *Algebr. Geom. Topol.* arXiv:1602.03856.

[Wil16] Michael Willis. Stabilization of the Khovanov homotopy type of torus links. To appear in *Int. Math. Res. Notices*, 2016. arXiv:1511.02742.

[Wit94] Edward Witten. Quantum field theory and the Jones polynomial. In *Braid group, knot theory and statistical mechanics, II*, volume 17 of *Adv. Ser. Math. Phys.*, pages 361–451. World Sci. Publ., River Edge, NJ, 1994.